Electronic Supplementary Material (ESI) for ChemComm.

Supporting information for:

Synthesis of fused B,N-heterocycles by alkyne cleavage, NHC ring-expansion and C-H activation at a diboryne

Tobias Brückner, Merle Arrowsmith, Merlin Heß, Kai Hammond, Marcel Müller and Holger Braunschweig*

Institut für Anorganische Chemie and the Institute for Sustainable Chemistry & Catalysis with Boron, Julius-Maximilians-Universität Würzburg, Am Hubland, 97074 Würzburg (Germany)

Table of contents

General Considerations

All manipulations were performed either under an atmosphere of dry argon or *in vacuo* using standard Schlenk line or glovebox techniques. Deuterated solvents were dried over molecular sieves and degassed by three freeze-pump-thaw cycles prior to use. All other solvents were distilled and degassed from appropriate drying agents. Solvents (both deuterated and non-deuterated) were stored under argon over activated 4 Å molecular sieves. NMR spectra were acquired on a Bruker Avance 500 NMR spectrometer (^{1}H: 500.1 MHz, ^{11}B: 160.5 MHz, ^{13}C{^{1}H}: 125.8 MHz, ^{19}F{^{1}H}: 470.6 MHz) or on a Bruker Avance 400 NMR spectrometer (^{1}H: 400.1 MHz, ^{11}B: 128.4 MHz, ^{13}C{^{1}H}: 125.8 MHz, ^{19}F{^{1}H}: 376.5 MHz) at 298 K unless otherwise stated. Chemical shifts (δ) are given in ppm and internally referenced to the carbon nuclei (^{13}C{^{1}H}) or residual protons (^{1}H) of the solvent. ^{11}B NMR spectra were referenced to [$BF_3 \cdot OEt_2$] as an external standard. High-resolution mass spectrometry data was obtained from a Thermo Scientific Exactive Plus spectrometer in ASAP or LIFDI mode. Elemental analysis was conducted on an Elementar vario MICRO cube elemental analyser.

4-Ethynyl-*N,N*-dimethylaniline, phenylacetylene and trimethylsilylacetylene were purchased from Sigma-Aldrich. SIDep,[1] 4-ethynyl-α,α,α-trifluorotoluene,[2] and ferrocenylacetylene[3] were synthesised following modified literature procedures. $B_2(SIDep)_2$[4] was synthesised following a literature procedure.

Synthetic procedures

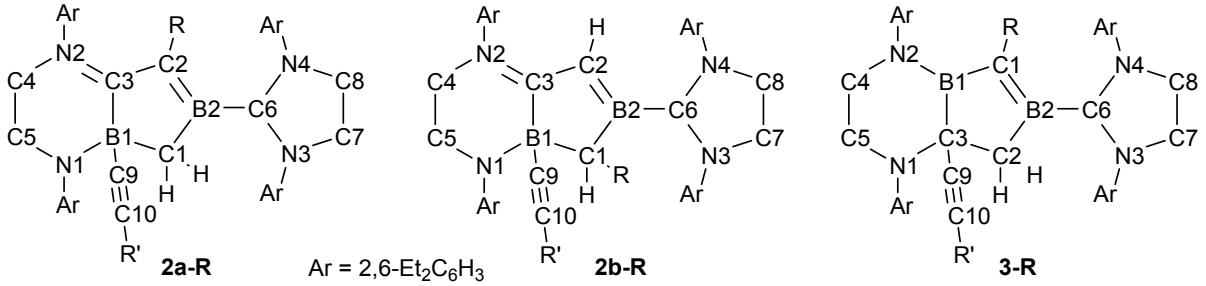

Figure S1. Numbering schemes employed for the NMR data assignment of compounds **2a-R**, **2b-R** and **3-R**.

Compound 2-H

50 mg $B_2(SIDep)_2$ (72.5 µmol) were dissolved in benzene (2 mL) and the argon atmosphere was exchanged with acetylene. Within one minute at room temperature the solution turned from red to brown. All volatiles were removed *in vacuo* and hexanes (5 mL) was added to the brown residue. After sonication a yellow precipitate was formed which was washed with hexanes (3 x 5 mL). Drying *in vacuo* provided the pure product as a yellow solid in 91% (66.0 µmol, 52.3 mg) yield as a single isomer. ^{1}H NMR (500 MHz, C_6D_6): δ = 7.29–7.28 (m, 1H, CH_{Ar}), 7.22–7.20 (m, 2H, CH_{Ar}), 7.12–7.07 (m, 5H, CH_{Ar}), 6.95–6.91 (m, 4H, CH_{Ar}), 4.98 (td, 1H, ^2J = 12.6 Hz, ^4J = 4.2 Hz, H4), 4.04 (s, 1H, H2), 3.73–3.63 (overlapping dq and dt, 2H, H5 + C$H_{2\text{-}Et}$), 3.57–3.50 (overlapping dq and br. d, 2H, H5 + C$H_{2\text{-}Et}$), 2.99 (s, 4H, H7/8), 2.96 (br. d, 1H, ^2J = 12.6 Hz, H4), 2.71 (dq, 1H, ^2J = 14.8 Hz, ^3J = 7.4 Hz, C$H_{2\text{-}Et}$), 2.62, 2.59, 2.56 (three overlapping dq, 2H each, ^2J = 15.2, 14.8 Hz, ^3J = 7.6, 7.4 Hz, C$H_{2\text{-}Et}$), 2.49 (dq, 2H, ^2J = 15.2 Hz, ^3J = 7.6 Hz, C$H_{2\text{-}Et}$), 2.29, 2.24 (two overlapping dq, 2H each, ^2J = 15.2 Hz, ^3J = 7.6 Hz, C$H_{2\text{-}Et}$), 1.90 (s, 1H, H10), 1.85 (dq, 1H, ^1J = 14.8 Hz, ^3J = 7.4 Hz, C$H_{2\text{-}Et}$), 1.58, 1.23, 1.19, 1.14 (four t, 3H each, ^3J = 7.4 Hz, C$H_{3\text{-}Et}$), 1.10, 1.00 (two t, 6H, ^3J = 7.6 Hz, C$H_{3\text{-}Et}$), –0.12 (d, 1H, ^2J = 16.3 Hz, H1), –0.74 (d, 1H, ^2J = 16.3 Hz, H1) ppm. ^{13}C{^{1}H} NMR (125.8 MHz, C_6D_6): δ = 216.2 (v. br., C3, detected by HMBC), 186.1 (C6), 152.9, 147.4, 145.7, 143.6, 143.4, 141.3, 141.2, 141.1, 134.5 ($C_{q\text{-}Ar}$), 129.7, 127.2, 126.8, 126.4, 126.1, 125.5, 123.1 (CH$_{Ar}$), 109.2 (br., C2), 76.8 (br., C9), 71.0 (C10), 54.0 (C4/5), 53.2 (C4/5), 51.3 (C7/8), 26.2, 25.1, 24.4, 23.9, 23.8 (CH$_{2\text{-}Et}$), 19.6 (v. br., C1, detected by HSQC), 17.2, 16.6, 16.2, 15.6, 14.2, 13.9 (CH$_{3\text{-}Et}$) ppm. ^{11}B NMR (160.5 MHz, C_6D_6): δ = 54.0 (br., B2), –10.2 (B1) ppm.

HRMS (LIFDI): m/z ($C_{50}H_{65}B_2N_4$) = calc.: 743.5390, found: 743.5343.

General procedure for all compounds

50 mg $B_2(SIDep)_2$ (72.5 μmol) were dissolved in benzene (2 mL) and 2 equiv. (30 equiv. for TMS acetylene) of the relevant acetylene. Within one minute at room temperature the solution turned from red to brown. All volatiles were removed *in vacuo* and hexanes (5 mL) was added to the brown residue. After sonication a yellow precipitate was formed, which was washed with hexanes (3 x 5 mL). Drying *in vacuo* provided the pure product as a yellow solid.

Note: for the minor isomers, only the characteristically distinct NMR resonances are provided, excluding the aromatic and alkyl resonances, which greatly overlap with those of the major product.

Compounds 2/3-Ph

Isolated: 36.9 mg, 41.3 μmol, 57% yield. Isomer ratio **2a-Ph/2b-Ph/3-Ph** = 82:3:15 (determined by ^{1}H NMR).

NMR data for **2a-Ph**

^{1}H NMR (500 MHz, C_6D_6): δ = 7.77–7.78 (m, 3H, *o/p*-C≡CC_6H_5), 7.29–7.34 (m, 2H, *m*-C≡CCC_6H_5, detected by COSY), 6.72–7.36 (m 7H, H_{Ar}), 6.43–6.58 (m, 3H, H_{Ar}), 5.45 (br., 1H, H_{Ar}), 5.22 (dt, 1H, ^2J = 12.6, ^3J = 4.1 Hz, H4), 3.58–3.68 (m, 3H, C$H_{2\text{-Et}}$ + H5), 3.57–3.47 (m, 3H, C$H_{2\text{-Et}}$ + H5), 2.91–3.08 (m, 5H, C$H_{2\text{-Et}}$+H7/8), 2.17–2.75 (m, 2H, C$H_{2\text{-Et}}$), 2.70 (m, 1H, H4), 1.67 (t, 3H, ^3J = 7.6 Hz, C$H_{3\text{-Et}}$), 1.50–1.59 (m, 1H, C$H_{2\text{-Et}}$), 1.06–1.28 (m, 15H, C$H_{3\text{-Et}}$), 0.95–0.80 (m, 6H, C$H_{3\text{-Et}}$), 0.30 (d, 1H, ^1J = 16.2 Hz, H1), –0.68 (d, 1H, ^1J = 16.2 Hz, H1) ppm. ^{13}C{^{1}H} NMR (125.8 MHz, C_6D_6): δ = 208.7 (C3), 186.1(C6), 134.1–152.8 ($C_{q\text{-Ar}}$), 122.4–132.4 (CH_{Ar}), 126.9 (C9 detected by HMBC), 125.1 (br., C2, detected by HMBC), 92.9 (C10), 55.8 (C4), 53.7 (C5), 52.2, 51.0 (C7/8), 26.7–22.1 (C$H_{2\text{-Et}}$), 21.4 (v. br., C1, identified by HSQC), 13.5–17.4 (C$H_{3\text{-Et}}$). ^{11}B NMR (160.5 MHz, C_6D_6): δ = 55.1 (br, B2), –9.9 (B1) ppm.

Characteristic resonances for **2b-Ph**

^{1}H NMR (500 MHz, C_6D_6): δ = 4.79 (dt, 1H, ^2J = 12.3, ^3J = 4.3 Hz, H4), 3.99 (s, 1H, H2), 3.74 (m, 1H, H5), 3.40 (m, 1H, H5, detected by COSY), 2.96 (m, 1H, H4, detected by COSY) ppm. ^{13}C{^{1}H} NMR (125.8 MHz, C_6D_6): 113.3 (C2, detected by HSQC), 52.8 (C4, detected by HSQC), 53.5 (C5, detected by HSQC). *Note: other characteristic ^{1}H and ^{13}C NMR resonances of **2b-Ph** could not be detected due to the species representing only 3% of the sample.* ^{11}B NMR (160.5 MHz, C_6D_6): δ = –8.1 (B1) ppm.

Characteristic resonances for **3-Ph**

^{1}H NMR (500 MHz, C_6D_6): δ = 3.96 (ddd, 1H, ^{2}J = 11.6 Hz, ^{3}J = 7.9, 4.1 Hz, H4), 3.50 (m, 1H, H4/5, detected by COSY), 3.21 (ddd, 1H, ^{2}J = 11.3 Hz, ^{3}J = 5.5, 4.1 Hz, H5), 3.08 (m, 1H, H4/5, detected by COSY), 1.16 (H2 overlapping with $CH_{3\text{-Et}}$, detected by COSY), 0.60 (d, 1H, ^{2}J = 11.6 Hz, H2) ppm. ^{13}C{^{1}H} NMR (125.8 MHz, C_6D_6): δ = 106.4 (C9), 81.9 (C10), 53.4 (br., C3), 52.2 (C4), 52.0 (C5), 51.7 (br. C7/8), 51.3 (br. C7/8), 30.9 (br., C2, identified by HSQC) ppm. *Note: other characteristic ^{13}C NMR resonances of* ***3-Ph*** *could not be detected due to the species representing only 15% of the sample*.^{11}B NMR (160.5 MHz, C_6D_6): δ = 37.1 (v. br., B1) ppm. HRMS (LIFDI): m/z ($C_{62}H_{73}B_2N_4$) = calc.: 895.5959, found: 895.6016.

Compounds 2/3-Ph^{CF3}

Isolated: 45.5 mg, 44.2 µmol, 61% yield. Isomer ratio **2a-Ph^{CF3}/2b-Ph^{CF3}/3-Ph^{CF3}** = 55:10:35 (determined by ^{19}F NMR).

NMR data for **2a-Ph^{CF3}**

^{1}H NMR (500 MHz, C_6D_6): δ = 7.60, 7.50 (two d, 2H each, ^{3}J = 7.9 Hz, *o/m*-C≡C$C_6H_4CF_3$), 7.35 (dd, 1H, ^{3}J = 7.4 Hz, ^{4}J = 1.4 Hz, *o*-B$CC_6H_4CF_3$), 7.22, 7.27 (two d, 1H each, ^{3}J = 7.4 Hz, *m*-B$CC_6H_4CF_3$), 7.11 (dd, 1H, ^{3}J = 7.4 Hz, ^{4}J = 1.4 Hz, *o*-B$CC_6H_4CF_3$), 6.89–7.10 (m, 5H, H_{Ar}), 6.81 (t, 1H, ^{3}J = 7.6 Hz, *p*-H_{Ar}), 6.73 (d, 1H, ^{3}J = 7.6 Hz, *m*-H_{Ar}), 6.69 (d overlapping with br. m, 1H each, ^{3}J = 7.4 Hz, *m*-H_{Ar}), 6.40 (d, 1H, ^{3}J = 7.4 Hz, *m*-H_{Ar}), 6.11 (d, 1H, ^{3}J = 7.7 Hz, *m*-H_{Ar}), 5.39 (br., 1H, H_{Ar}), 5.06 (dt, 1H, ^{2}J = 12.6, ^{3}J = 4.1 Hz, H4), 3.88 (ddd, 1H, ^{2}J = 11.5 Hz, ^{3}J = 4.1, 7.9 Hz, H7/8), 3.52–3.57 (q overlapping with m, 3H, ^{3}J = 7.6 Hz, C$H_{2\text{-Et}}$ + H5), 3.42 (ddd, 1H, ^{2}J = 9.9 Hz, ^{3}J = 4.1, 1.4 Hz, H5), 3.31–3.40 (m, 2H, C$H_{2\text{-Et}}$), 3.15 (dt, 1H, ^{2}J = 11.5 Hz, ^{3}J = 5.0 Hz, H7/8), 2.91–2.97 (m, 2H, H7/8), 2.67 (m, 1H, H4), 1.48–2.90 (m, 16H, C$H_{2\text{-Et}}$), 1.64 (t, 3H, ^{3}J = 7.6 Hz, C$H_{3\text{-Et}}$) 0.83–1.28 (m, 21H, C$H_{3\text{-Et}}$), 0.22 (d, 1H, ^{1}J = 16.2 Hz, H1), –0.72 (d, 1H, ^{1}J = 16.2 Hz, H1) ppm. ^{13}C{^{1}H} NMR (125.8 MHz, C_6D_6): δ = 209.3 (C3), 185.6 (C6), 134.1–158.1 ($C_{q\text{-Ar}}$), 122.4–132.3 (CH_{Ar}), 125.4 (C9 detected by HMBC), 122.4 (br., C2, detected by HMBC), 92.7 (C10), 56.2 (C4), 53.6 (C5), 52.2, 52.0 (C7/8), 52.1, 23.1–26.9 (*C*$H_{2\text{-Et}}$), 21.1 (v. br., C1, identified by HSQC), 13.8–17.6 (*C*$H_{3\text{-Et}}$). ^{11}B NMR (160.5 MHz, C_6D_6): δ = 57 (br., B2), –10.1 (B1) ppm. ^{19}F NMR (470.6 MHz, C_6D_6): δ = –61.70 (B=CPhCF_3), –61.75 (C≡CPhCF_3) ppm.

Characteristic resonances for **2b-Ph^{CF3}**.

^{1}H NMR (500 MHz, C_6D_6): δ = 4.61 (dt, 1H, ^{2}J = 12.3, ^{3}J = 4.3 Hz, H4), 3.97 (s, 1H, H2), 3.68 (m, 1H, H5), 3.31 (H5, detected by COSY), 2.91 (H4, detected by COSY) ppm. ^{13}C{^{1}H} NMR (125.8 MHz, C_6D_6): δ = 182.8 (C6), 114.0 (v. br., C2, detected by HSQC), 53.9 (C4), 53.6 (C5, detected by HSQC), 51.8 (C7/8) ppm. *Note: the other characteristic ^{13}C NMR resonances of*

2b-Ph^{CF3} *could not be detected due to the species representing only 10% of the sample.* ^{11}B NMR (160.5 MHz, C_6D_6): δ = –8.0 (B1) ppm. ^{19}F NMR (470.6 MHz, C_6D_6): δ = –60.55 (B=CPhCF_3), –61.78 (C≡CPhCF_3) ppm.

Characteristic resonances for **3-Ph^{CF3}**

^{1}H NMR (500 MHz, C_6D_6): δ = 3.86 (ddd, 1H, ^2J = 11.6 Hz, ^3J = 7.9, 4.1 Hz, H4), 3.37 (m, 1H, H4/5, detected by COSY), 3.15 (ddd, 1H, ^2J = 11.3 Hz, ^3J = 5.5, 4.1 Hz, H5), 3.03 (m, 1H, H4/5, detected by COSY), 1.08 (H2 overlapping with $CH_{3\text{-Et}}$, detected by COSY), 0.54 (d, 1H, ^2J = 11.6 Hz, H2) ppm. ^{13}C{^{1}H} NMR (125.8 MHz, C_6D_6): δ = 186.7 (C6), 129.1 (broadened into baseline, C1, identified by HMBC), 106.8 (C9), 81.7 (C10), 55.4 (br., C3), 52.5 (br., C7/8), 52.3 (C5), 52.1 (C4), 51.5 (br., C7/8), 31.0 (br., C2, identified by HSQC) ppm.^{11}B NMR (160.5 MHz, C_6D_6): δ = 38.4 (v. br., B1) ppm. ^{19}F NMR (470.6 MHz, C_6D_6): δ = –61.17 (BCPhCF_3). ^{19}F NMR (470.6 MHz, C_6D_6): δ = –60.88 (B=CPhCF_3), –61.99 (C≡CPhCF_3) ppm.

HRMS (LIFDI): m/z ($C_{64}H_{71}B_2N_4F_6$) = calc.: 1031.5764, found: 1031.5702.

Compounds 2/3-Ph^{NMe2}

Isolated: 37.6 mg, 38.4 µmol, 53% yield. Isomer ratio **2a-Ph^{NMe2}/2b-Ph^{NMe2}/3-Ph^{NMe2}** = 93:1:6 (determined by ^{1}H NMR).

NMR data for **2a-Ph^{NMe2}**

^{1}H NMR (500 MHz, C_6D_6): δ = 7.77 (dm, 2H, ^3J = 8.8 Hz, *o*-C≡CC_6H_4NMe_2), 7.38 (dd, 1H, ^3J = 7.4 Hz, ^4J = 1.6 Hz, *o*-BCC_6H_4NMe_2), 7.28, 7.26 (two d, 1H each, ^3J = 7.4 Hz, *m*-BCC_6H_4NMe_2), 7.19–7.26 (br. m, 4H, H_{Ar}), 7.16 (dd, ^3J = 7.4 Hz, ^4J = 1.6 Hz, *o*-BCC_6H_4NMe_2), 7.00–7.10 (br. m, 3H, H_{Ar}), 6.84 (br. m overlapping with d, 1H each, ^3J = 7.6 Hz, *m*-H_{Ar}), 6.77 (dm overlapping with t, 2H and 1H, ^3J = 8.8 Hz, *m*-C≡CC_6H_4NMe_2, ^3J = 7.6 Hz, *p*-*H*Ar), 6.52 (d, 1H, ^3J = 7.6 Hz, *m*-H_{Ar}), 6.48, 6.34, 5.91 (three br. m, 1H each, *H*Ar), 5.35 (td, 1H, ^2J = 12.6 Hz, ^3J = 4.0 Hz, H4), 5.31 (br. m, 1H, *H*Ar), 3.78–3.64 (m, 4H, H5 + C$H_{2\text{-Et}}$), 3.56 (ddd, 1H, ^2J = 9.6 Hz, ^3J = 4.1, 1.4 Hz, H5), 3.11 (dq, 2H, ^2J = 15.2 Hz, ^3J =7.6 Hz, C$H_{2\text{-Et}}$), 2.93–3.06 (m, 4H, H6/7), 2.83 (dq, 2H, ^2J = 15.2 Hz, ^3J =7.6 Hz, C$H_{2\text{-Et}}$), 2.74 (ddd, 1H, ^2J = 12.6 Hz, ^3J = 3.8, 1.4 Hz, H4), 2.50–2.70 (m, 4H, C$H_{2\text{-Et}}$), 2.66 (s, 6H, NCH_3), 2.61 (s, 6H, NCH_3), 2.25–2.39 (overlapping br. m and dq, 3H, C$H_{2\text{-Et}}$), 1.77–1.85 (br. m, 1H, C$H_{2\text{-Et}}$), 1.73 (t, 3H, ^3J = 7.6 Hz, C$H_{3\text{-Et}}$), 1.63 (dq, 1H, ^2J = 15.2 Hz, ^3J =7.6 Hz, C$H_{2\text{-Et}}$), 1.42–1.50 (br. m, 1H, C$H_{2\text{-Et}}$), 1.38 (t, 3H, ^3J = 7.6 Hz, C$H_{3\text{-Et}}$), 1.28 (t, 3H, ^3J = 7.6 Hz, C$H_{3\text{-Et}}$), 1.18 (br. t, 6H, ^3J = 7.6 Hz, C$H_{3\text{-Et}}$), 1.11 (t, 3H, ^3J = 7.6 Hz, C$H_{3\text{-Et}}$), 0.94–0.98, 0.85–0.91 (two br. m, 3H each, C$H_{3\text{-Et}}$), 0.31 (d, 1H, ^1J = 16.5 Hz, H1), –0.72 (d, 1H, ^1J = 16.5 Hz, H1) ppm. ^{13}C{^{1}H} NMR (125.8 MHz, C_6D_6): δ = 209.8 (C3), 186.6 (C6), 112.6 (C2), 100.0 (C9), 92.6 (C10), 55.3 (C7),

53.8 (C8), 52.1 (C4), 51.0 (C5), 41.7 (NCH_3), 40.6 (NCH_3), 26.7 ($CH_{2\text{-Et}}$), 24.8 ($CH_{2\text{-Et}}$), 24.0 ($CH_{2\text{-Et}}$), 24.0 ($CH_{2\text{-Et}}$), 21.4 (br., C1) 17.4–13.6 ($CH_{3\text{-Et}}$) ppm. ^{11}B NMR (160.5 MHz, C_6D_6): δ = 55.8 (br., B2), –9.8 (s, B1) ppm.

Characteristic resonances for **2b-Ph^{NMe2}**

^{1}H NMR (500 MHz, C_6D_6): δ = 4.90 (dt, 1H, ^2J = 12.3 Hz, ^3J = 4.3 Hz, H4), *Note: the other characteristic ^{1}H and ^{13}C NMR resonances of **2b-Ph^{NMe2}** could not be detected due to the species representing only 1% of the sample.* ^{11}B NMR (160.5 MHz, C_6D_6): δ = –8.0 (B1) ppm.

Characteristic resonances for **3-Ph^{NMe2}**

^{1}H NMR (500 MHz, C_6D_6): δ = 4.05 (ddd, 1H, ^2J = 11.6 Hz, ^3J = 7.9, 4.1 Hz, H4), 1.17 (H2, detected by COSY), 0.59 (d, 1H, ^2J = 11.6 Hz, H2) ppm. ^{13}C{^{1}H} NMR (125.8 MHz, C_6D_6): δ = 111.3 (C9), 78.0 (C10), 54.1 (br., C3, detected by HMBC), 51.6 (C4), 30.6 (br., C2, detected by HSQC). *Note: other characteristic ^{1}H, ^{13}C NMR or ^{11}B NMR resonances of **3-Ph^{NMe2}** could not be detected due to the species representing only 6% of the sample.*

HRMS (LIFDI): m/z ($C_{66}H_{63}B_2N_6$) = calc.: 981.6860, found: 981.6801.

Compounds 2-TMS/2-H

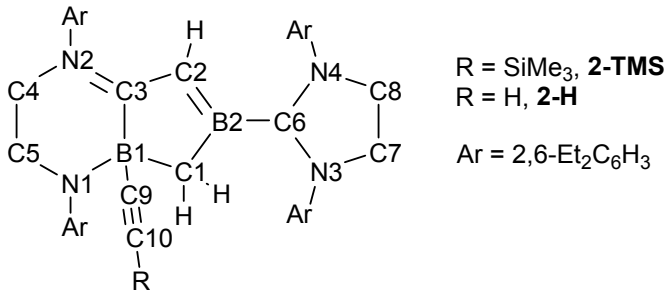

Figure S2. Numbering scheme employed for NMR assignment in compound **2-TMS**.

Isolated: 48.3 mg, 59.4 µmol, 82% yield. Ratio of **2-TMS**/**2-H** = 79:21 (determined by ^{1}H NMR).

NMR data for **2-TMS** (for **2-H**, *vide supra*)

^{1}H NMR (500 MHz, C_6D_6): δ = 7.29–7.26 (m, 1H, CH_{Ar}), 7.20–7.19 (m, 2H, CH_{Ar}), 7.14–7.06 (m, 5H, CH_{Ar}), 6.99–6.91 (m, 4H, CH_{Ar}), 5.02–4.95 (m. 1H, H1), 4.00 (s, 1H, H2), 3.81–3.43 (m, 4H, H4/5), 3.00–2.94 (m, 5H, H1 + H4/5), 2.74–2.18 (m, 13H, C$H_{2\text{-Et}}$), 1.73–1.64 (qt, 1H, C$H_{2\text{-Et}}$), 1.56, 1.23, 1.20, 1.14 (four t, 3H each, ^3J =7.6 Hz, C$H_{3\text{-Et}}$), 1.12, 0.98 (two t, 6H each, ^3J =7.6 Hz, C$H_{3\text{-Et}}$), 0.98 (m, 6H, C$H_{3\text{-Et}}$), 0.44 (s, 9H, SiCH_3), –0.24 (d, 1H, ^2J = 16.7 Hz, H1),

–0.86 (d, 1H, ^{2}J = 16.7 Hz, H1) ppm. $^{13}C\{^{1}H\}$ NMR (125.8 MHz, C_6D_6): δ = 211.1 (br., C3, identified by HMBC) 185.8 (C6), 152.8, 147.5, 145.9, 143.4, 143.3, 141.2, 141.1, 141.0, 134.5 ($C_{q\text{-}Ar}$), 129.7, 127.3, 126.7, 126.4, 126.3, 126.0,125.5, 123.1 (CH_{Ar}), 109.9 (br., C2), 93.4 (C9), 76.8 (C10), 53.8 (C4/5), 53.0 (C4/5), 51.4 (C7/8), 26.2, 25.1, 24.4, 23.9, 23.8 ($CH_{2\text{-}Et}$), 18.1 (v. br., C1, detected by HSQC), 17.2, 16.6, 16.2, 15.6, 14.2, 13.9 ($CH_{3\text{-}Et}$), 2.0 ($SiCH_3$) ppm. ^{11}B NMR (160.5 MHz, C_6D_6): δ = 54.3 (br, B2), –10.4 (B1) ppm.
HRMS (LIFDI): m/z ($C_{53}H_{73}B_2N_4Si$) = calc.: 815.5785, found: 815.5733.

Compounds 3-Fc/4-Fc

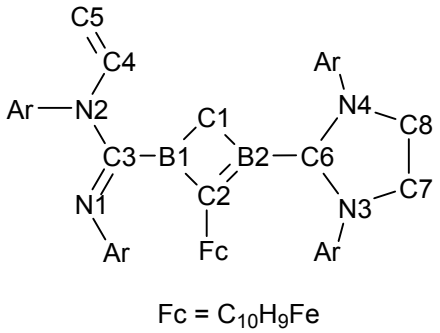

Figure S3. Numbering scheme employed for NMR assignment in compound **4-Fc**.

1st fraction isolated: 52.8 mg, 58.7 µmol, 81% yield. Ratio of **3-Fc**/**4-Fc** 33:66 (determined by ^{1}H NMR).

2nd fraction isolated from hexane filtrate: **3-Fc** 100%.

NMR Data for pure **3-Fc**

^{1}H NMR (500 MHz, C_6D_6): δ = 7.19–7.32 (m, 6H, H_{Ar}), 7.06–7.12 (m, 2H, H_{Ar}), 6.97–7.00 (m, 2H, H_{Ar}), 6.94 (d, 2H, ^{3}J = 7.4 Hz, H_{Ar}), 6.84 (d, 2H, ^{3}J = 7.4 Hz, H_{Ar}), 4.74 (dt, 1H, ^{3}J = 2.2 Hz, ^{4}J = 1.1 Hz, H_{Cp}), 4.52 (dt, 1H, ^{3}J = 2.4 Hz, ^{4}J = 1.3 Hz, H_{Cp}), 4.30 (overlapping s, 6H + m, 1H + br., 1H, C_5H_5 + H_{Cp} + H4), 4.13 (s, 5H, C_5H_5), 4.06 (td, 1H, ^{3}J = 2.4 Hz, ^{4}J = 1.3 Hz, H_{Cp}), 3.98 (td, 1H, ^{3}J = 2.4 Hz, ^{4}J = 1.3 Hz, H_{Cp}), 3.87 (td, 1H, ^{3}J = 2.3 Hz, ^{4}J = 1.2 Hz, H_{Cp}), 3.77 (td + br., 2H, ^{3}J = 2.4 Hz, ^{4}J = 1.3 Hz, H_{Cp}), 3.56 (m, 1H, $CH_{2\text{-}Et}$), 3.28 (m, 2H, H7/8), 3.35 (m, 2H, H5, detected by COSY), 3.14 (m, 1H, H4, detected by HSQC), 3.07, 2.98 (two m, 1H each, H7/8), 2.25–3.47 (m, 16H, $CH_{2\text{-}Et}$), 1.54 (t, 3H, ^{3}J = 7.5 Hz, $CH_{3\text{-}Et}$), 1.48 (t, 3H, ^{3}J = 7.5 Hz, $CH_{3\text{-}Et}$), 1.30 (q, 6H, ^{3}J = 7.5 Hz, $CH_{3\text{-}Et}$), 1.04 (t, 3H, ^{3}J = 7.5 Hz, $CH_{3\text{-}Et}$), 0.94–0.98 (m, 0.89 (t, 3H, ^{3}J = 7.5 Hz, $CH_{3\text{-}Et}$), 0.76–0.85 (m, 2H, H2) ppm. *Note: The spectra contain residual hexane from washing at 1.23 (m) and 0.89 ppm (t, overlapping with $CH_{3\text{-}Et}$).* $^{13}C\{^{1}H\}$ NMR (125.8 MHz, C_6D_6): δ = 190.9 (C6), 135.6–149.3 ($C_{q\text{-}Ar}$), 125.6–129.4 (CH_{Ar}), 119.4 (C10, detected by HMBC), 98.3 (C9), 97.5 ($C_{q\text{-}Cp}$), 71.1, 70.8, 70.6 ($CH_{\text{-}Cp}$), 70.2 (C_5H_5), 69.3 (C_5H_5),

68.0, 67.7, 67.5, 66.4, 65.2 (CH_{Cp}), 66.0 ($C_{q\text{-}Cp}$), 56.1 (br., C3), 54.4 (C5), 52.4 (C7/8), 51.7 (C7/8), 50.8 (C4), 31.4 (br. C2, detected by HSQC), 23.1–27.0 ($CH_{2\text{-}Et}$), 14.4–17.6 ($CH_{3\text{-}Et}$) ppm. ^{11}B NMR (160.5 MHz, C_6D_6): δ = 43.4 (v. br., B2), 39.3 (br. B1) ppm.

NMR data for **4-Fc**

*Note: the complete ^{1}H NMR data was determined from the difference between the spectra of the **3-Fc**/**4-Fc** mixture and pure **3-Fc**, respectively, generated in TopSpin.* ^{1}H NMR (500 MHz, C_6D_6): δ = 6.93-7.31 (m, 12H, H_{Ar}), 6.45 (dd, 1H, $^3J_{cis}$ = 8.8 Hz, $^3J_{trans}$ = 15.2 Hz, H4), 4.37 (br.), 4.20 (t, 2H, ^3J = 1.8 Hz), 4.00 (s, 5H, C_5H_5) 3.59 (d, 1H, $^3J_{trans}$ = 15.2 Hz, H5), 3.45 (d, 1H each, $^3J_{cis}$ = 8.8 Hz, H5), 3.12 (s, 4H, H7/8), 2.88, 2.81, 2.57 2.51 (four dq, 4H, 6H, 2H and 4H, respectively, ^3J = 7.5 Hz, $CH_{2\text{-}Et}$), 1.46, 1.22, 1.13 (three t, 3H, 3H and 6H, respectively, ^3J = 7.5 Hz, $CH_{3\text{-}Et}$), –0.06 (s, 2H, H1) ppm. ^{13}C{^{1}H} NMR (125.8 MHz, C_6D_6): δ = 191.2 (C6) 158.7 (C3, detected by HBMC), 140.8 (C4, detected by HSQC), 85.7 (C5, detected by HSQC), 52.2 (C7/8), 16.9 (v. br. C1, detected by HSQC) ppm. *Note: other characteristic ^{13}C NMR resonances of **4-Fc** could not be detected.* ^{11}B NMR (160.5 MHz, C_6D_6): δ = 24.6 (br, B1), 27.7 (v. br., B2) ppm.

HRMS (LIFDI): m/z ($C_{58}H_{70}B_2N_4Fe$) = calc.: 900.5136, found: 900.4916; ($C_{70}H_{80}B_2N_4Fe_2$) = calc.: 1110.5268, found: 1110.5261.

Compound 5-Ph$_2$

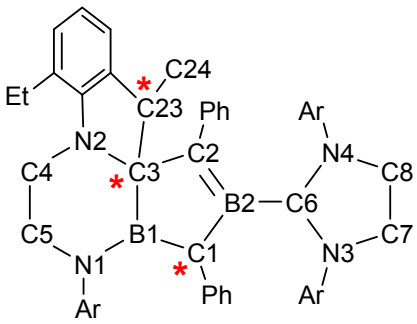

Figure S4. Numbering scheme employed for NMR assignment in compound **5-Ph$_2$**.

Isolated: 52.2 mg, 60.1 μmol, 83% yield. Three stereocentres, six diastereomers observed by ^{1}H NMR in a 77:13:5:3:1:1 ratio as determined by integration of the six aryl protons doublets in the 5.92 – 6.23 ppm region.

50 mg B_2(SIDep)$_2$ (72.5 μmol) were dissolved in benzene (2 mL) and one equiv. of diphenylacetylene was added. Within one minute at room temperature the solution turned from red to brown. All volatiles were removed *in vacuo* and hexanes (5 mL) was added to the brown

residue. After sonication a yellow precipitate was formed which was washed with hexanes (3 x 5 mL). Drying *in vacuo* provided the pure product as an orange solid. Only the NMR data for the major diastereomer, **7a**, is given. ^{1}H NMR (500 MHz, C_6D_6): δ = 7.09–6.57 (m, 23H, CH_{Ar}), 6.57 (t, 1H, ^{3}J = 7.3 Hz, *p*-CH_{Ar}), 6.02 (d, 1H, ^{3}J = 7.3 Hz, *m*-CH_{Ar}), 3.96 (q, 1H, ^{3}J = 7.5 Hz, H23), 3.68 (ddd, 1H, ^{2}J = 13.2 Hz, ^{3}J = 11.2, 2.0 Hz, H4), 3.42 (dt, 1H, ^{2}J = 13.2 Hz, ^{3}J = 2.0 Hz, H4), 3.25 (ddd, 1H, ^{2}J = 12.8 Hz, ^{3}J = 11.2, 1.5 Hz, H5), 3.16–3.02 (m, 8H, H7/8 + C$H_{2\text{-}Et}$), 2.78 (dq, 2H, ^{2}J = 15.0 Hz, ^{3}J = 7.5 Hz, C$H_{2\text{-}Et}$), 2.70, 2.60, 2.50, 2.46, 2.38, 2.33 (six dq, 2H, ^{2}J = 15.2 Hz, ^{3}J = 7.6 Hz, C$H_{2\text{-}Et}$), 2.39 (dm, 1H, ^{2}J = 12.8 Hz, H5), 2.08 (overlapping s and dq, 3H, ^{2}J = 15.0 Hz, H1, ^{3}J = 7.5 Hz, C$H_{2\text{-}Et}$), 1.95 (dq, 2H, ^{2}J = 15.6 Hz, ^{3}J = 7.8 Hz, C$H_{2\text{-}Et}$), 1.44, (d, 3H, ^{3}J = 7.5 Hz, H24), 1.30, (t, 6H, ^{3}J = 7.6 Hz, C$H_{3\text{-}Et}$), 1.22, 1.18, 1.07 (three t, 3H each, ^{3}J = 7.6 Hz, C$H_{3\text{-}Et}$), 0.92 (t, 6H, ^{3}J = 7.5 Hz, C$H_{3\text{-}Et}$) ppm. ^{13}C{^{1}H} NMR (125.8 MHz, C_6D_6): δ = 187.2 (C6, detected by HMBC), 152.5, 149.9, 148.4, 145.3, 142.5, 141.6, 140.9, 137.4 ($C_{q\text{-}Ar}$), 131.1, 130.6, 129.2, 128.9, 128.1 (CH$_{Ar}$), 127.8 (br., C2), 127.7, 126.8, 126.7, 126.2, 126.1, 125.9, 125.8, 122.0, 121.7, 120.0, 119.8 (CH$_{Ar}$), 74.1 (br., C3), 52.9 (C7/8), 52.5 (C5), 51.9 (C4), 45.5 (C23), 37.2 (br., C1), 25.7, 25.2, 25.0, 24.4 (CH$_{2\text{-}Et}$), 15.8, 15.6, 15.2 (CH$_{3\text{-}Et}$), 14.7 (C24 + CH$_{3\text{-}Et}$), 14.3 (CH$_{3\text{-}Et}$) ppm. ^{11}B NMR (160.5 MHz, C_6D_6): δ = 48.0 (br., B1), 23.4 (B2) ppm.

HRMS (LIFDI): m/z ($C_{60}H_{70}B_2N_4$) = calc.: 868.5787, found: 868.5783.

NMR Spectra

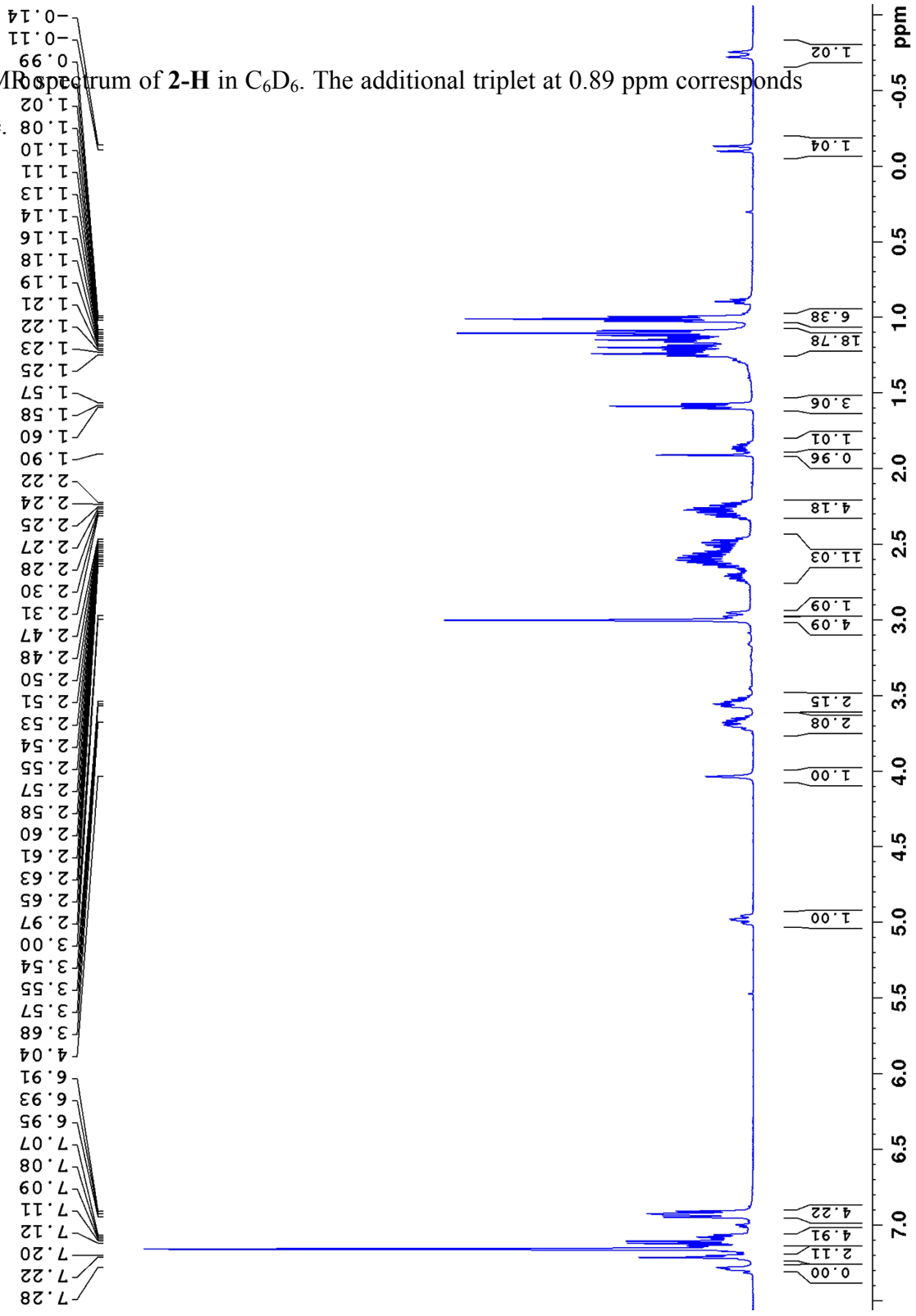

Figure S5. ^{1}H NMR spectrum of **2-H** in C_6D_6. The additional triplet at 0.89 ppm corresponds to residual hexane.

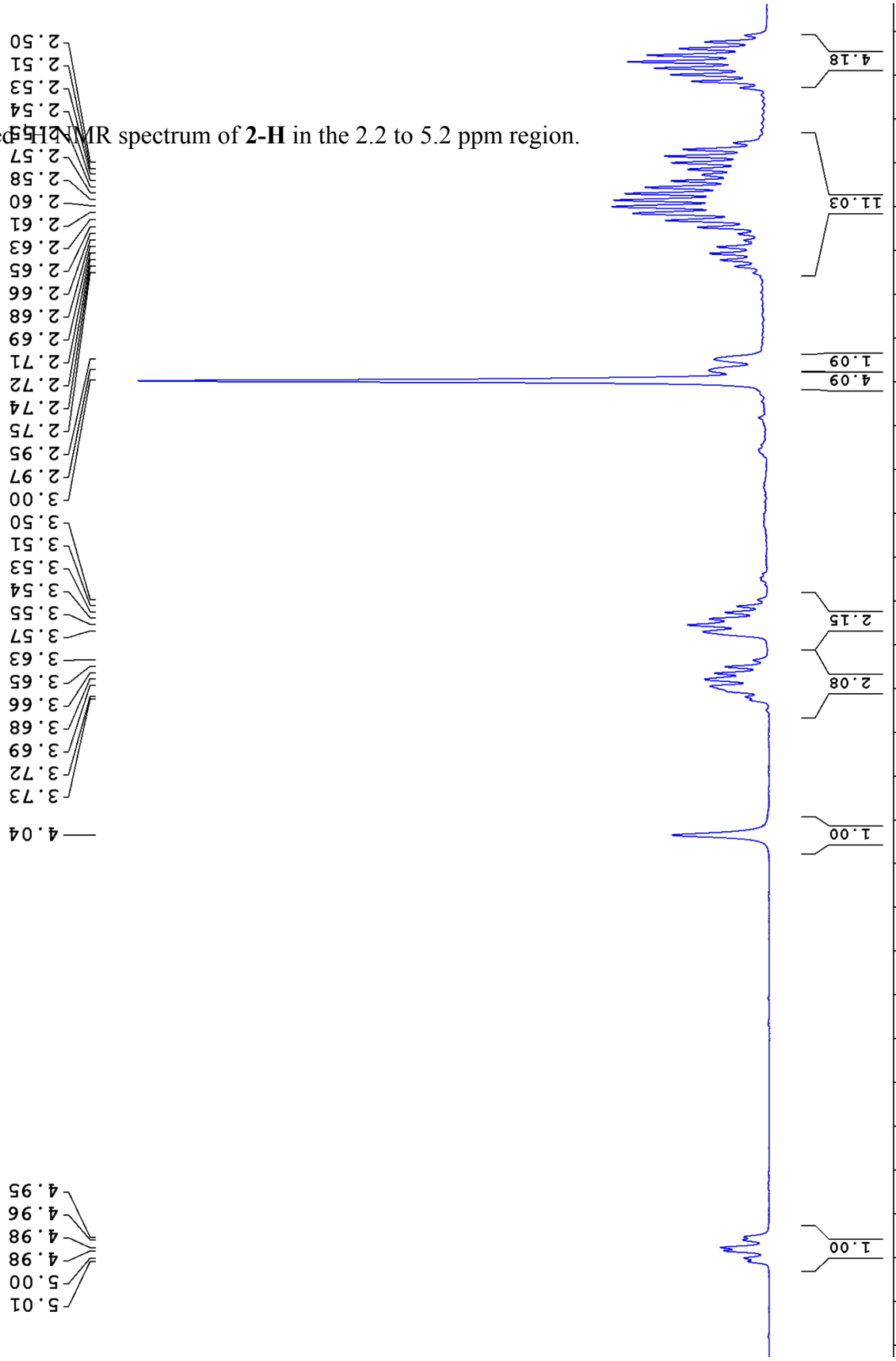

Figure S6. Annotated ^{1}H NMR spectrum of **2-H** in the 2.2 to 5.2 ppm region.

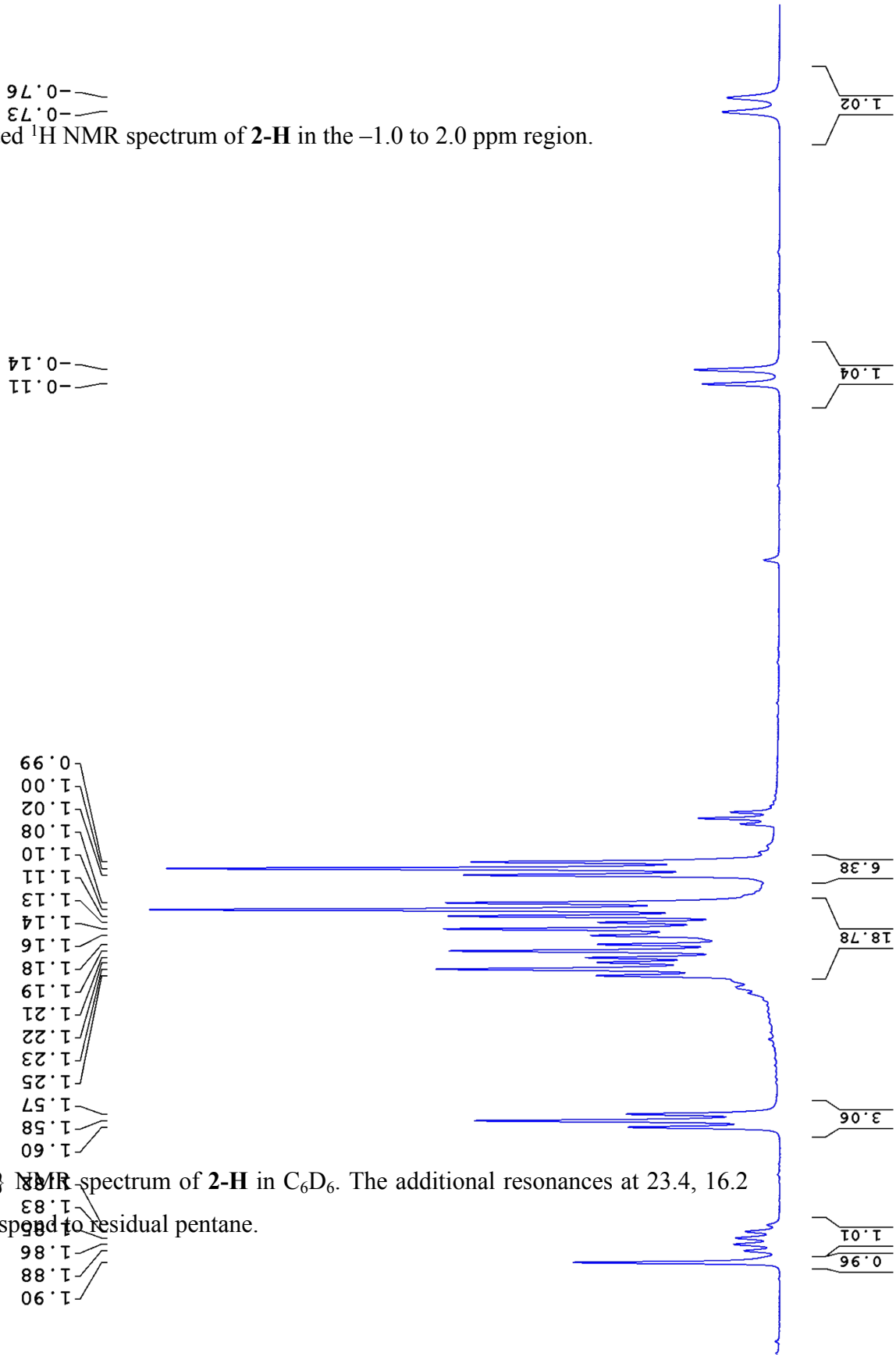

Figure S7. Annotated ^{1}H NMR spectrum of **2-H** in the –1.0 to 2.0 ppm region.

Figure S8. $^{13}C\{^{1}H\}$ NMR spectrum of **2-H** in C_6D_6. The additional resonances at 23.4, 16.2 and 14.7 ppm correspond to residual pentane.

16.62
17.19
19.61
23.75
23.87
24.26
24.45
25.11
26.23
51.33
53.20
54.04
71.03
76.76
109.21
123.07
125.49
126.08
126.37
126.57
126.82
127.24
129.67
134.49
141.15
141.16
141.25
143.40
143.58
145.71
147.40
152.93
186.07
216.11
100.00

Figure S9. HSQC plot of **2-H** in C_6D_6.

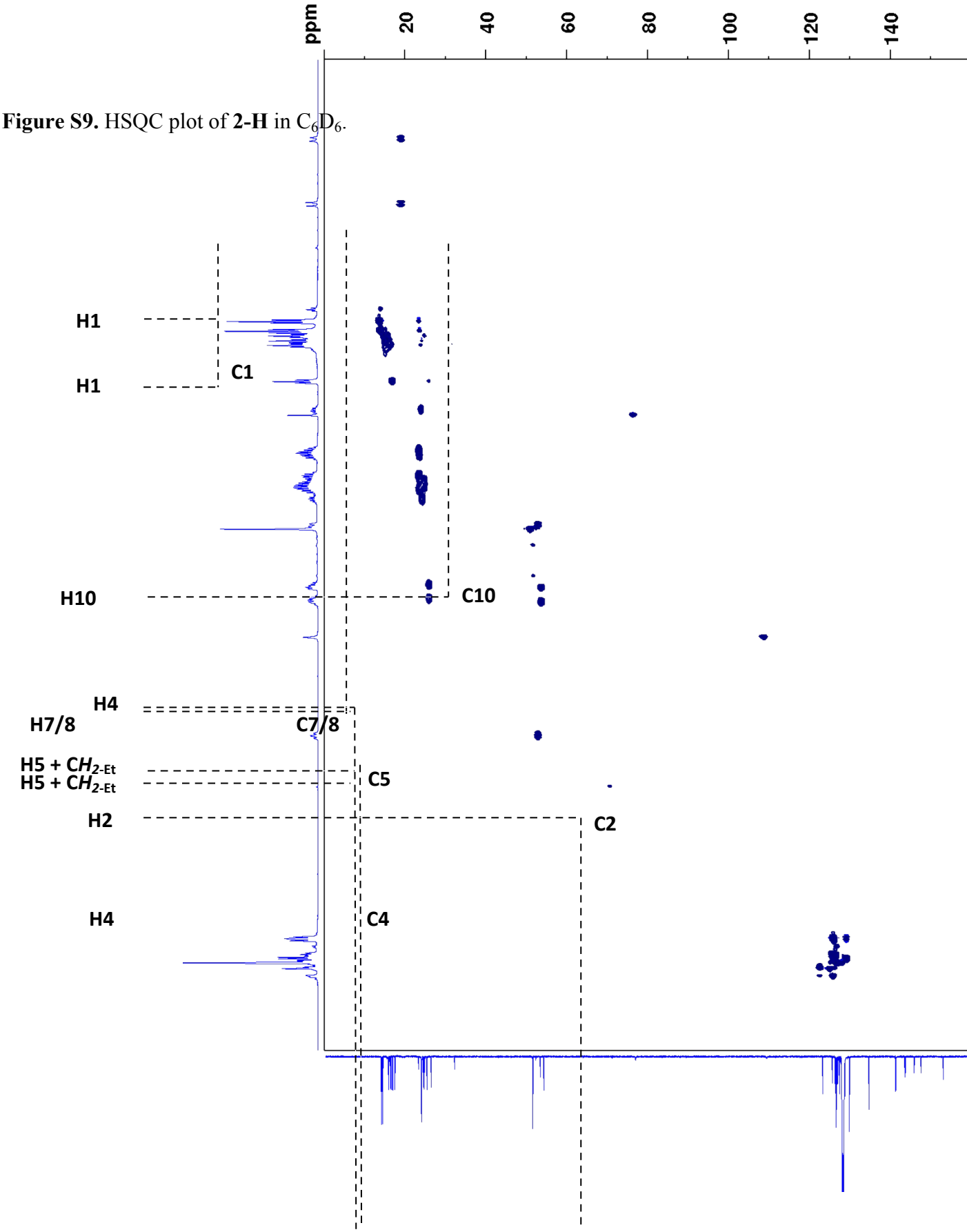

Figure S10. HMBC plot of **2-H** in C_6D_6.

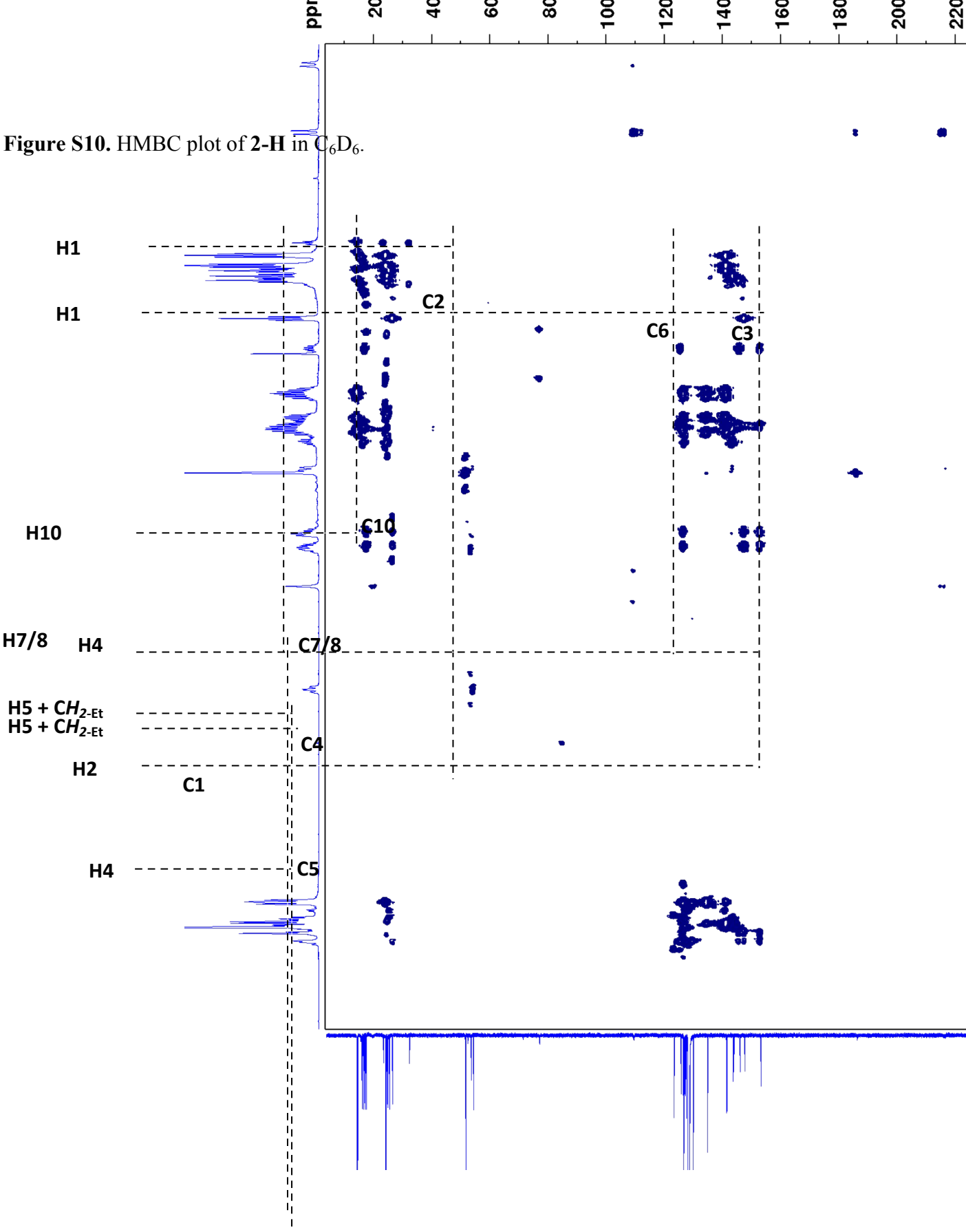

Figure S11. ^{11}B NMR spectrum of **2-H** in C_6D_6.

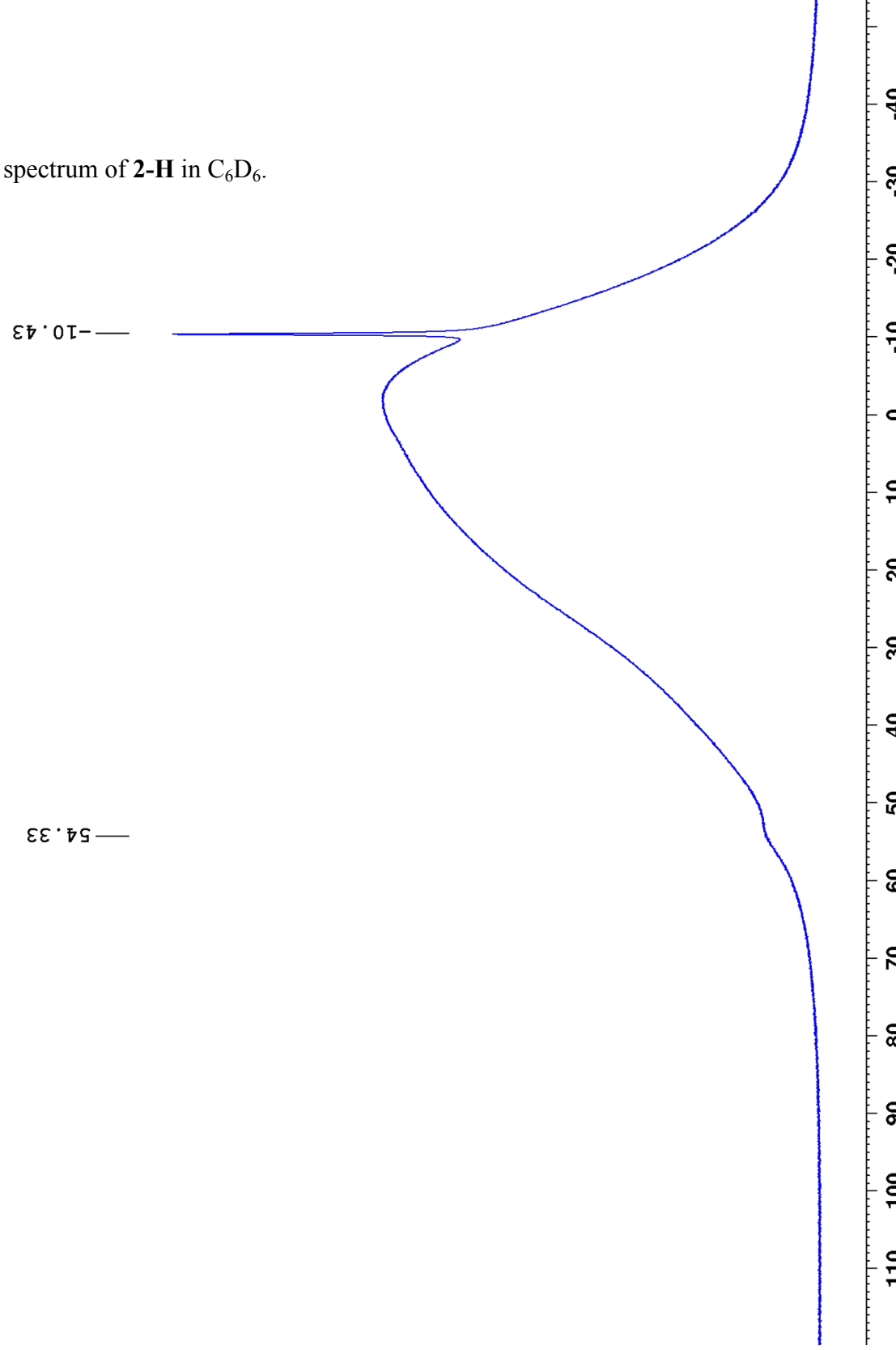

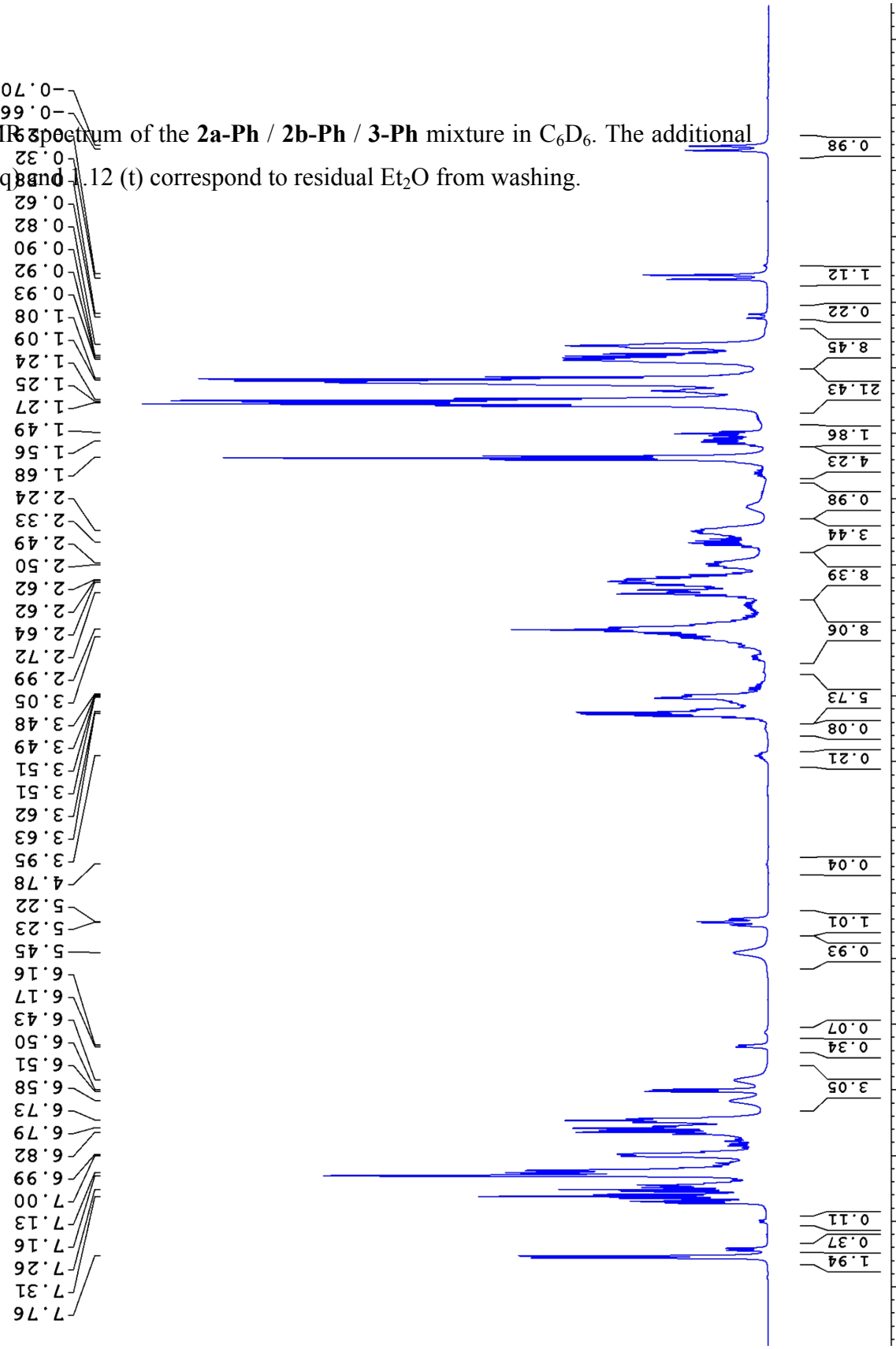

Figure S12. ^{1}H NMR spectrum of the **2a-Ph** / **2b-Ph** / **3-Ph** mixture in C_6D_6. The additional resonances at 3.27 (q) and 1.12 (t) correspond to residual Et_2O from washing.

Figure S13. Annotated ^{1}H NMR spectrum of the **2a-Ph** (●) / **2b-Ph** (♦) / **3-Ph** (■) mixture in the 3.7 to 8.0 ppm region.

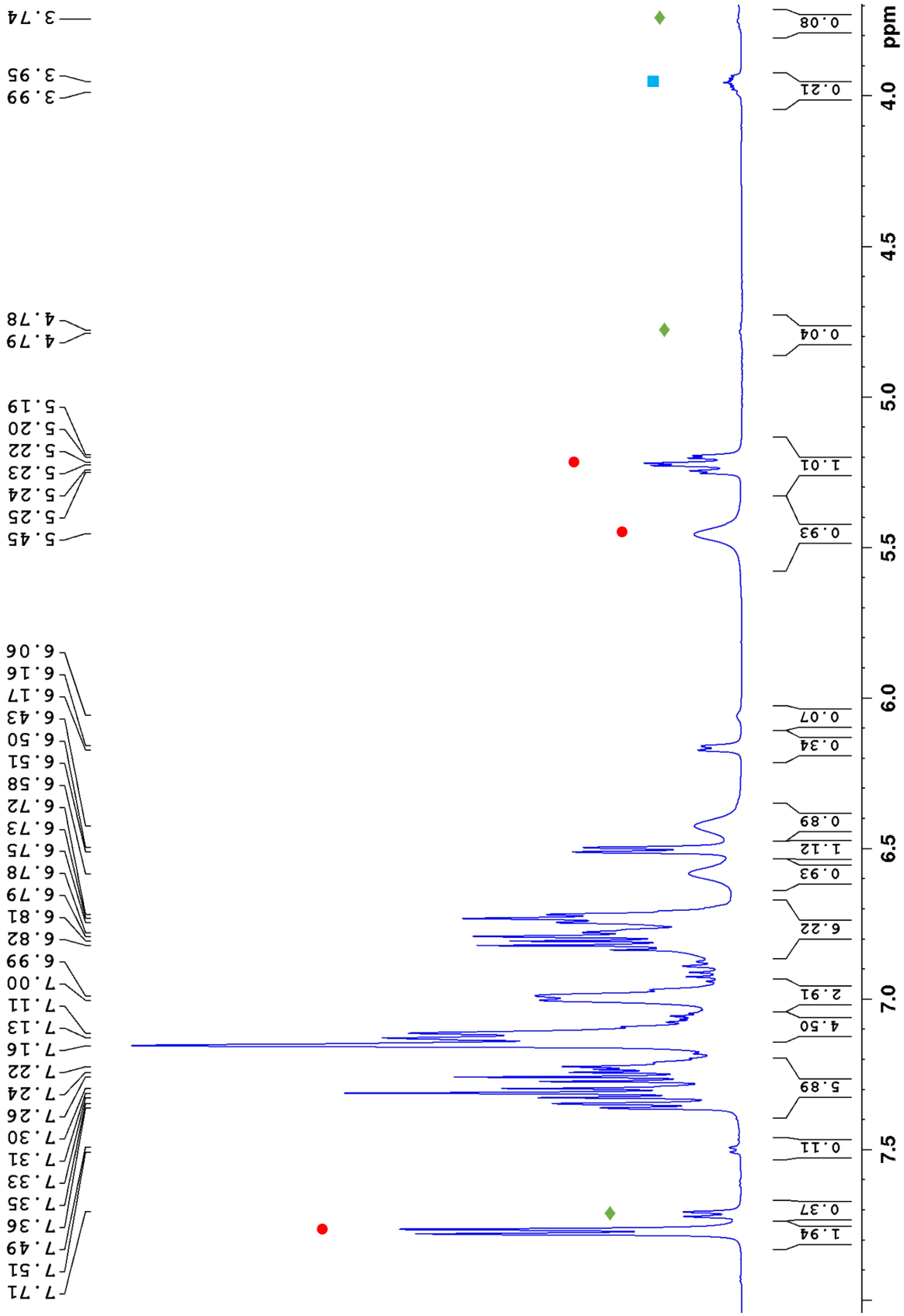

Figure S14. Annotated ^{1}H NMR spectrum of the **2a-Ph** (●) / **2b-Ph** (♦) / **3-Ph** (■) mixture in the –1.0 to 1.9 ppm region.

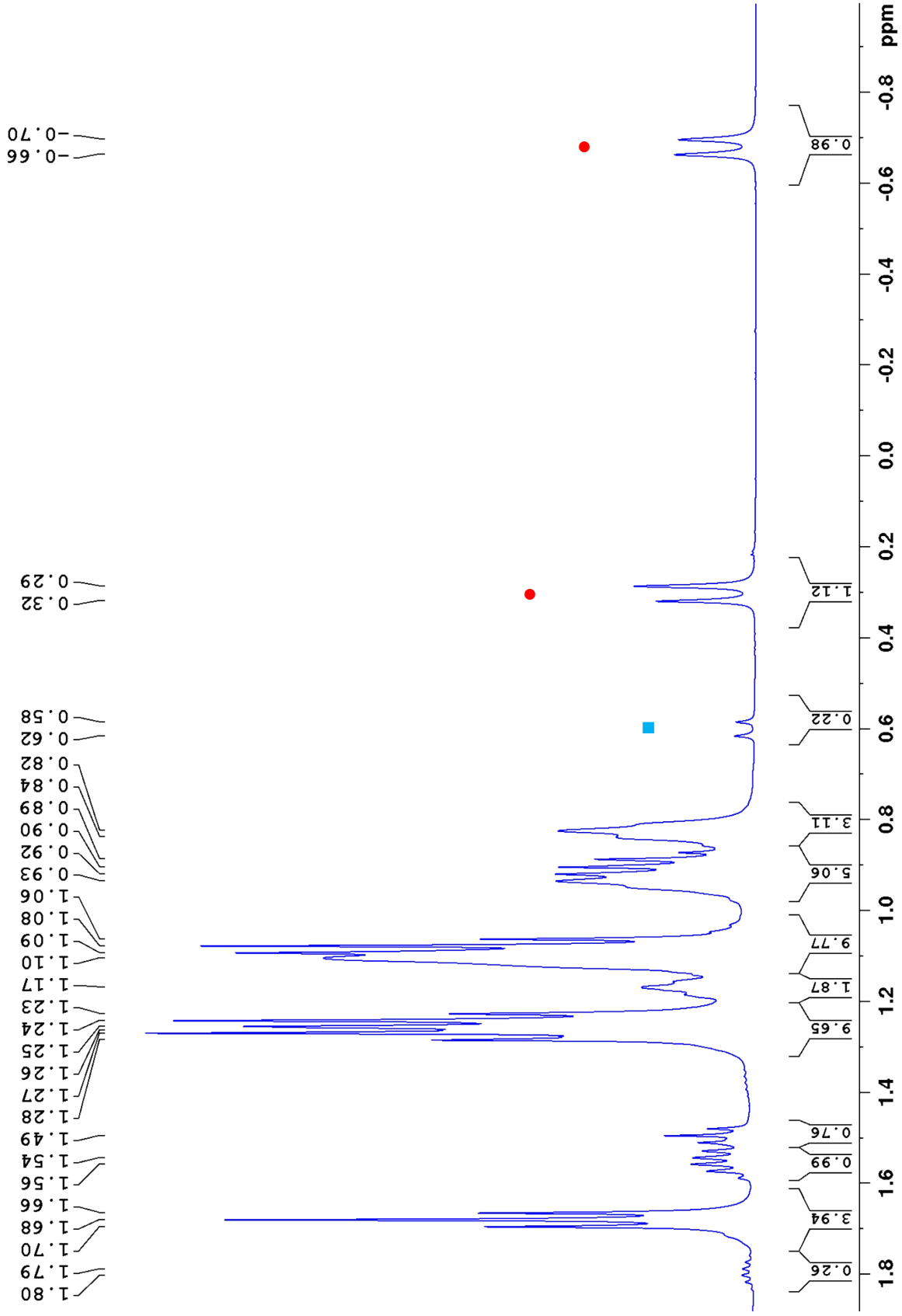

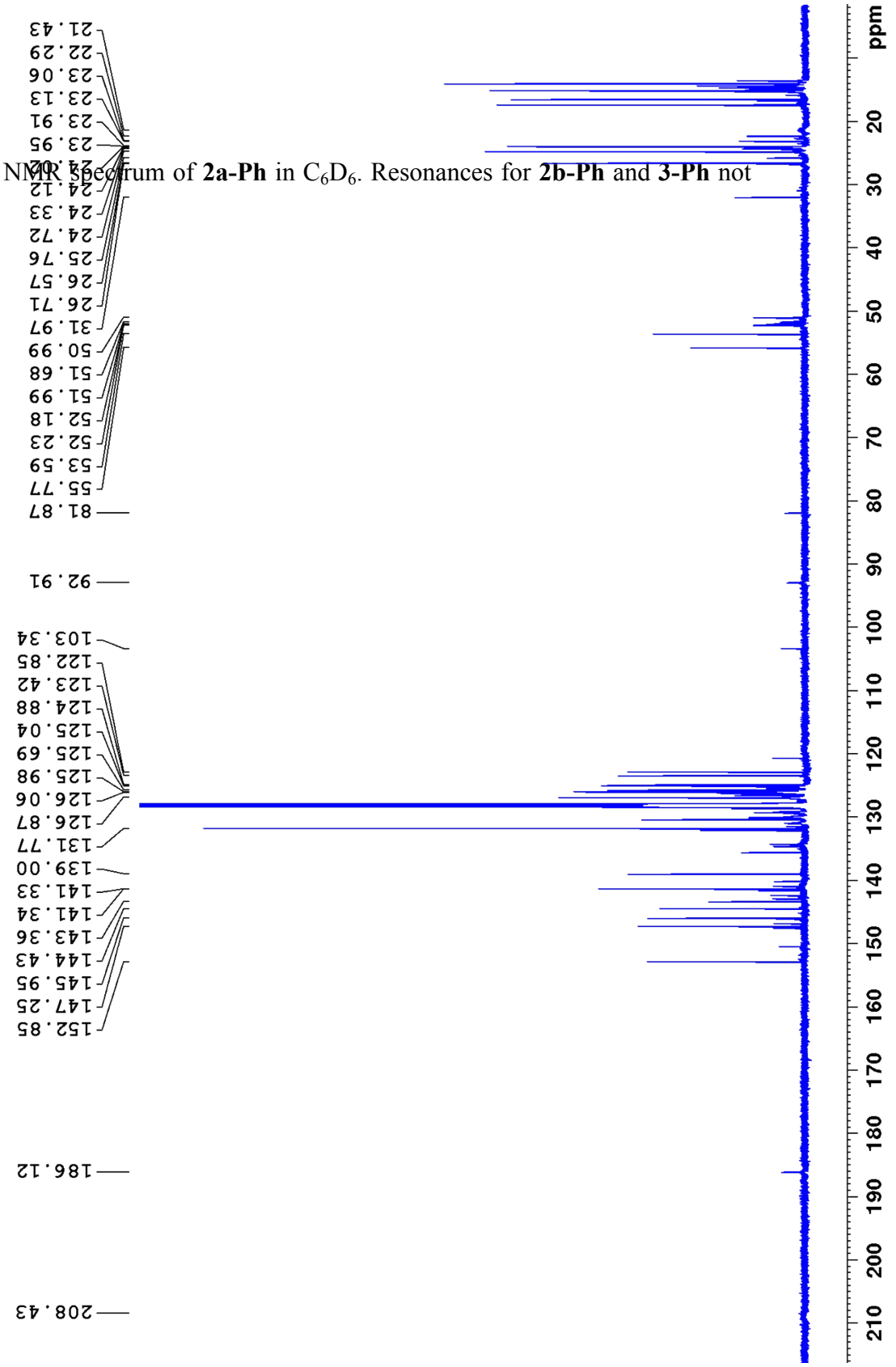

Figure S15. $^{13}C\{^{1}H\}$ NMR spectrum of **2a-Ph** in C_6D_6. Resonances for **2b-Ph** and **3-Ph** not visible.

Figure S16. HSQC plot of the **2a-Ph** / **2b-Ph** / **3-Ph** mixture in C_6D_6.

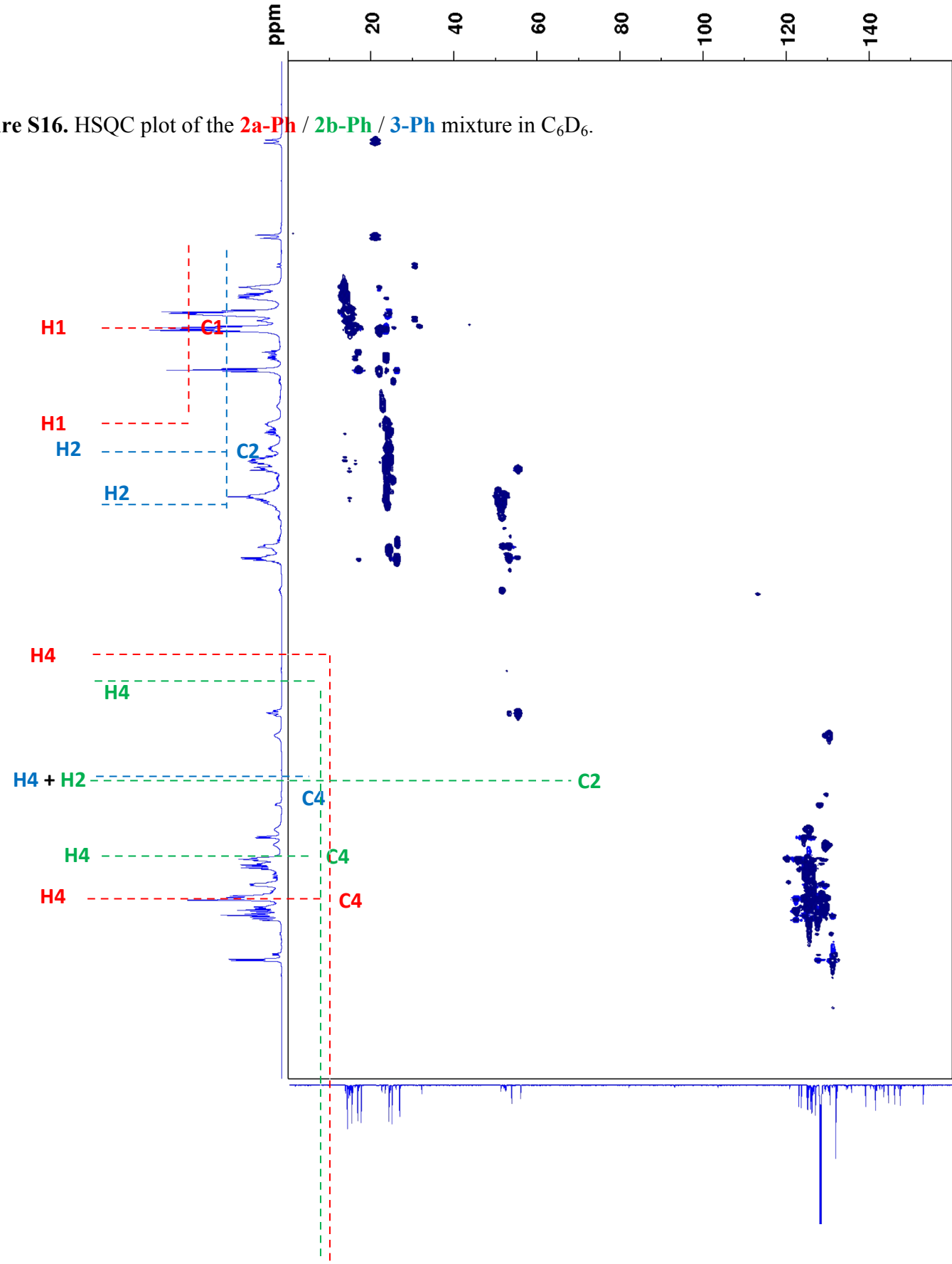

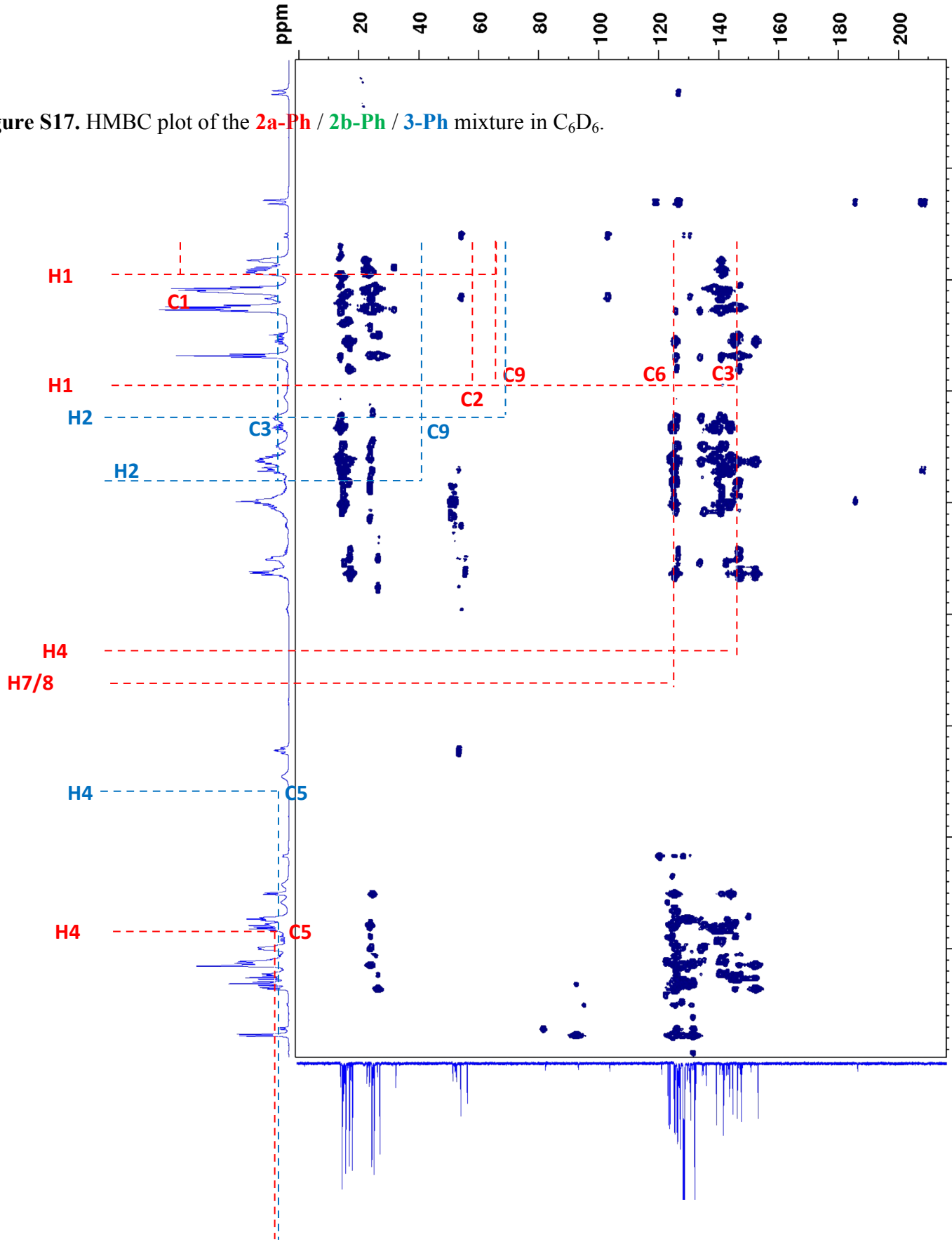

Figure S17. HMBC plot of the **2a-Ph** / **2b-Ph** / **3-Ph** mixture in C_6D_6.

Figure S18. ^{11}B NMR spectrum of the **2a-Ph** (●) / **2b-Ph** (♦) / **3-Ph** (■) mixture in C_6D_6.

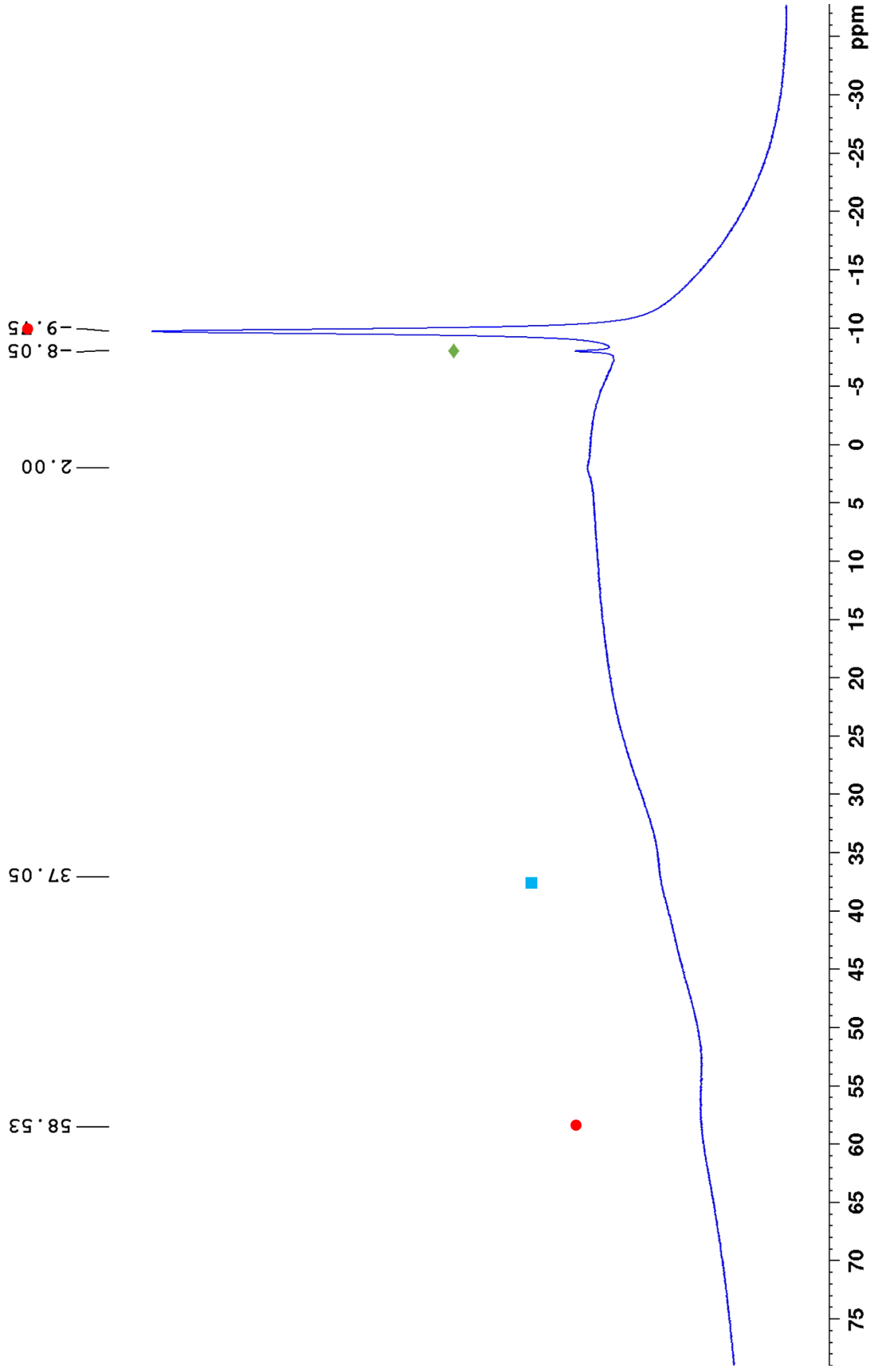

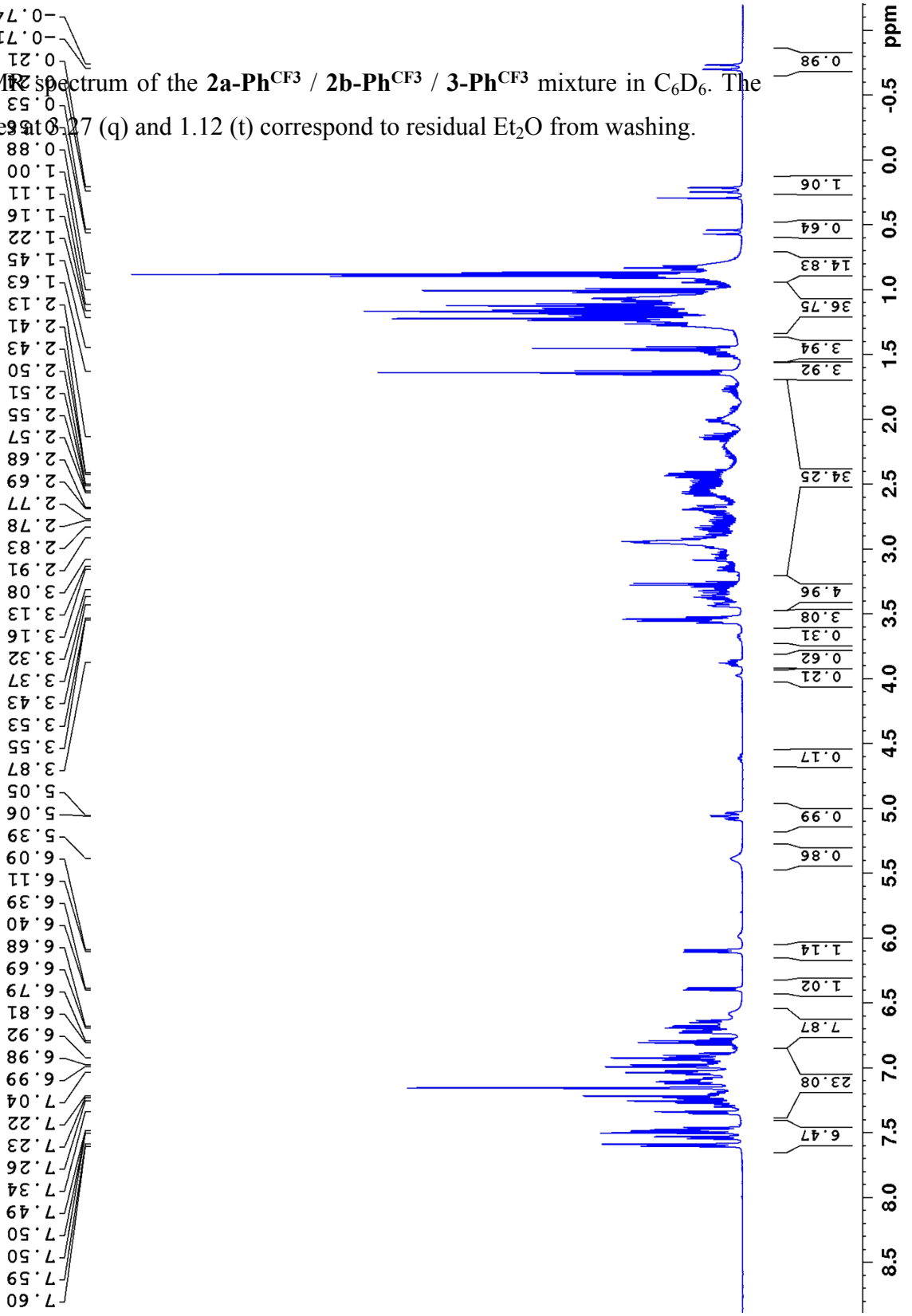

Figure S19. ^{1}H NMR spectrum of the **2a-Ph^{CF3}** / **2b-Ph^{CF3}** / **3-Ph^{CF3}** mixture in C_6D_6. The additional resonances at 3.27 (q) and 1.12 (t) correspond to residual Et_2O from washing.

Figure S20. Annotated ^{1}H NMR spectrum of the **2a-Ph^{CF3}** (●) / **2b-Ph^{CF3}** (♦) / **3-Ph^{CF3}** (■) mixture in the 3.6 to 6.5 ppm region.

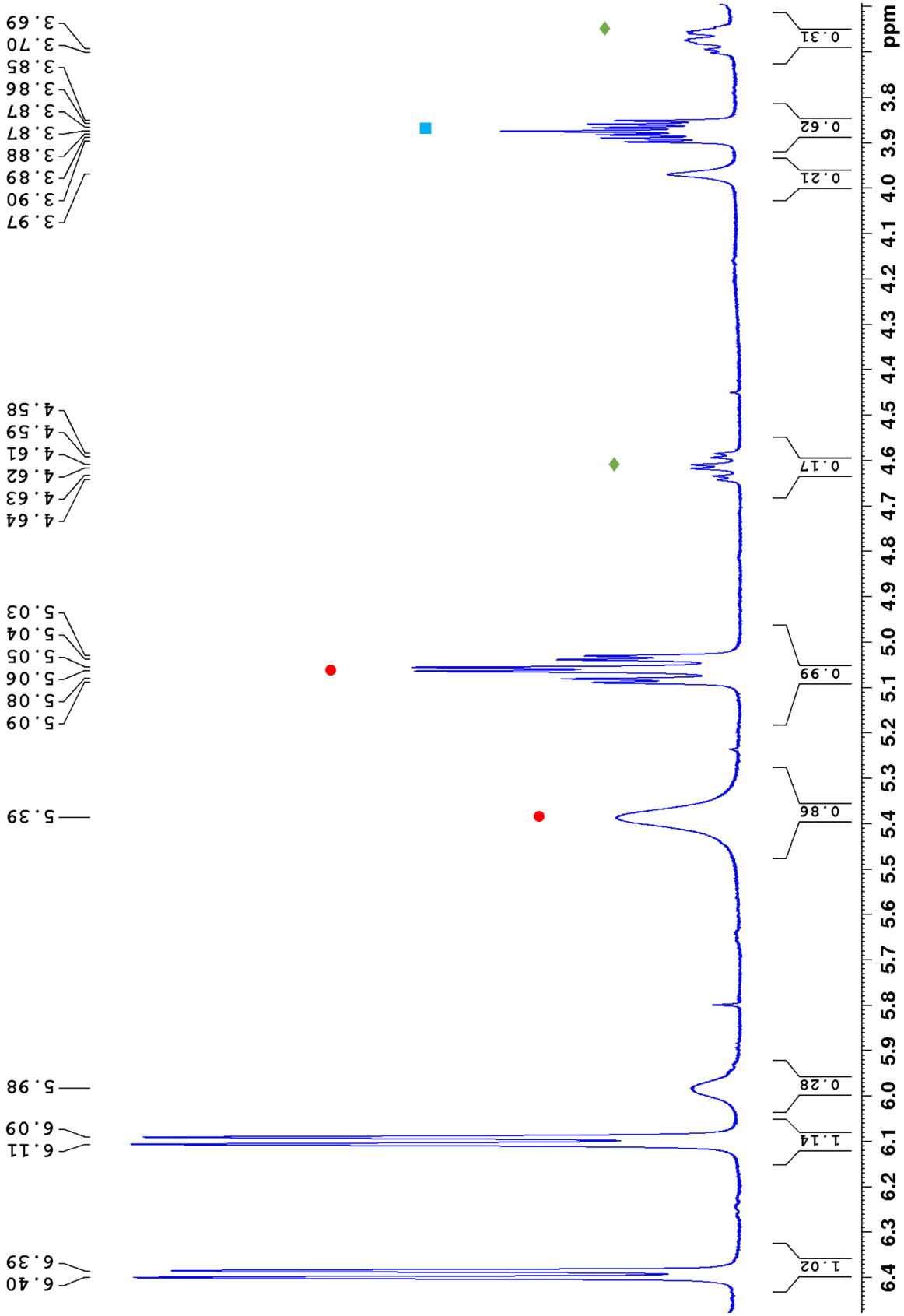

Figure S21. Annotated ^{1}H NMR spectrum of the **2a-Ph^{CF3}** (●) / **2b-Ph^{CF3}** (♦) / **3-Ph^{CF3}** (■) mixture in the –1.0 to 1.8 ppm region.

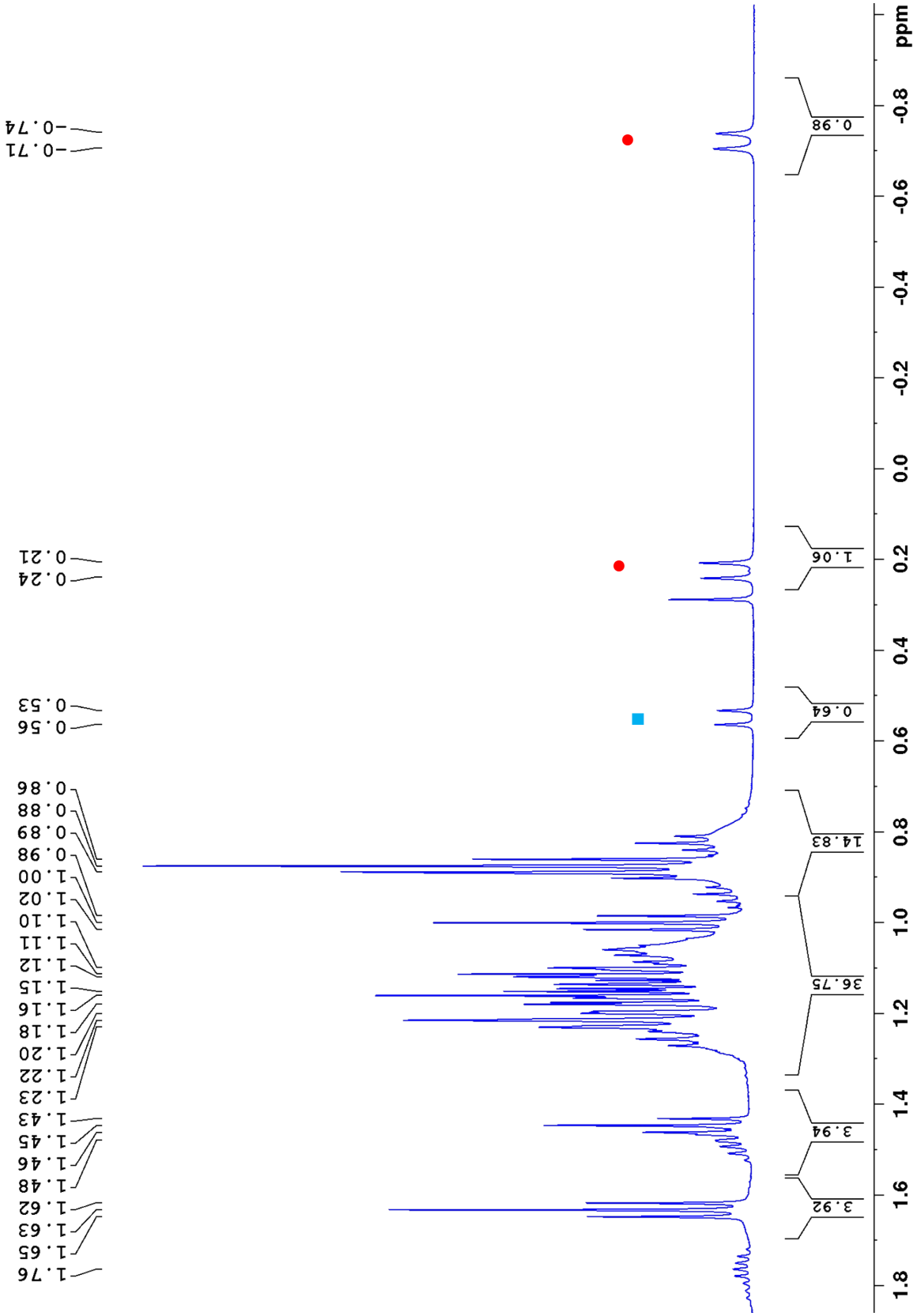

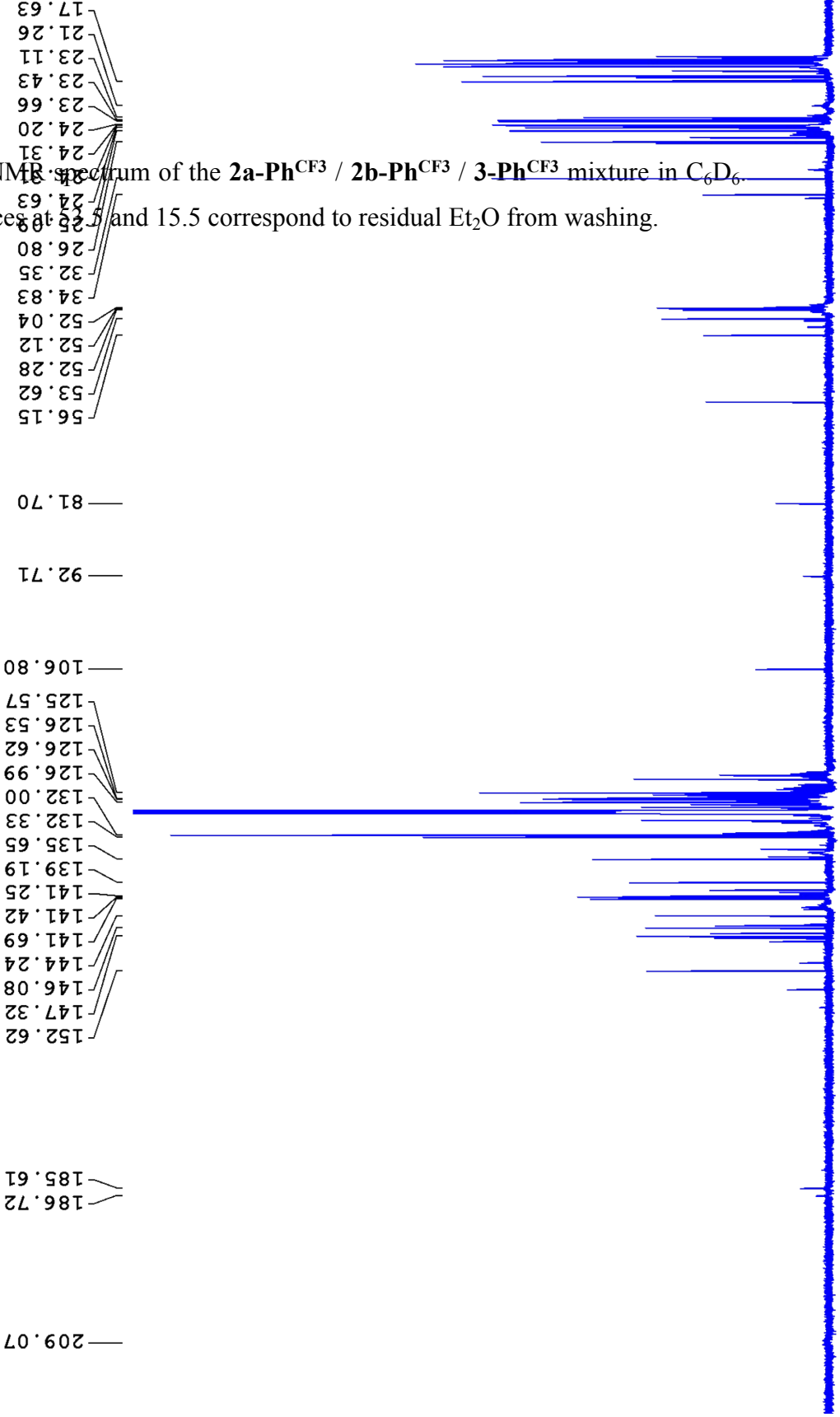

Figure S22. $^{13}C\{^{1}H\}$ NMR spectrum of the **2a-Ph^{CF3}** / **2b-Ph^{CF3}** / **3-Ph^{CF3}** mixture in C_6D_6. The additional resonances at 52.5 and 15.5 correspond to residual Et_2O from washing.

Figure S23. HSQC plot of the **2a-Ph^{CF3}** / **2b-Ph^{CF3}** / **3-Ph^{CF3}** mixture in C_6D_6.

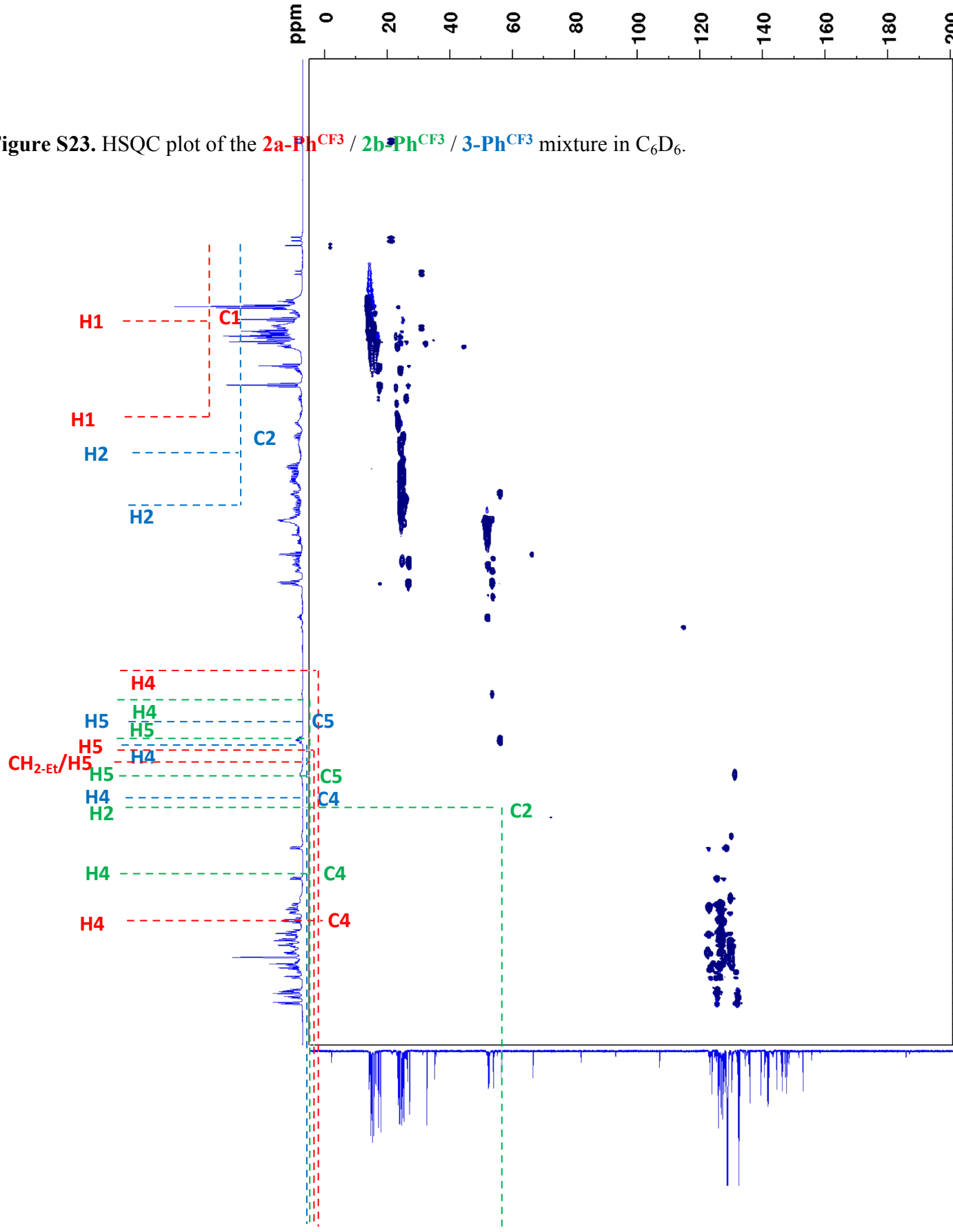

Figure S24. HMBC plot of the **2a-Ph^{CF3}** / **2b-Ph^{CF3}** / **3-Ph^{CF3}** mixture in C_6D_6.

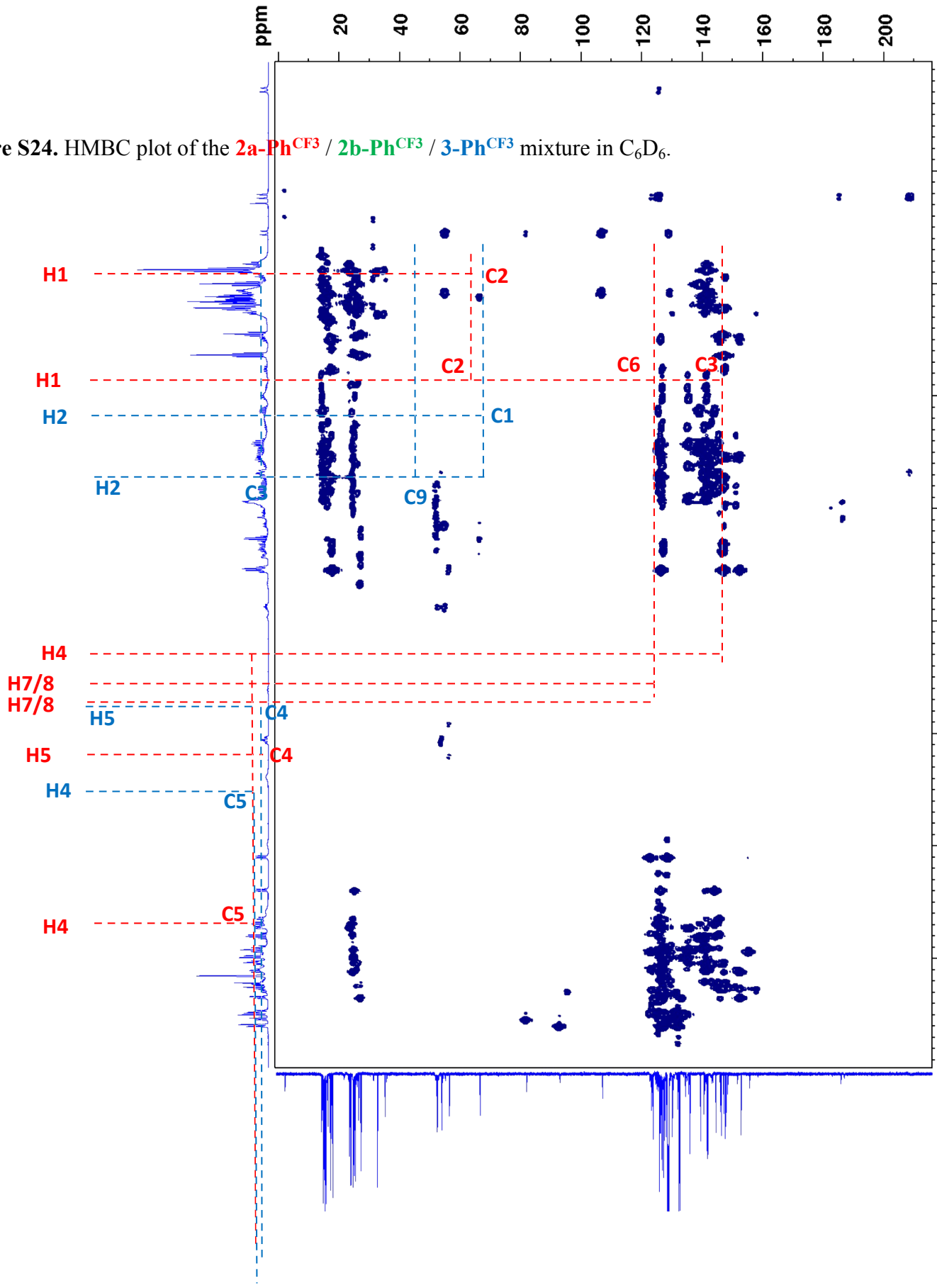

Figure S25. ^{11}B NMR spectrum of the **2a-Ph^{CF3}** (●) / **2b-Ph^{CF3}** (♦) / **3-Ph^{CF3}** (■) mixture in C_6D_6.

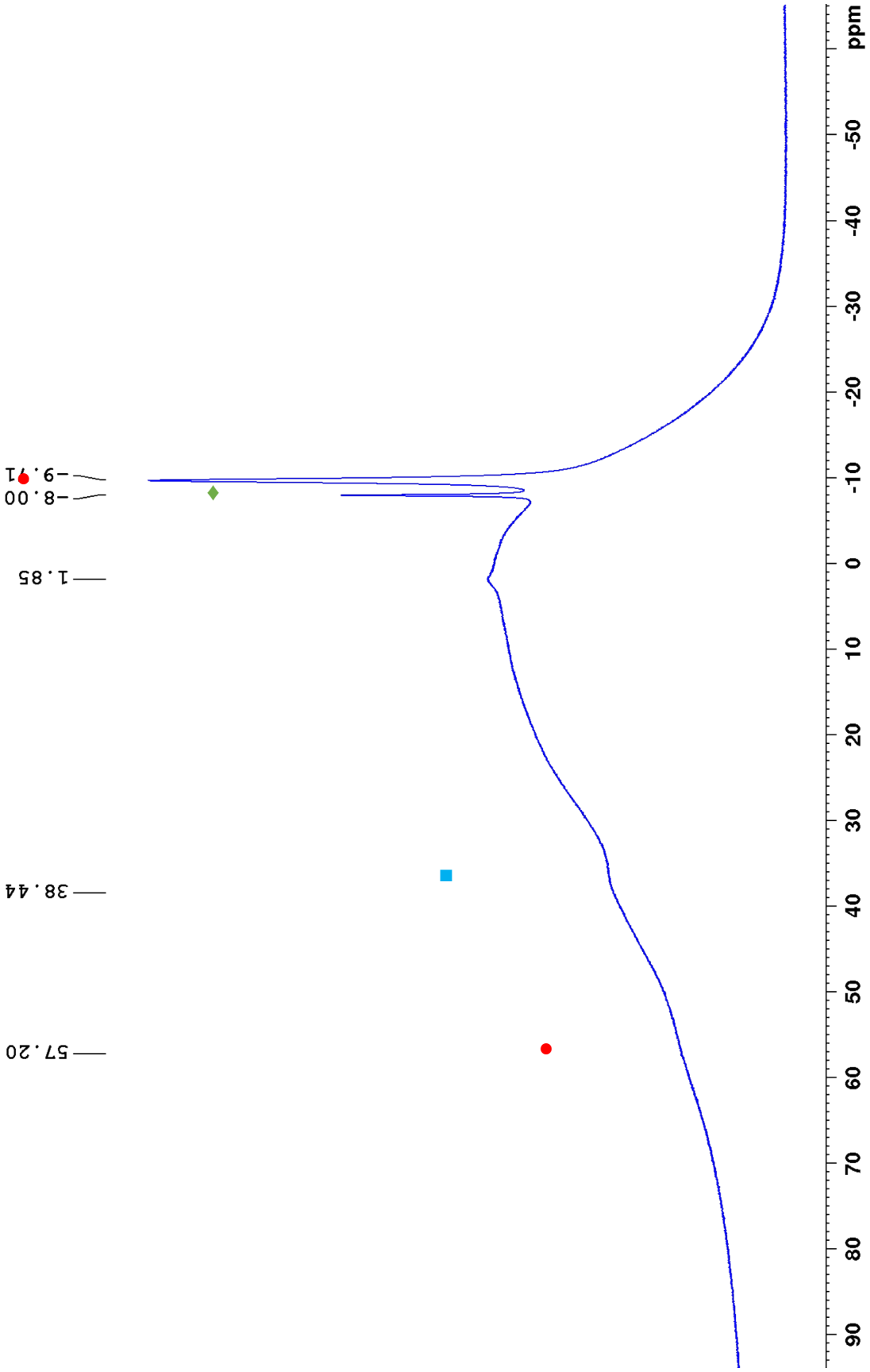

Figure S26. ^{19}F NMR spectrum of the **2a-Ph^{CF3}** (●) / **2b-Ph^{CF3}** (♦) / **3-Ph^{CF3}** (■) in C_6D_6.

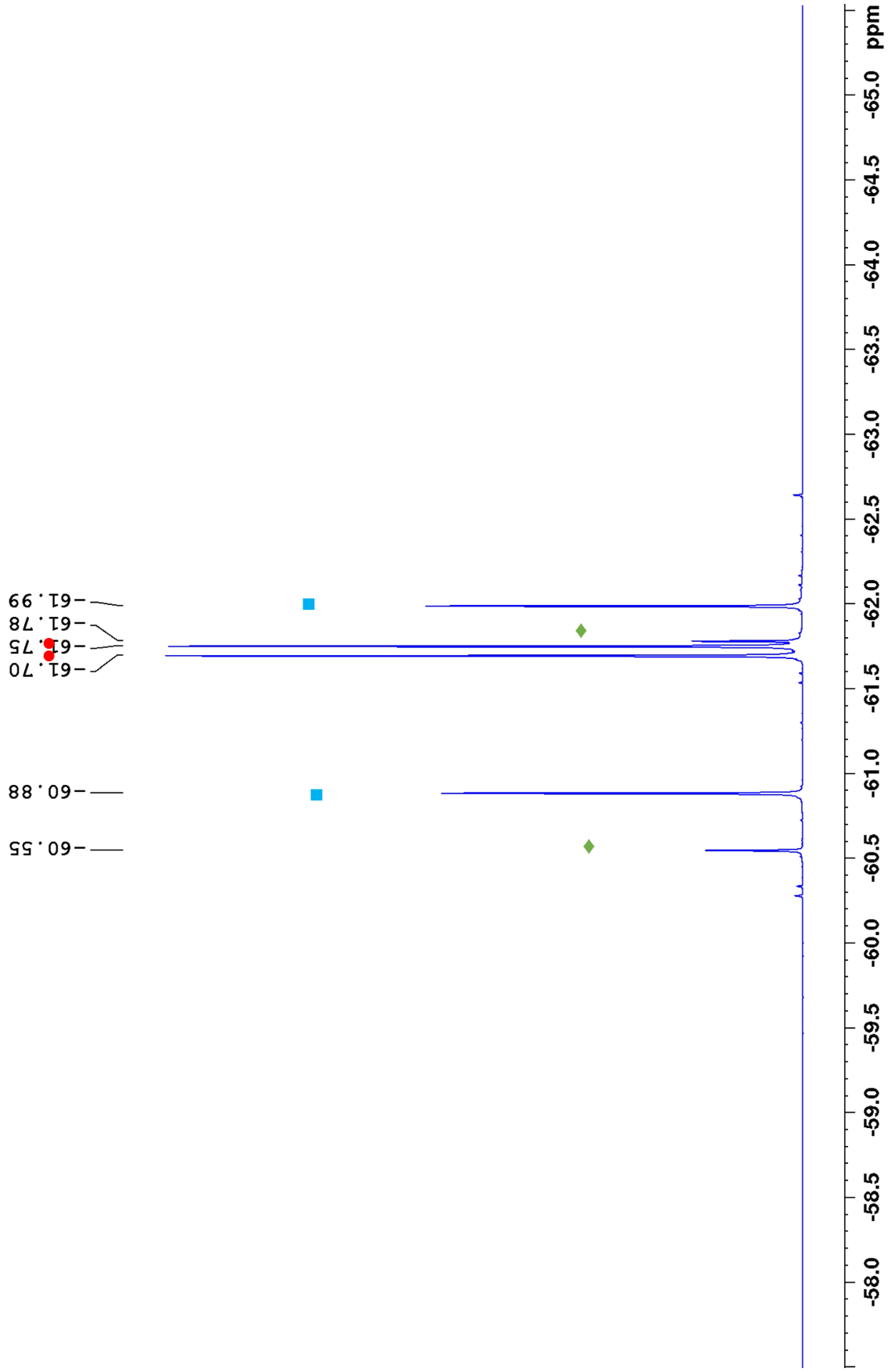

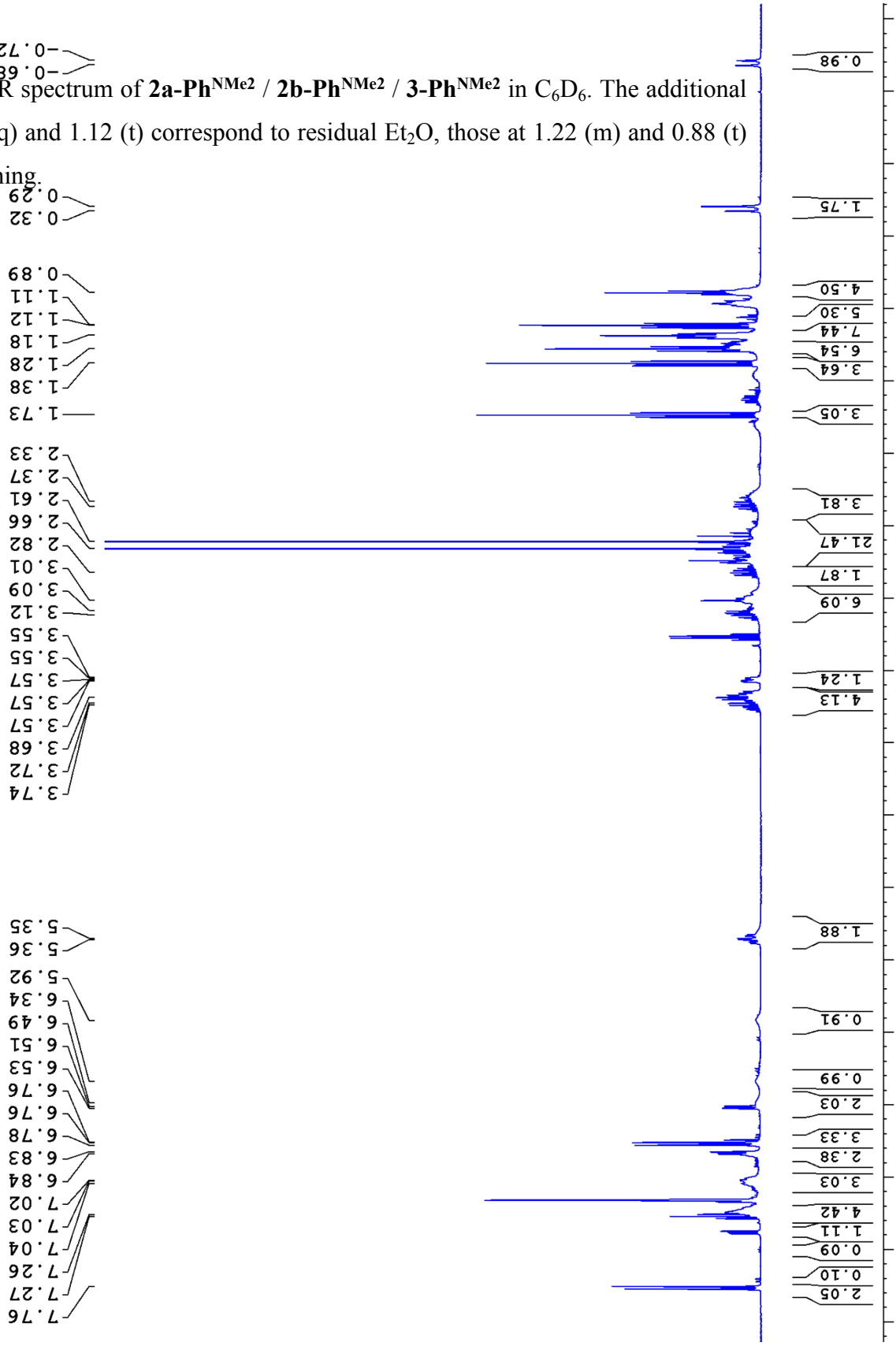

Figure S27. ^{1}H NMR spectrum of **2a-Ph^{NMe2}** / **2b-Ph^{NMe2}** / **3-Ph^{NMe2}** in C_6D_6. The additional resonances at 3.27 (q) and 1.12 (t) correspond to residual Et_2O, those at 1.22 (m) and 0.88 (t) to hexane from washing.

Figure S28. Annotated ^{1}H NMR spectrum of **2a-Ph^{NMe2}** (●) / **2b-Ph^{NMe2}** (♦) / **3-Ph^{NMe2}** (■) in the 3.5 to 8.0 ppm region.

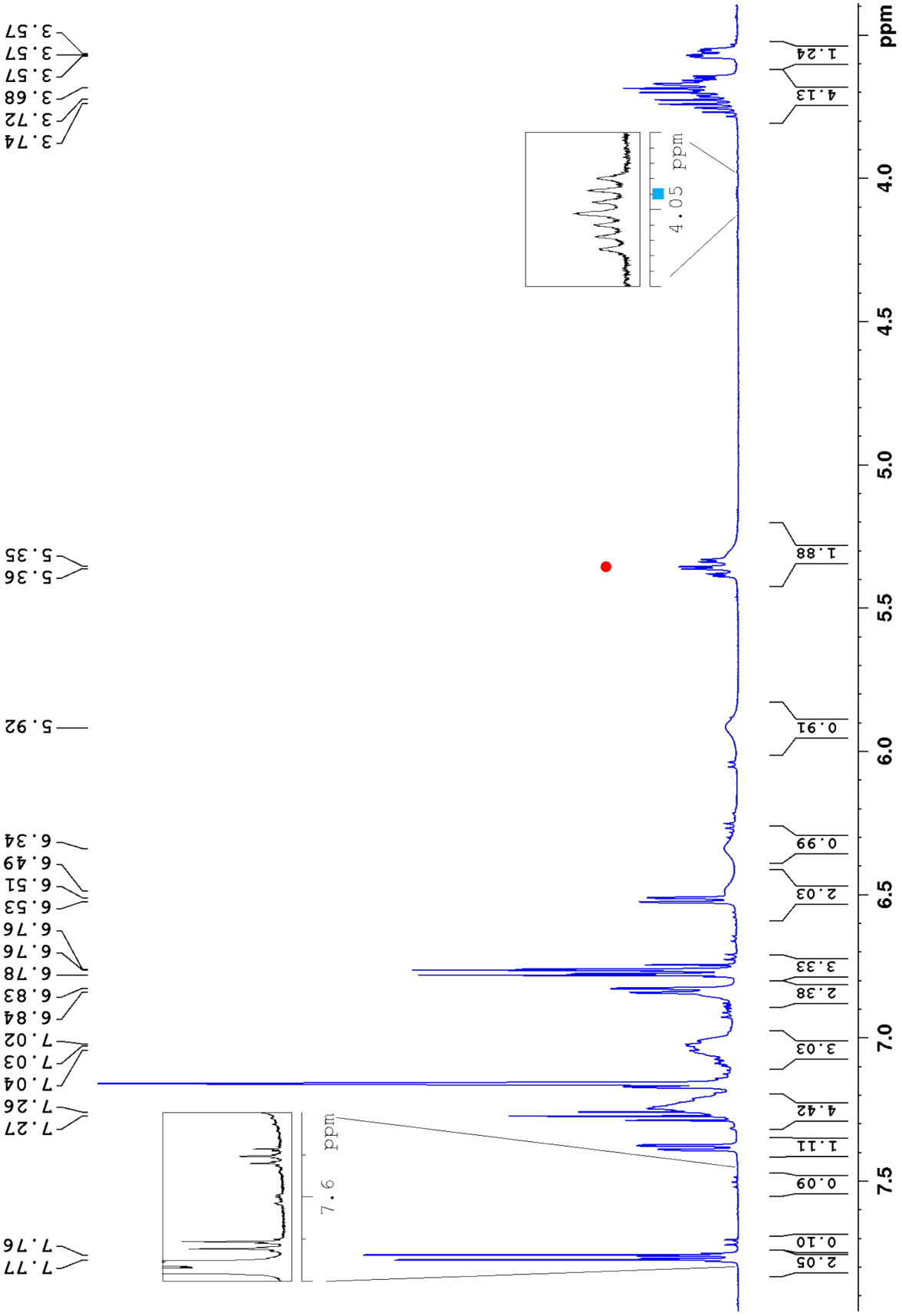

Figure S29. Annotated ^{1}H NMR spectrum of **2a-Ph^{NMe2}** (●) / **2b-Ph^{NMe2}** (♦) / **3-Ph^{NMe2}** (■) in the –1.0 to 3.2 ppm region.

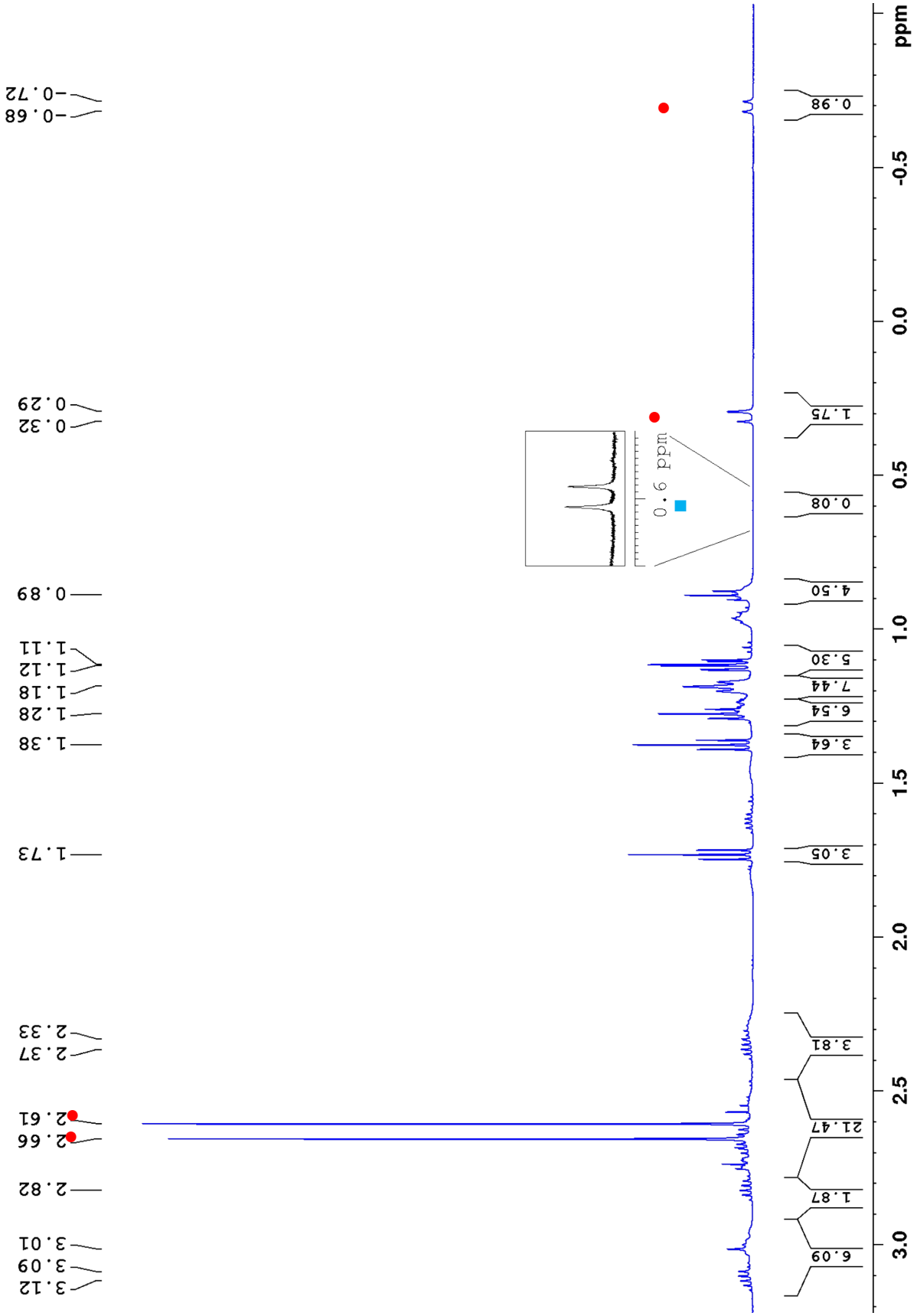

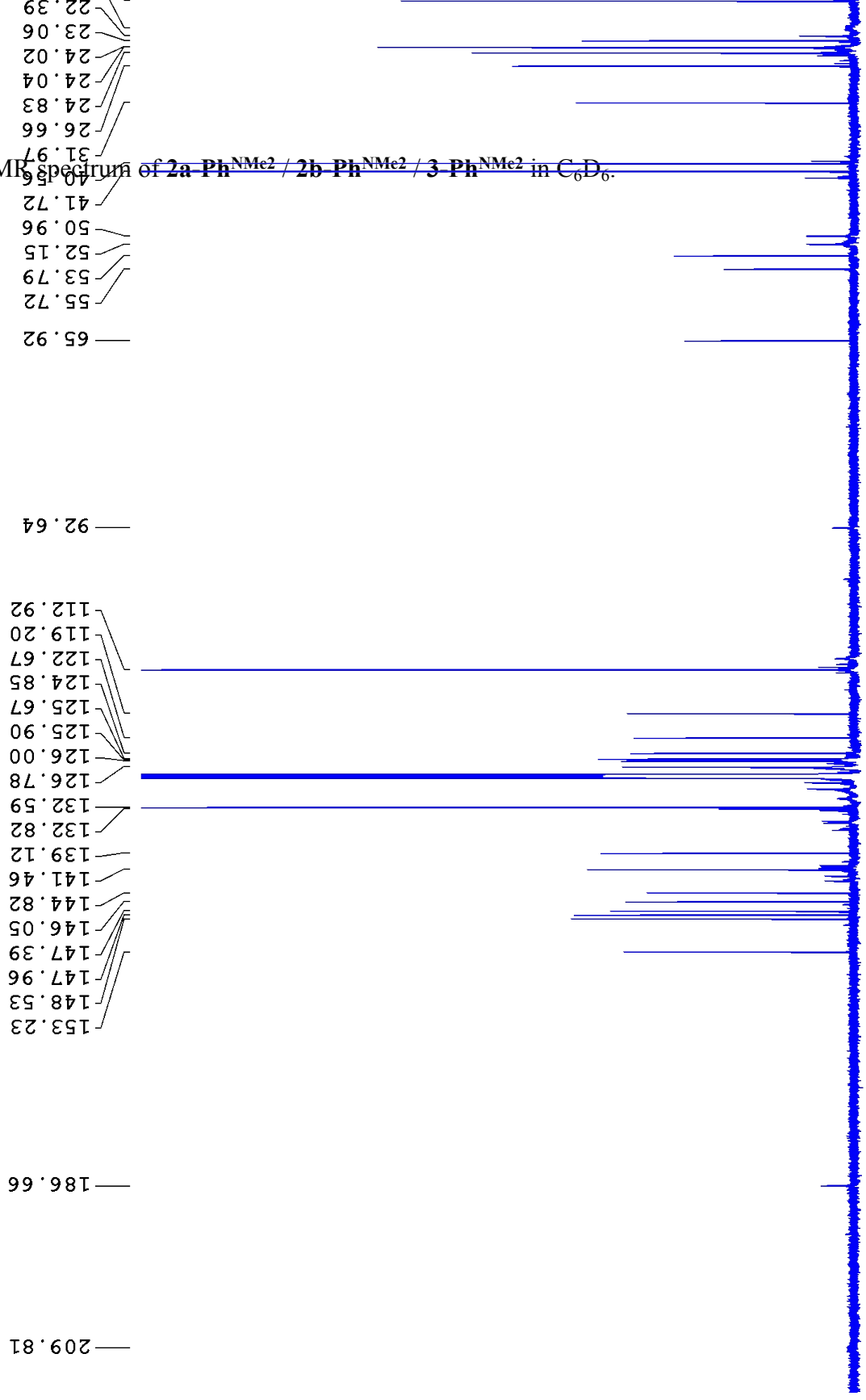

Figure S30. $^{13}C\{^{1}H\}$ NMR spectrum of **2a-Ph^{NMe2}** / **2b-Ph^{NMe2}** / **3-Ph^{NMe2}** in C_6D_6.

Figure S31. HSQC plot of **2a-Ph^{NMe2}** / **2b-Ph^{NMe2}** / **3-Ph^{NMe2}** in C_6D_6.

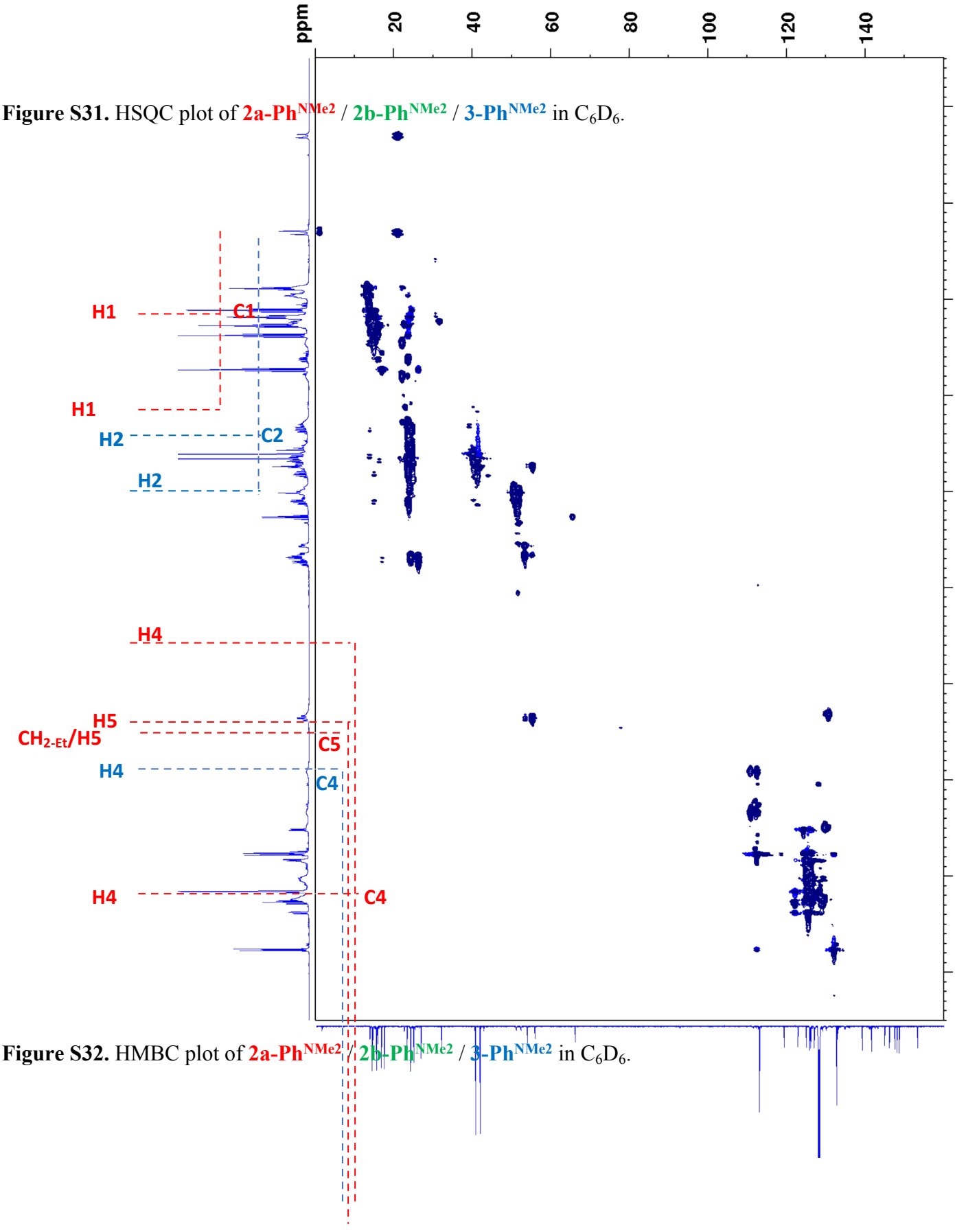

Figure S32. HMBC plot of **2a-Ph^{NMe2}** / **2b-Ph^{NMe2}** / **3-Ph^{NMe2}** in C_6D_6.

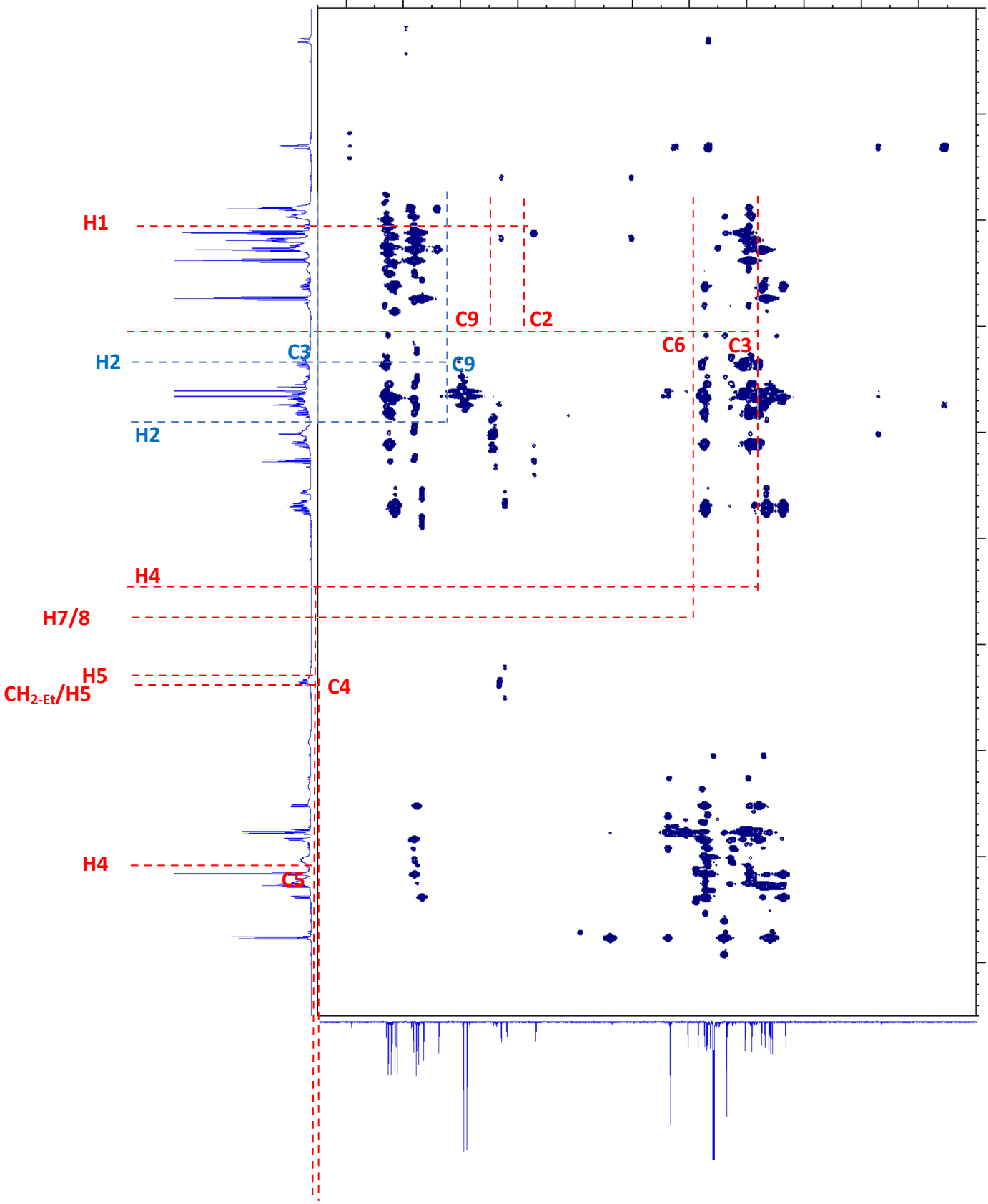
H1
C9
C2
H2
C3
C9
C6
C3
H2
H4
H7/8
H5
CH2-Et/H5
C4
H4
C5

Figure S33. ^{11}B NMR spectrum of **2a-Ph^{NMe2}** (●) / **2b-Ph^{NMe2}** (♦) / **3-Ph^{NMe2}** (■) in C_6D_6.

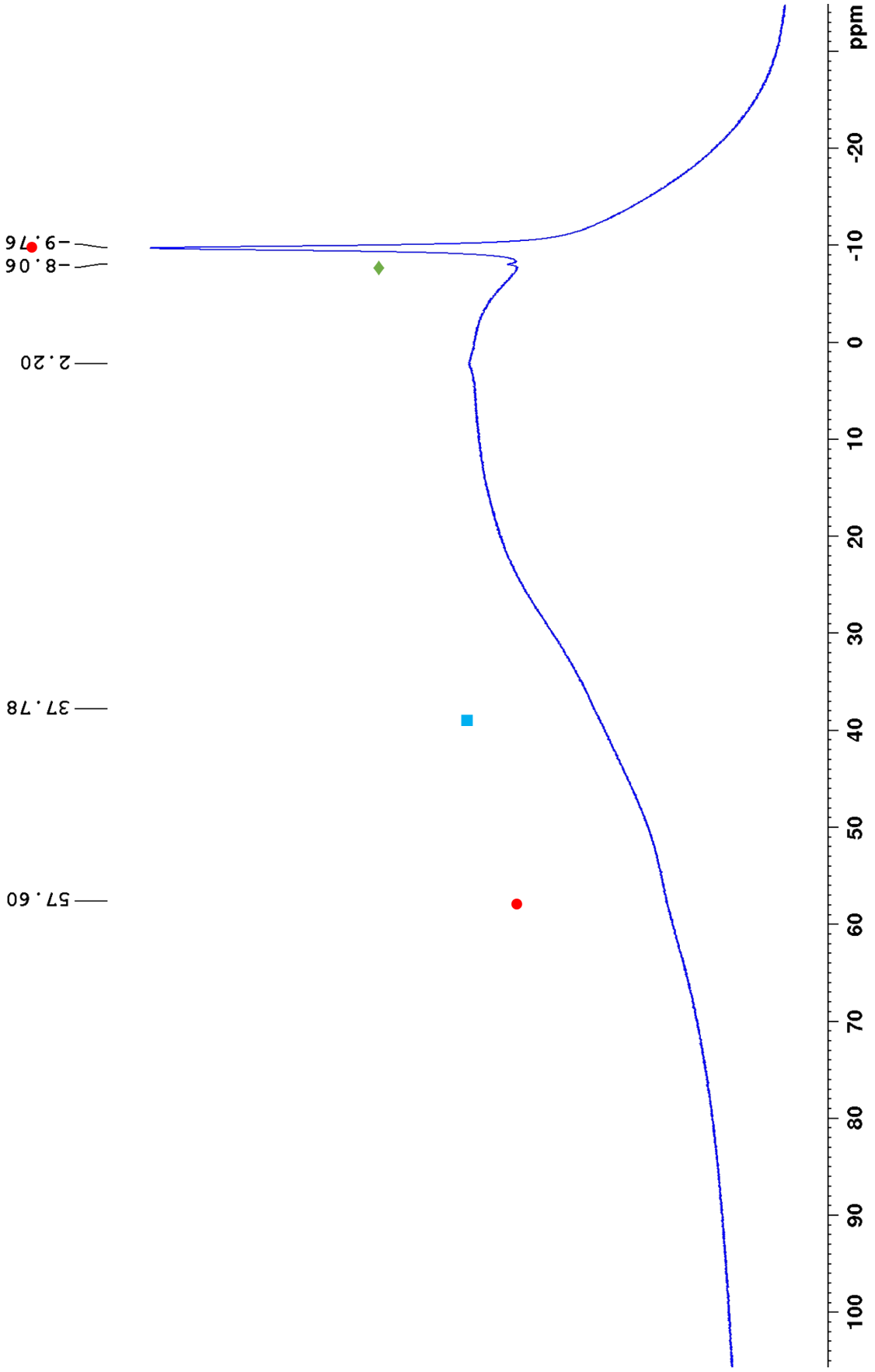

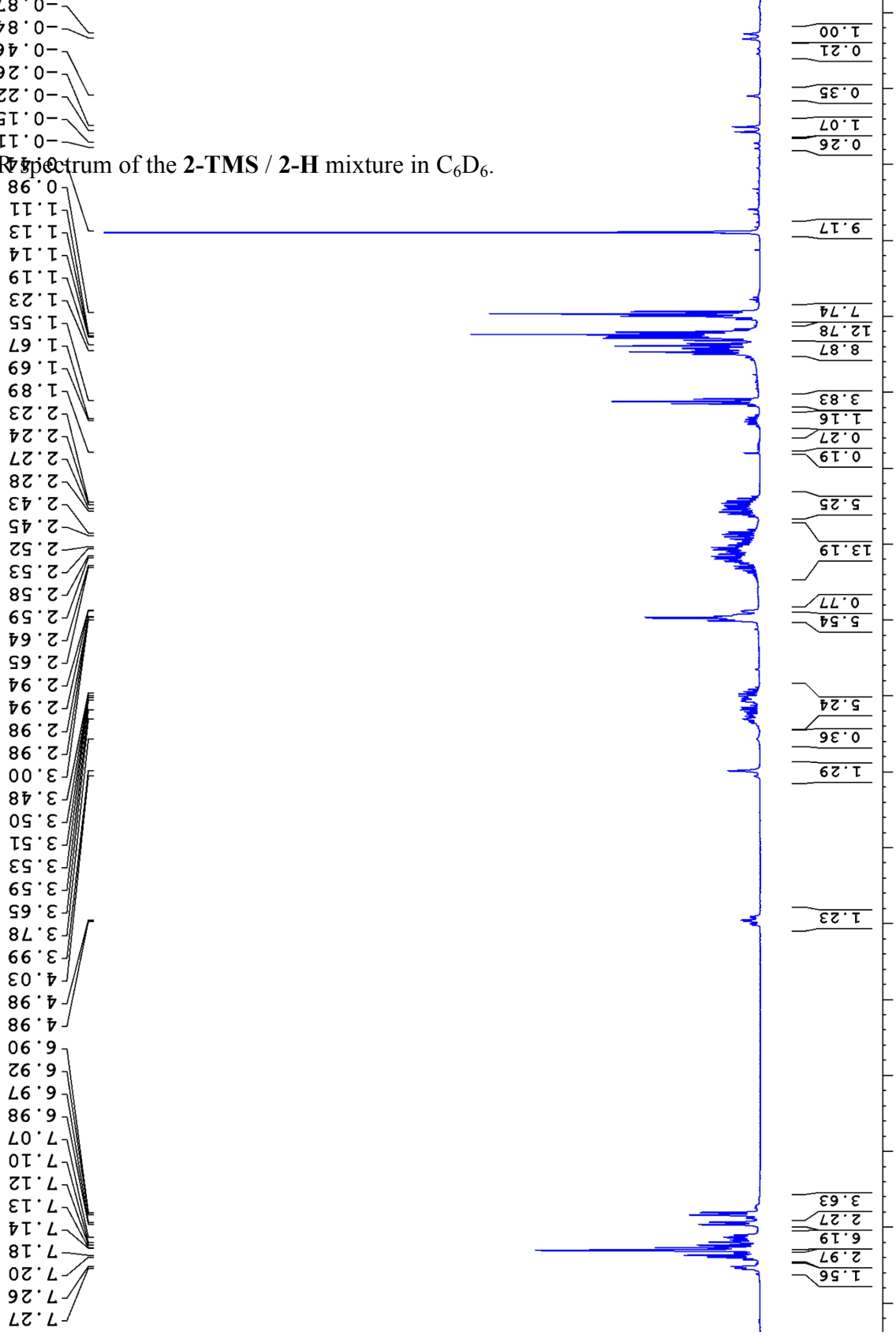

Figure S34. ^{1}H NMR spectrum of the **2-TMS** / **2-H** mixture in C_6D_6.

Figure S35. Overlay of th
between **1** and trimethlysil

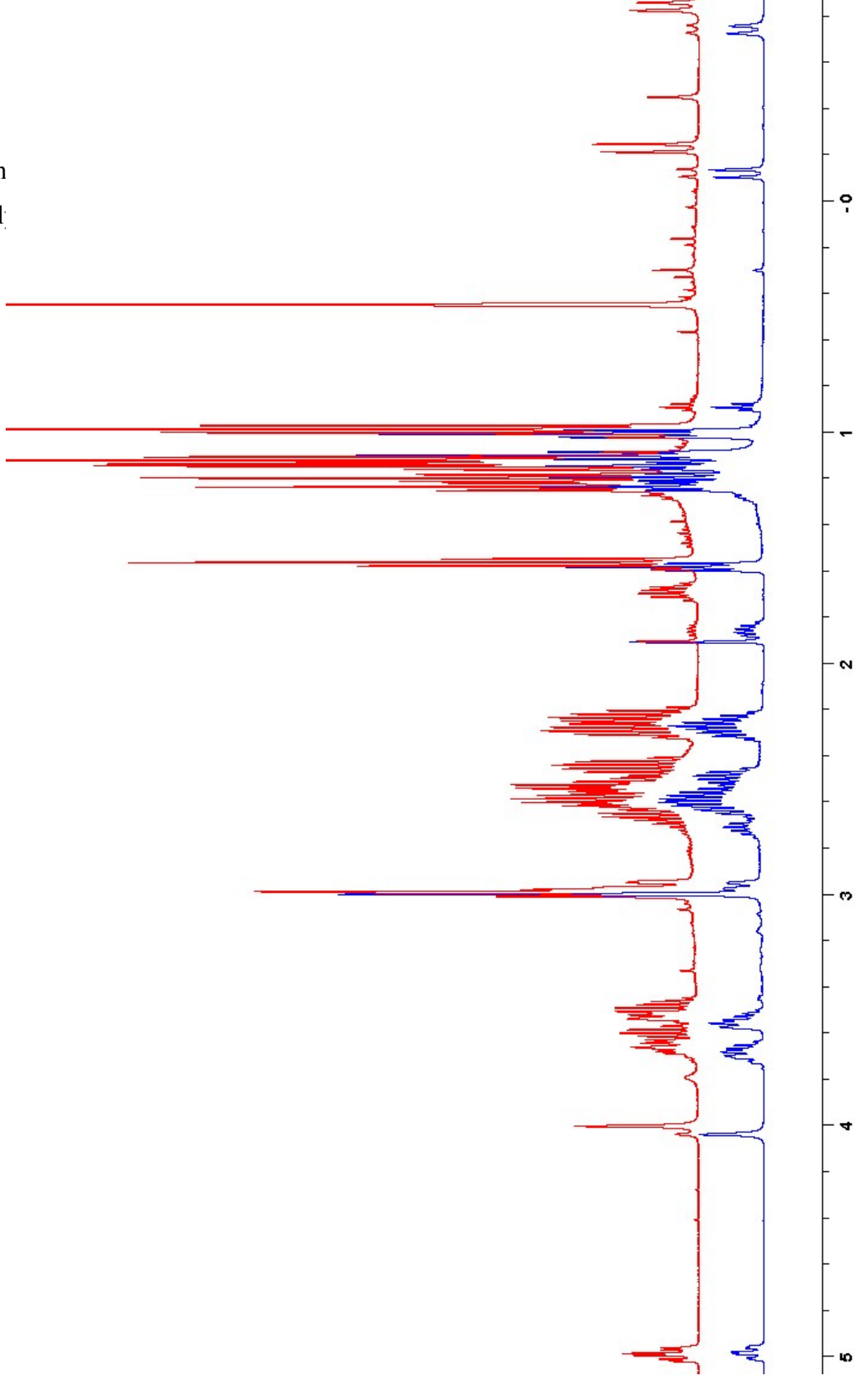

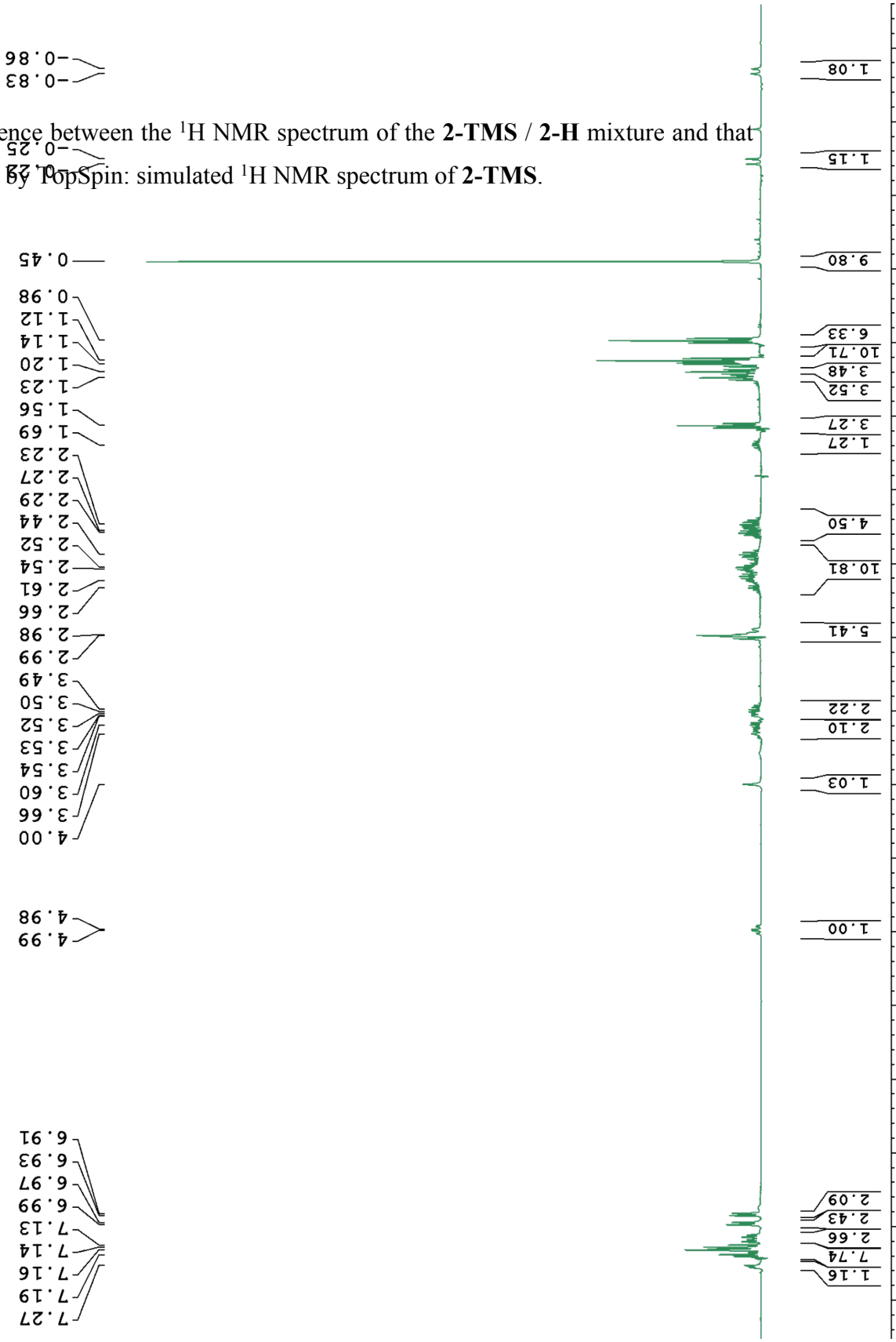

Figure S36. Difference between the ^{1}H NMR spectrum of the **2-TMS** / **2-H** mixture and that of pure **2-H** plotted by TopSpin: simulated ^{1}H NMR spectrum of **2-TMS**.

Figure S37. ^{1}H NMR spectrum of the **2-TMS** (●) / **2-H** (♦) mixture in the 3.4 to 5.1 ppm region.

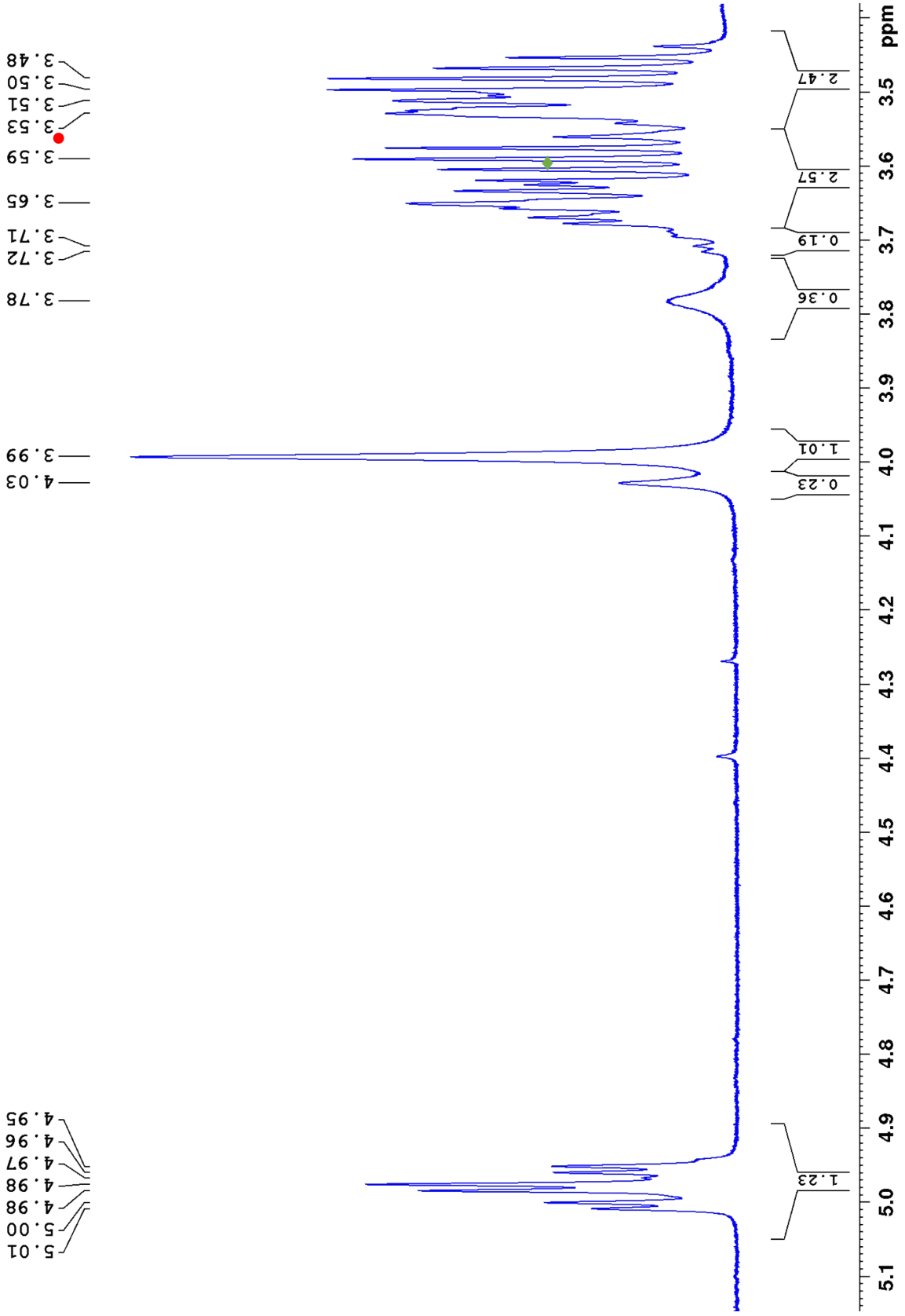

Figure S38. ^{1}H NMR spectrum of the **2-TMS** (●) / **2-H** (♦) mixture in the –1.0 to 2.0 ppm region.

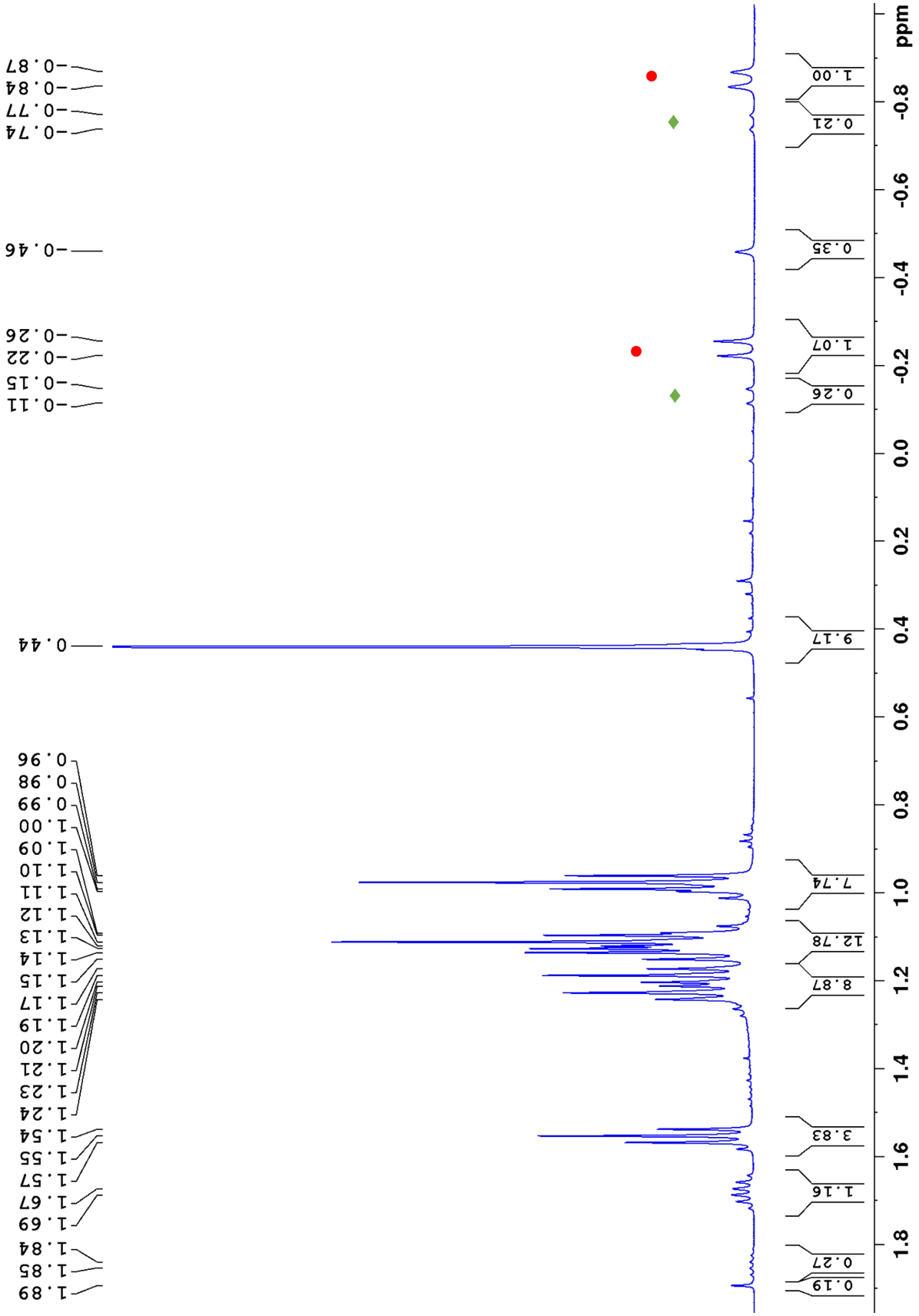

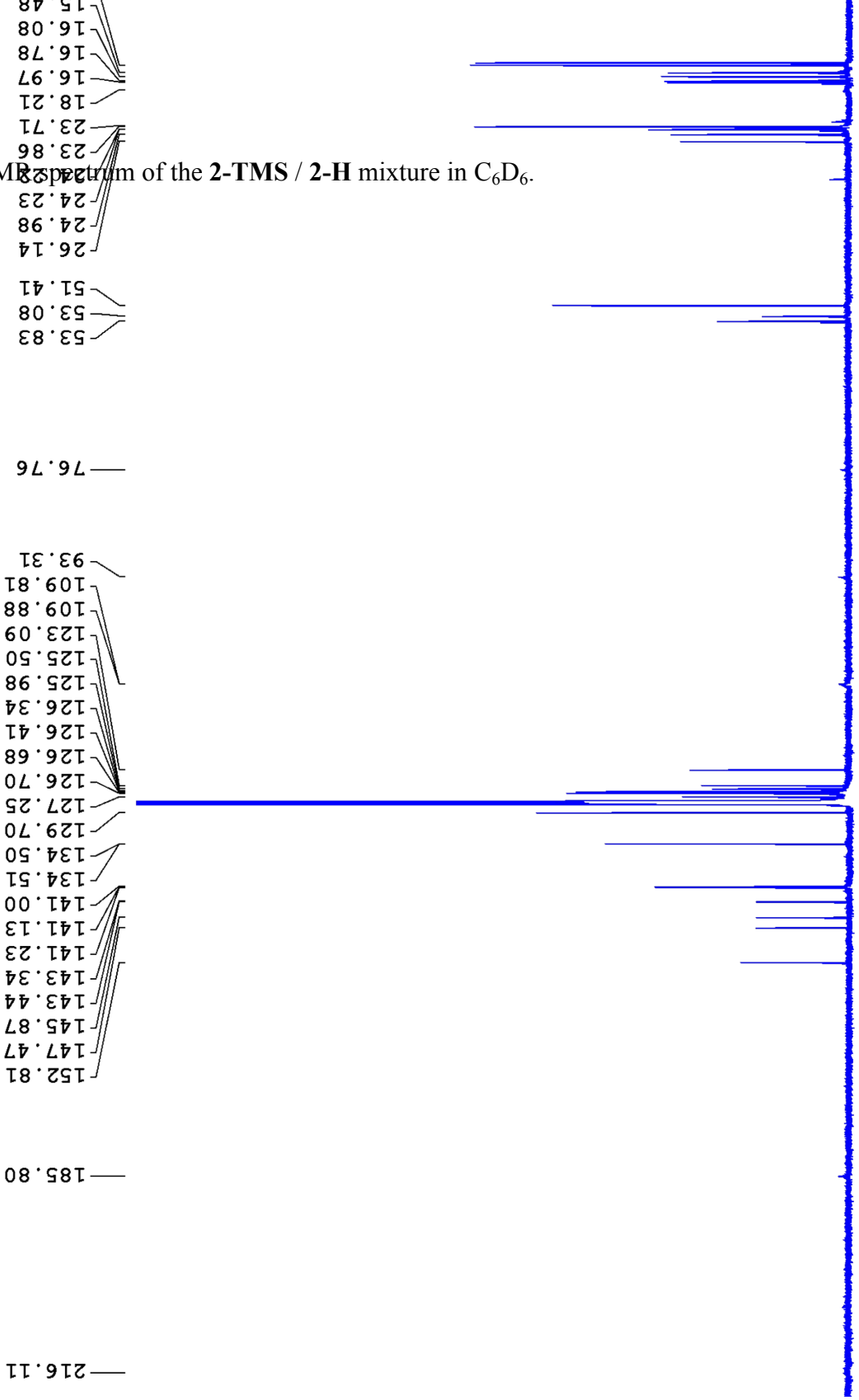

Figure S39. $^{13}C\{^{1}H\}$ NMR spectrum of the **2-TMS** / **2-H** mixture in C_6D_6.

Figure S40. HSQC plot of the **2-TMS** / **2-H** mixture in C_6D_6.

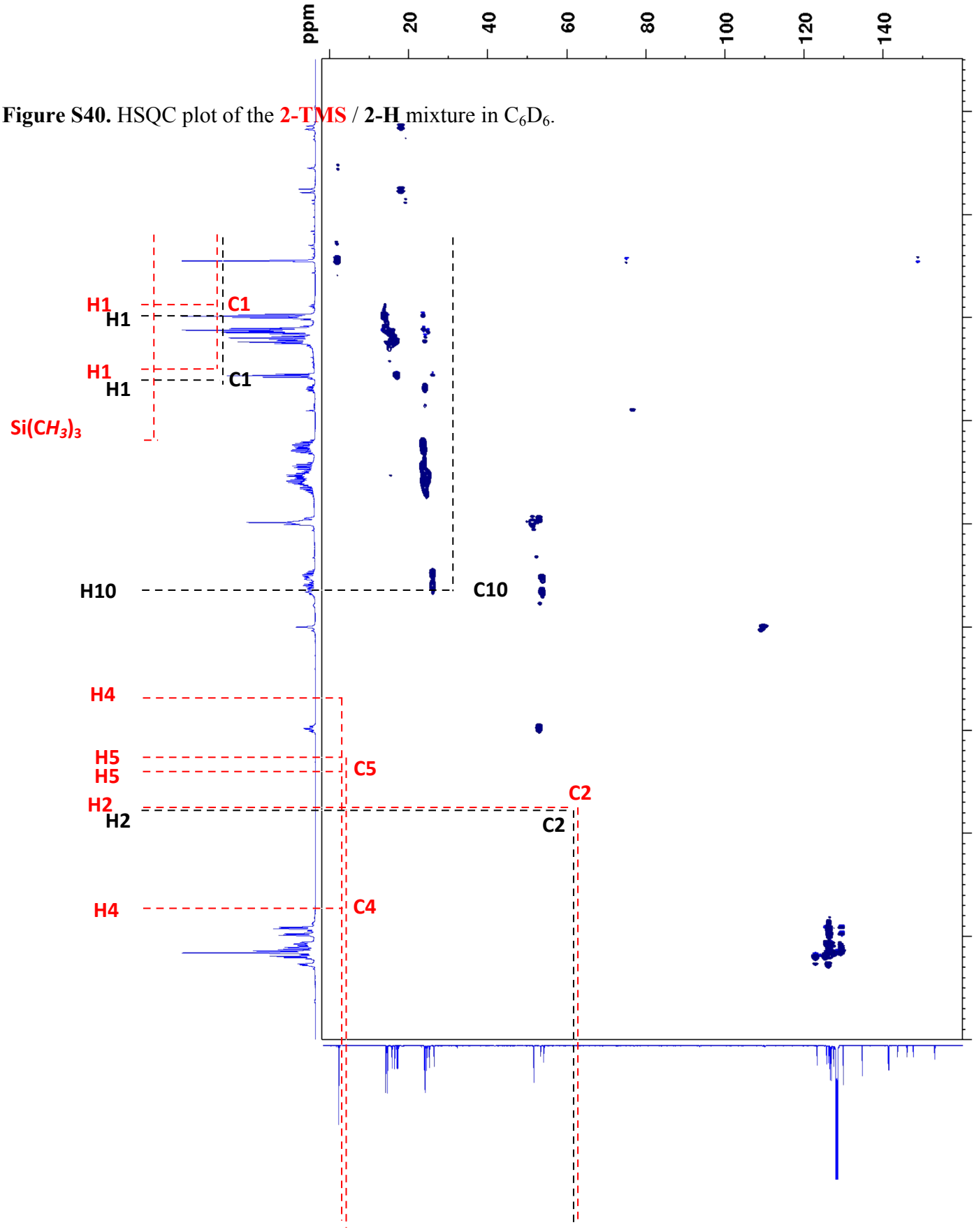

Figure S41. HMBC plot of the **2-TMS** / **2-H** mixture in C_6D_6.

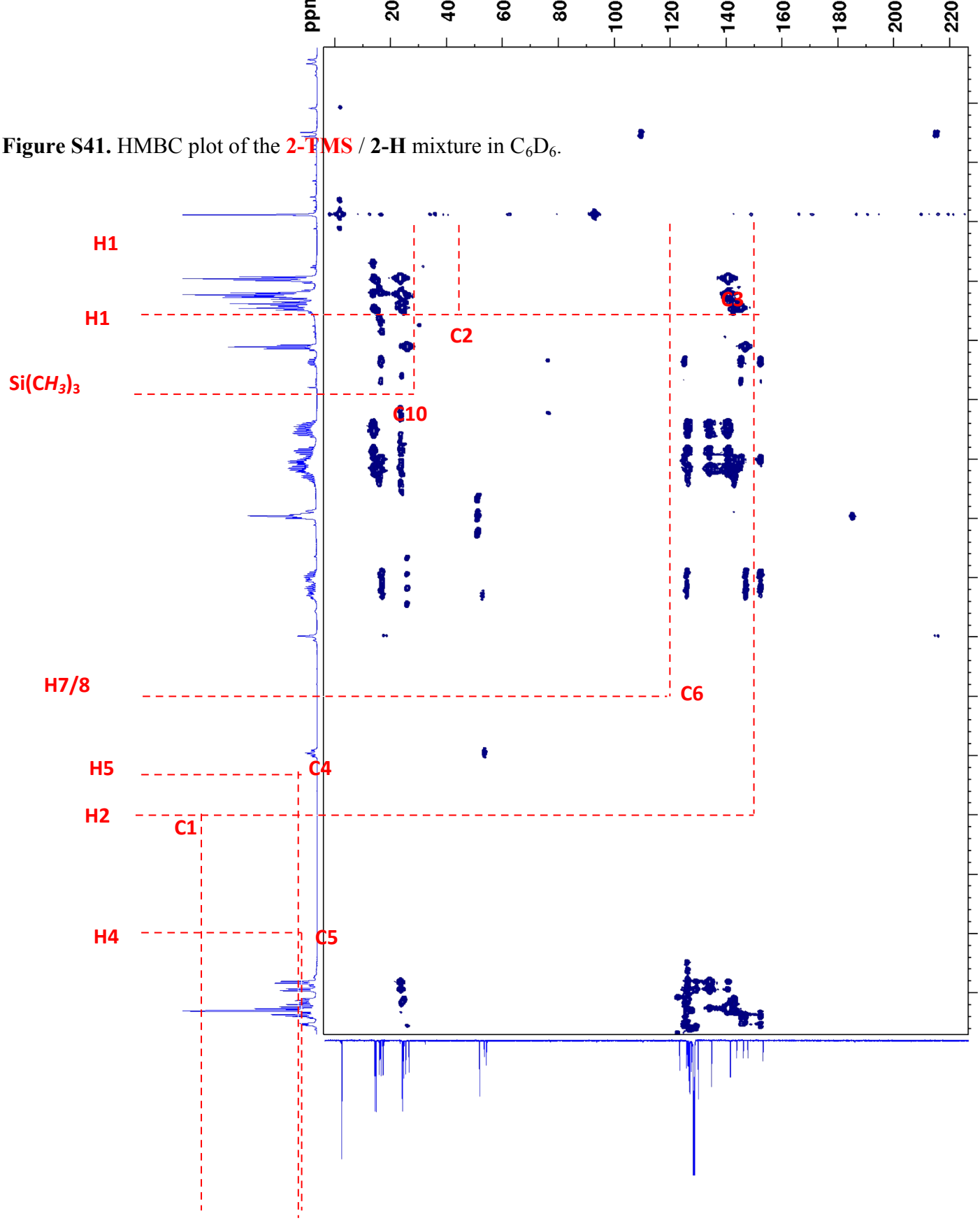

Figure S42. ^{11}B NMR spectrum of **2-TMS** / **2-H** in C_6D_6.

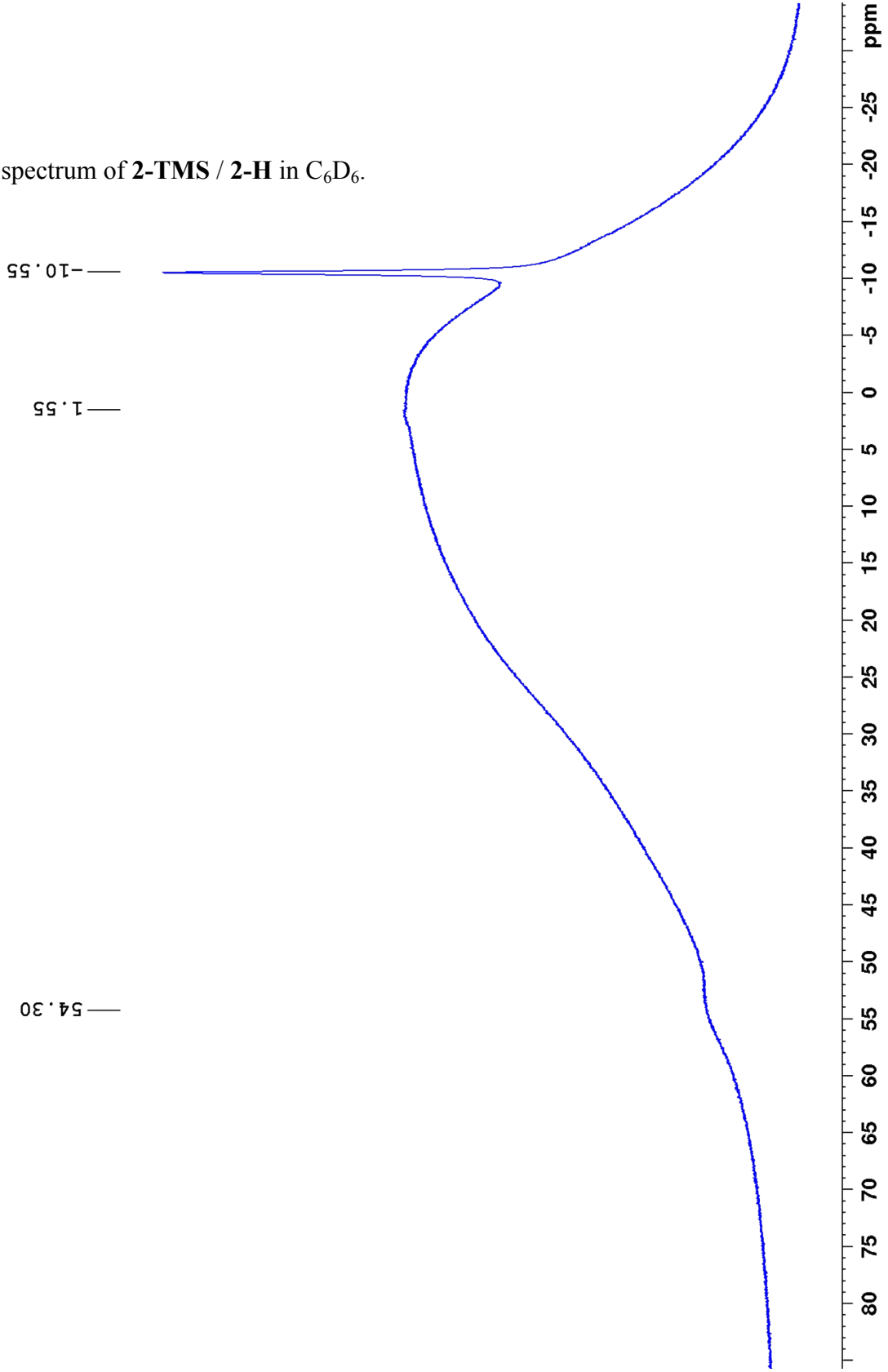

Figure S43. Annotated ^{1}H NMR spectrum of the reaction mixture of **1** + 80 equiv. $Me_3SiC{\equiv}CH$ after full consumption of **1** (18h, rt): **2-TMS** (●), **2-H** (♦).

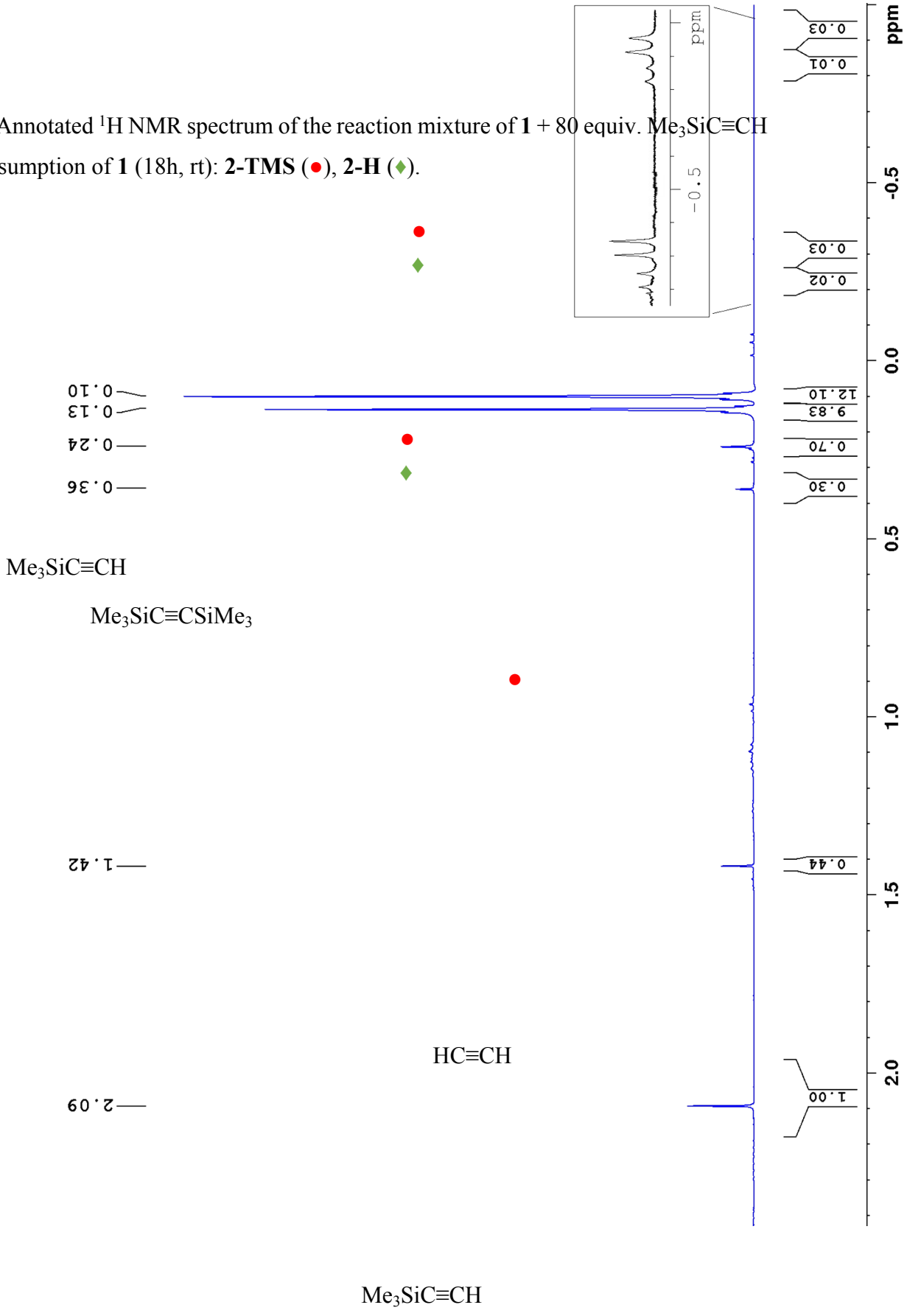

Figure S44. Overlay of the ^{29}Si NMR spectra of the reaction mixture of **1** + 80 equiv. $Me_3SiC{\equiv}CH$ after full consumption of **1** (red) and $Me_3SiC{\equiv}CSiMe_3$ (blue).

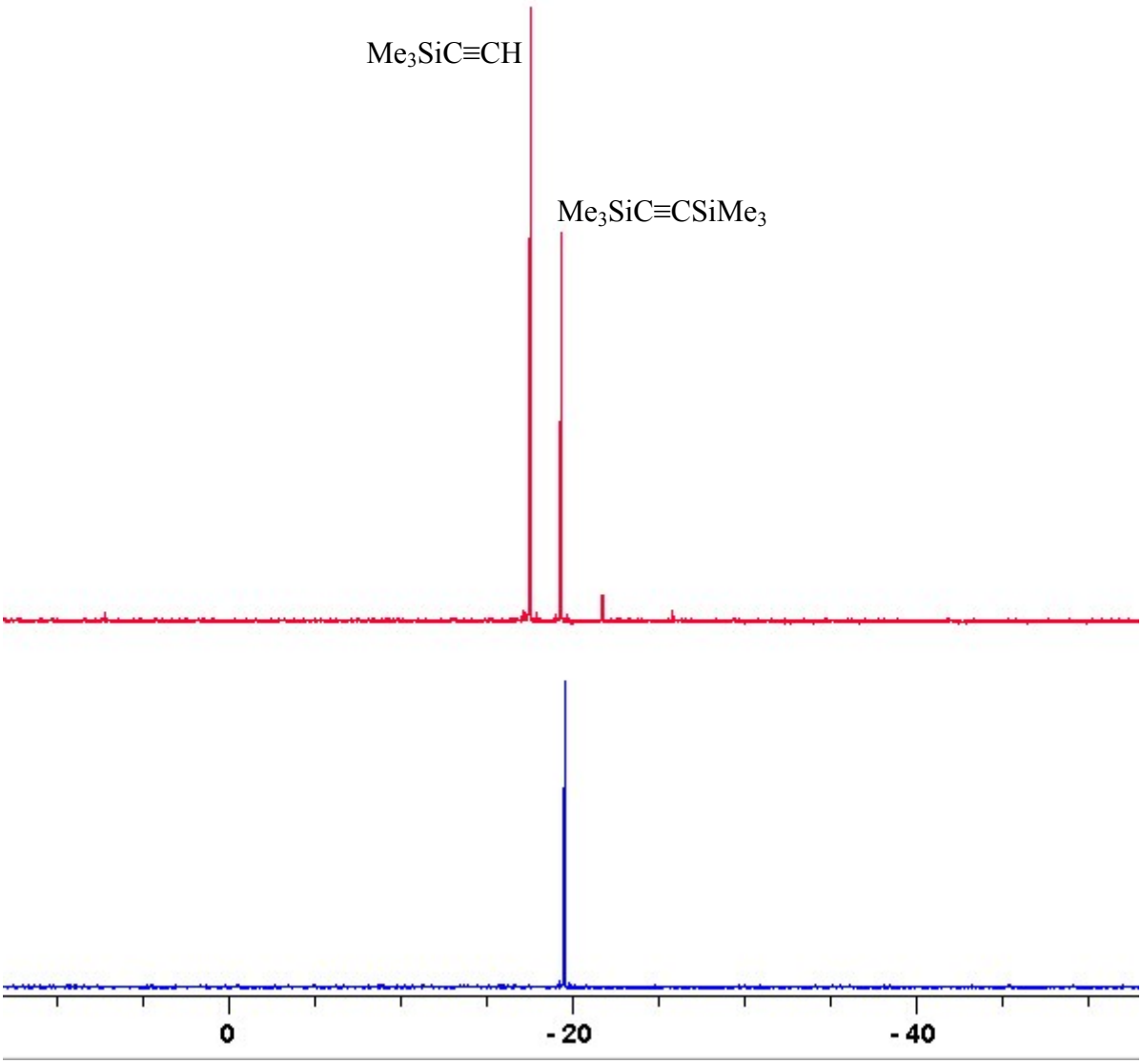

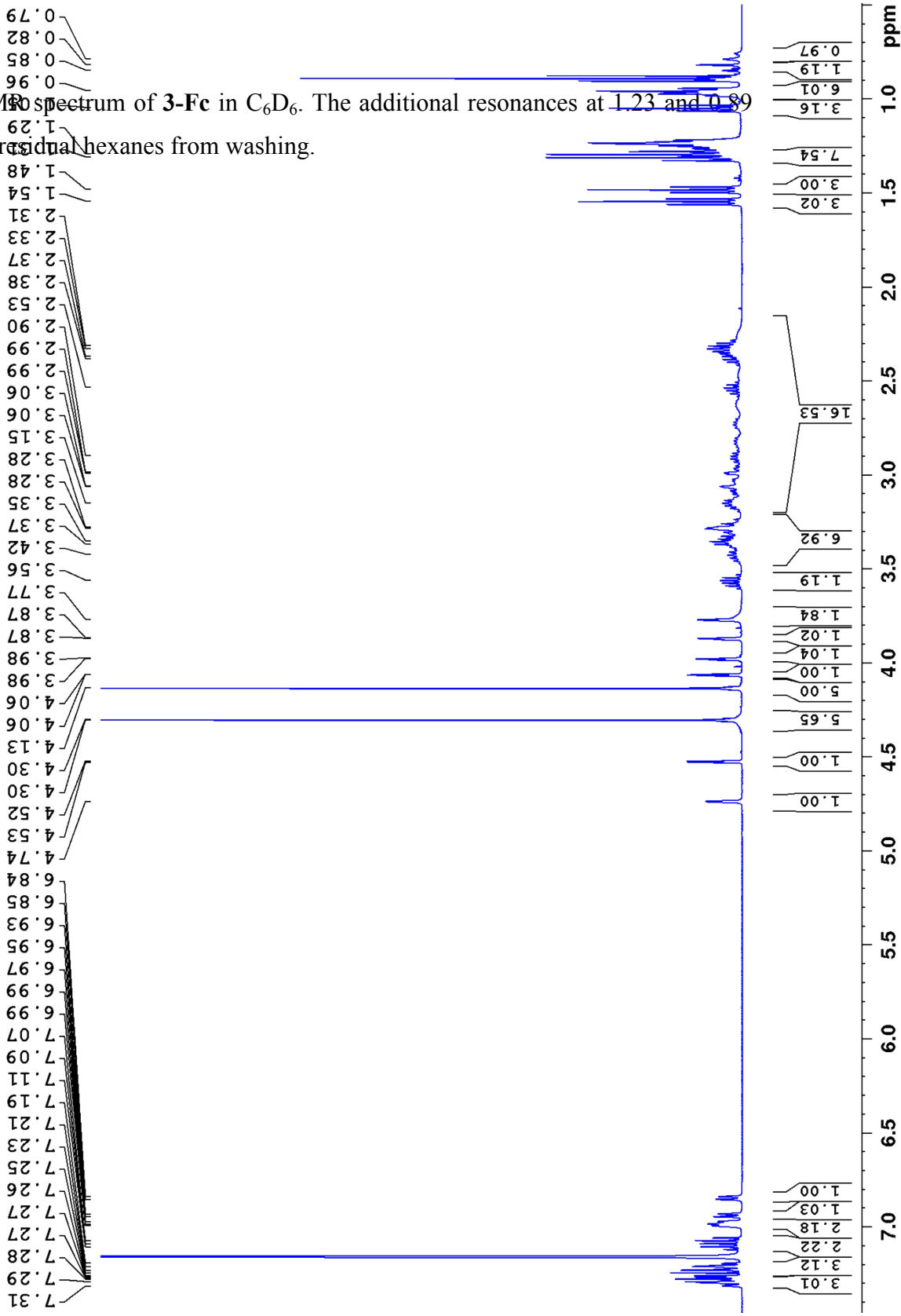

Figure S45. ^{1}H NMR spectrum of **3-Fc** in C_6D_6. The additional resonances at 1.23 and 0.89 ppm correspond to residual hexanes from washing.

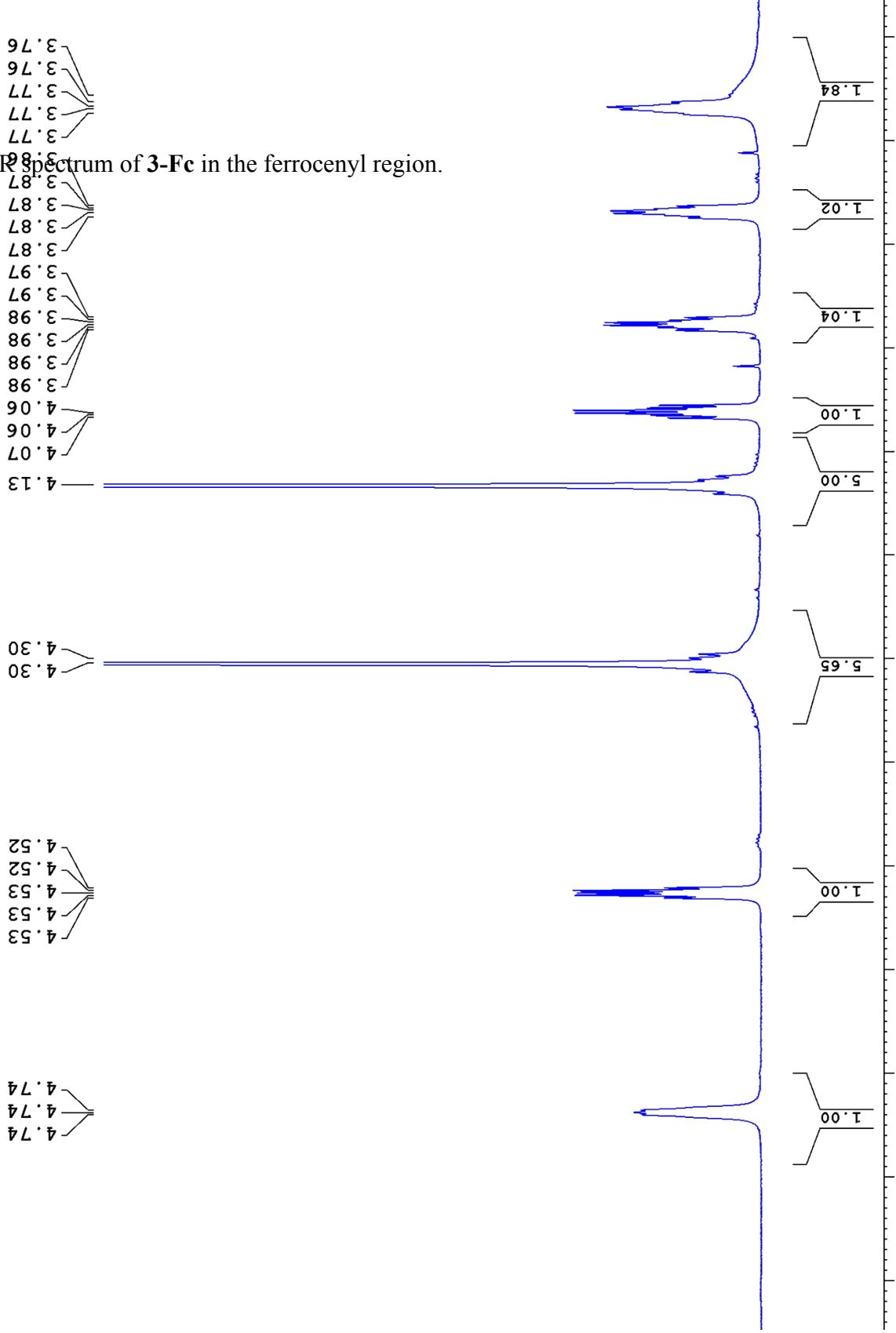

Figure S46. ^{1}H NMR spectrum of **3-Fc** in the ferrocenyl region.

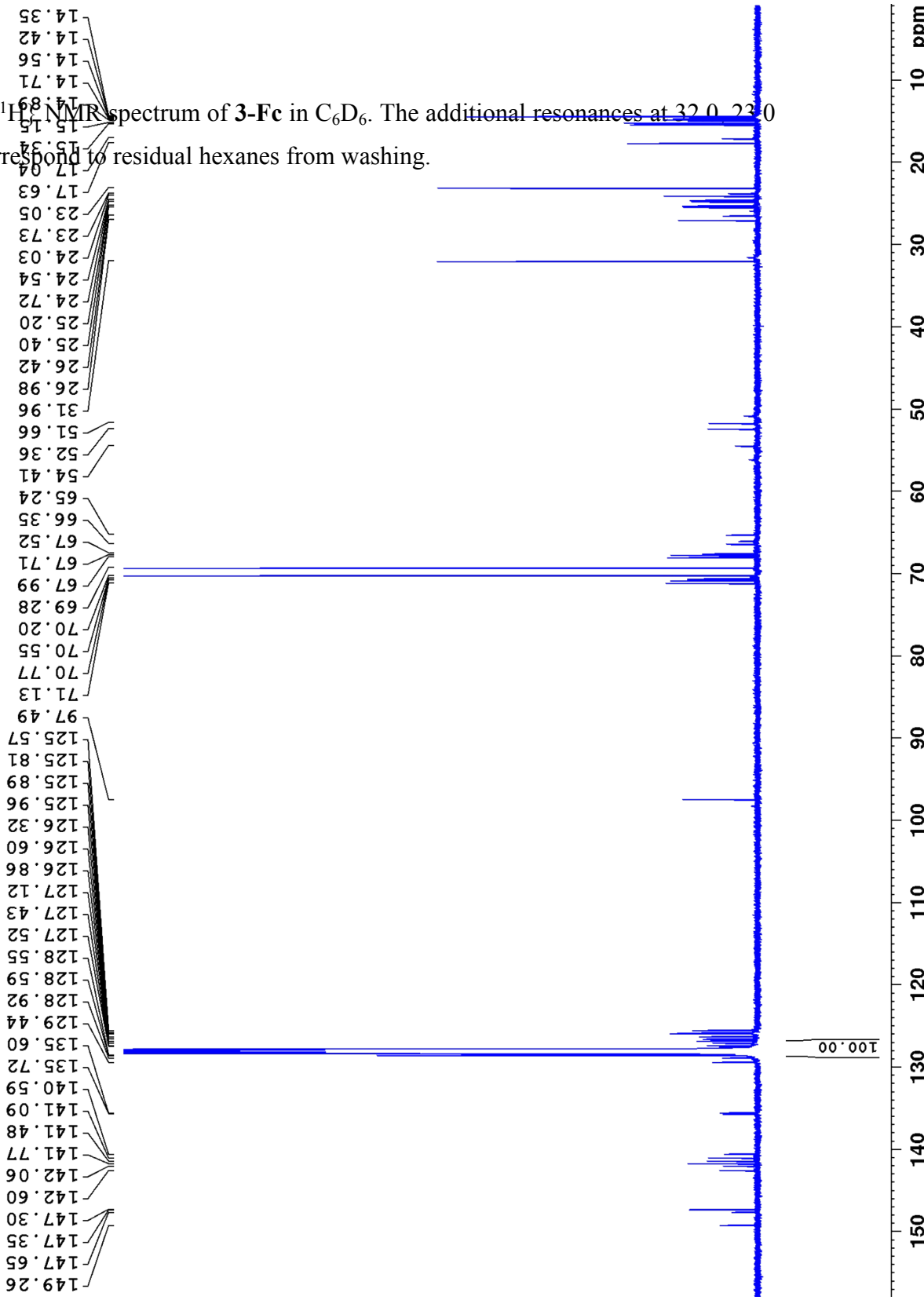

Figure S47. $^{13}C\{^{1}H\}$ NMR spectrum of **3-Fc** in C_6D_6. The additional resonances at 32.0, 23.0 and 14.3 ppm correspond to residual hexanes from washing.

Figure S48. HSQC plot of **3-Fc** in C_6D_6.

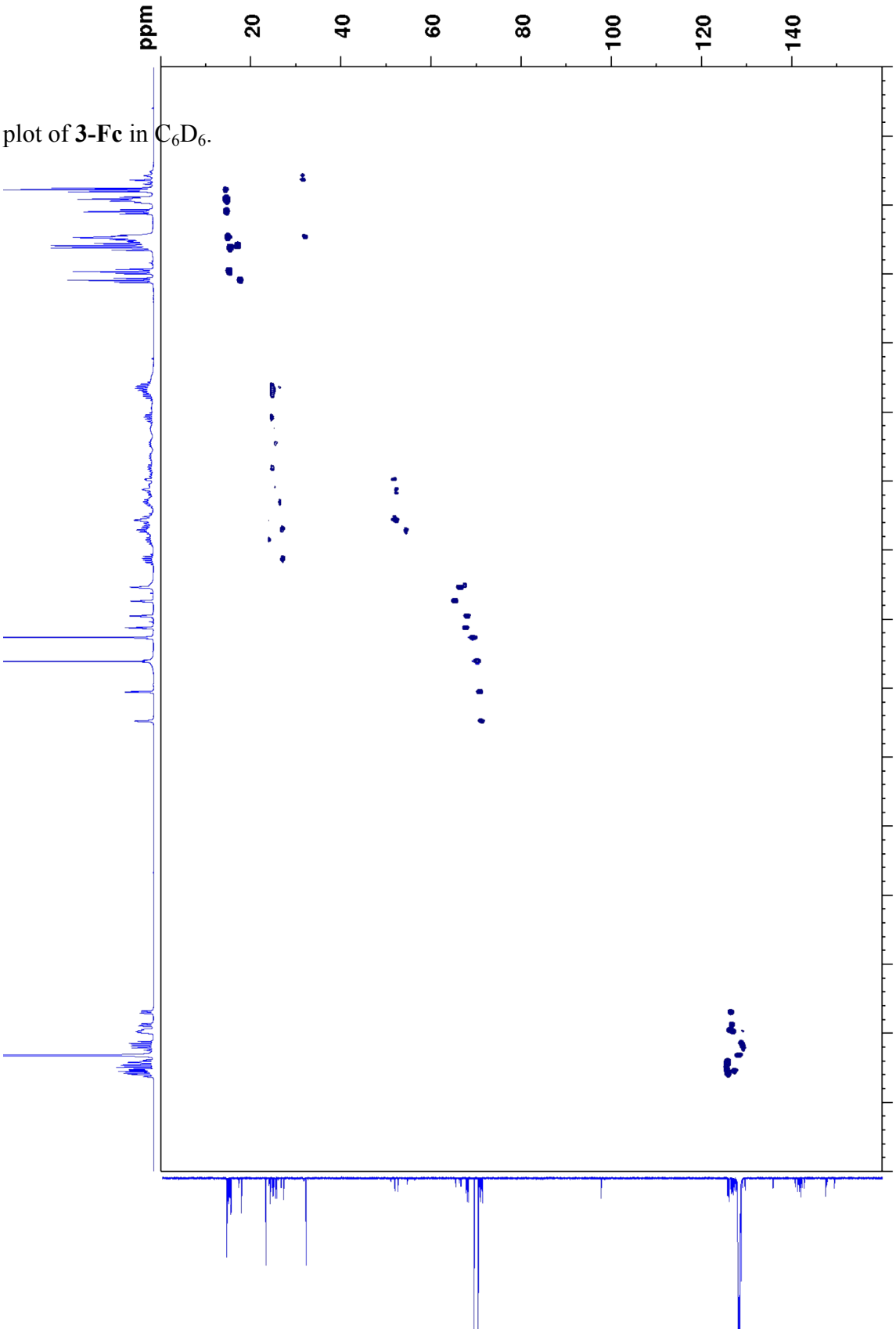

Figure S49. HMBC plot of **3-Fc** in C_6D_6.

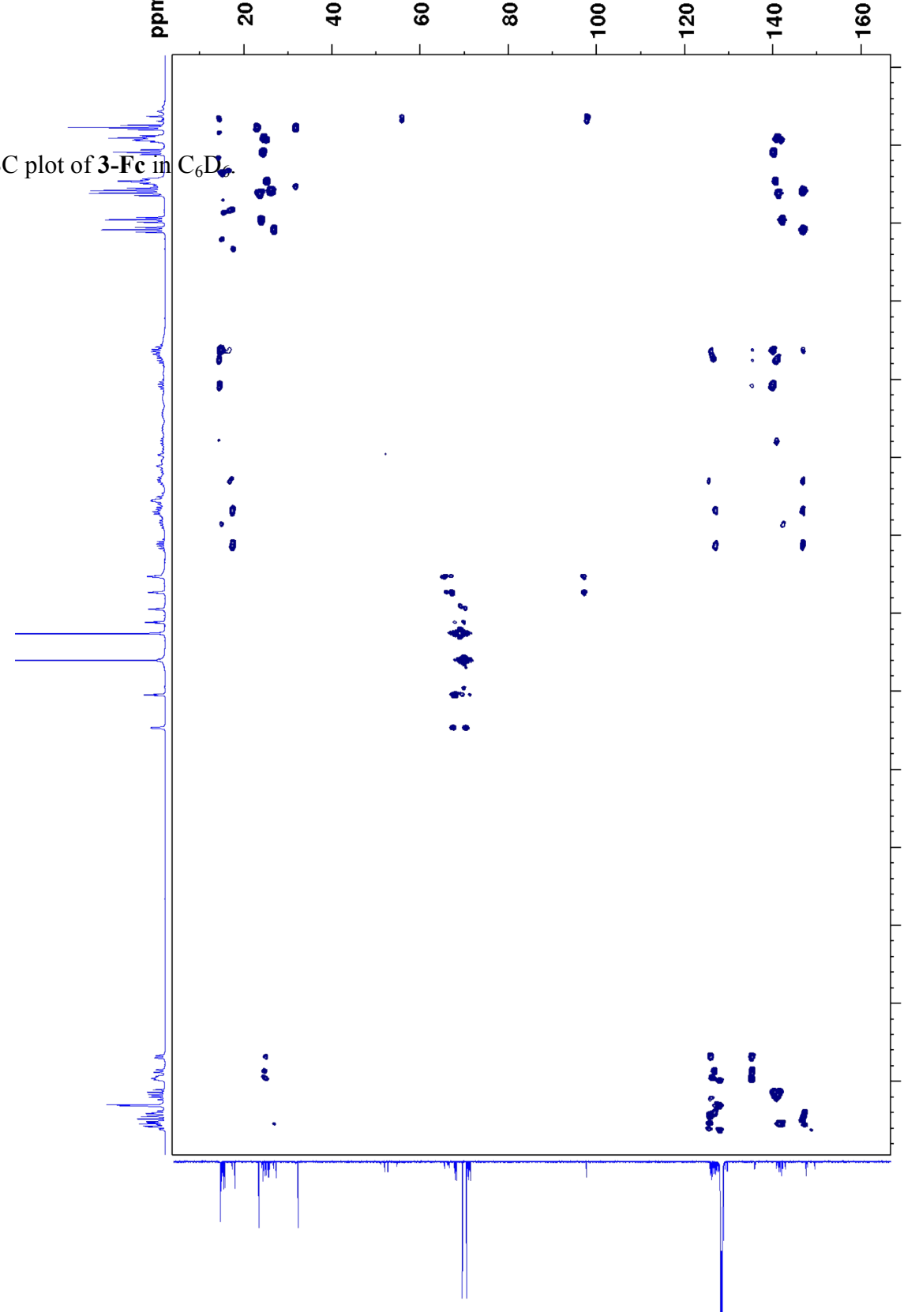

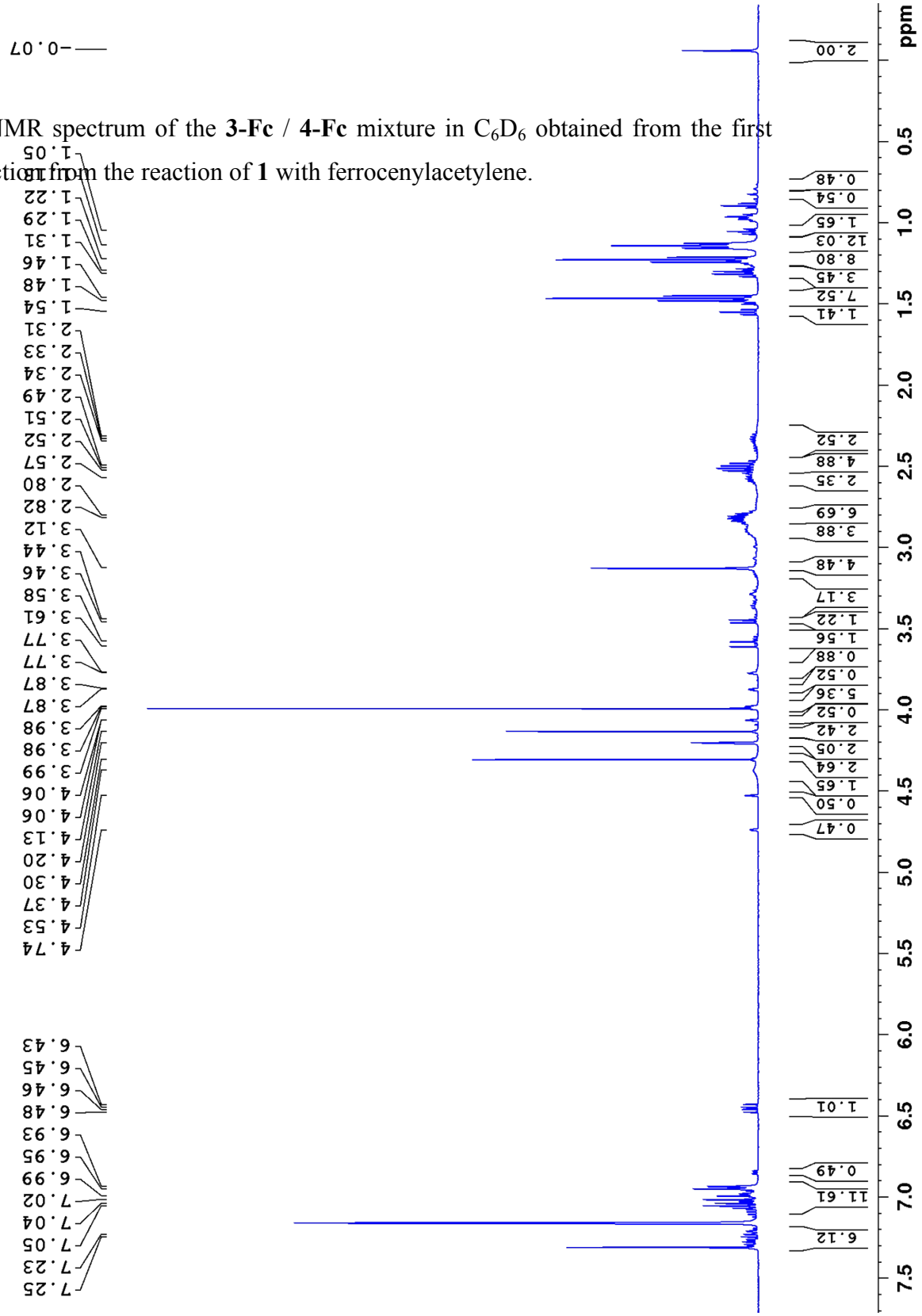

Figure S50. ^{1}H NMR spectrum of the **3-Fc** / **4-Fc** mixture in C_6D_6 obtained from the first crystallization fraction from the reaction of **1** with ferrocenylacetylene.

Figure S51. Overlay c
between **1** and trimeth
Fc.

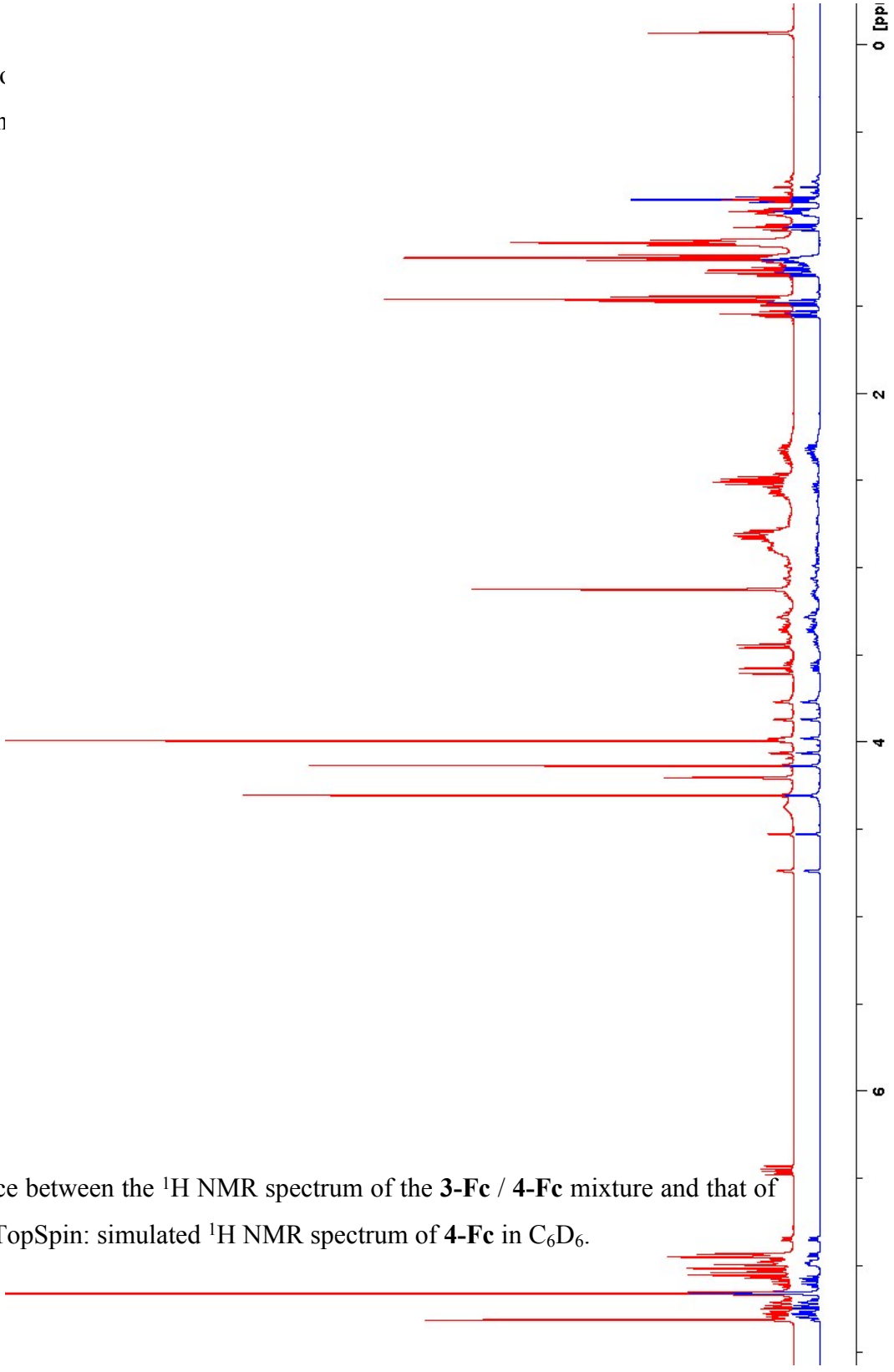

Figure S52. Difference between the ^{1}H NMR spectrum of the **3-Fc** / **4-Fc** mixture and that of pure **3-Fc** plotted by TopSpin: simulated ^{1}H NMR spectrum of **4-Fc** in C_6D_6.

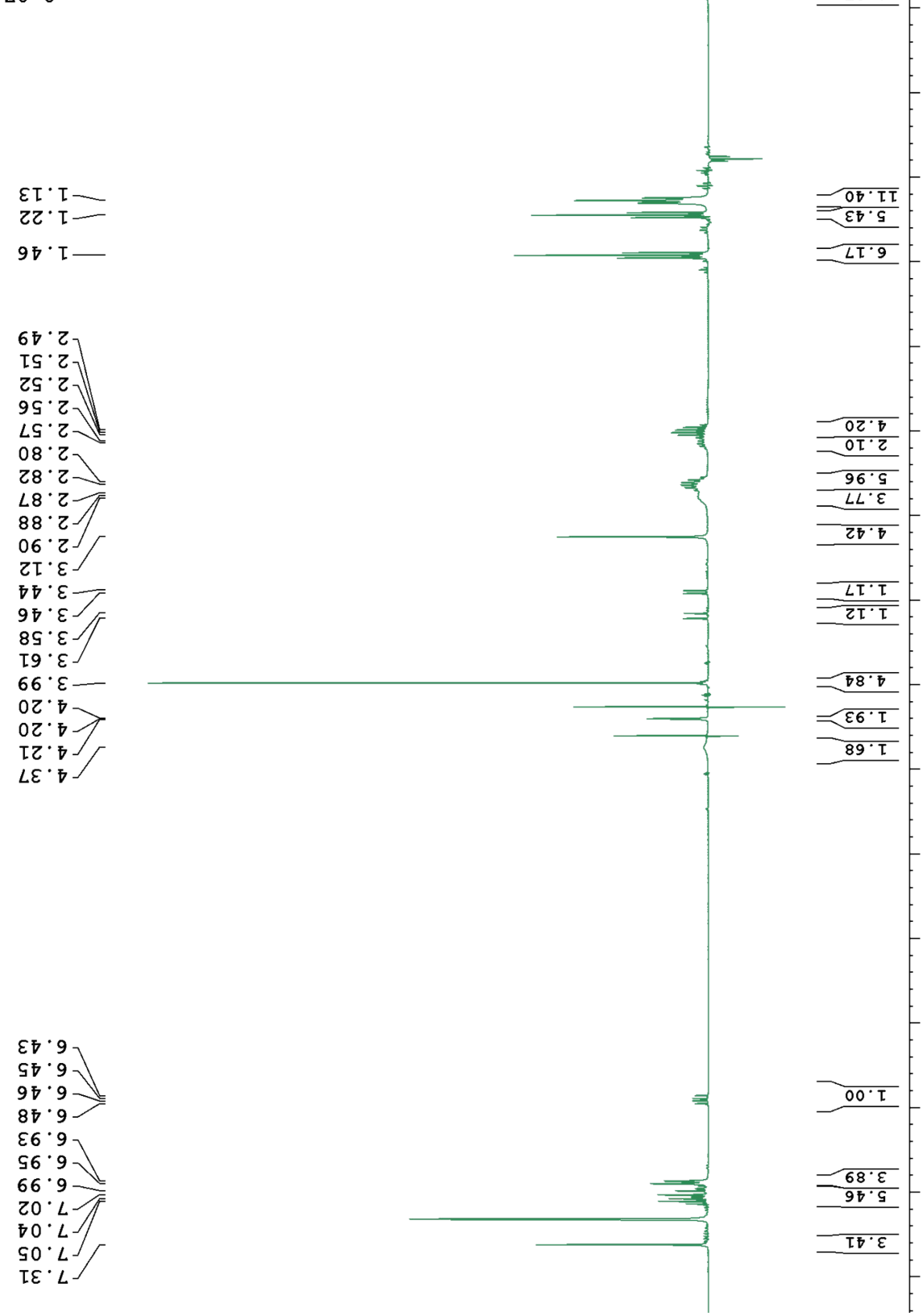
1.13
1.22
1.46
2.49
2.51
2.52
2.56
2.57
2.80
2.82
2.87
2.88
2.90
3.12
3.44
3.46
3.58
3.61
3.99
4.20
4.20
4.21
4.37
6.43
6.45
6.46
6.48
6.93
6.95
6.99
7.02
7.04
7.05
7.31
11.40
5.43
6.17
4.20
2.10
5.96
3.77
4.42
1.17
1.12
4.84
1.93
1.68
1.00
3.89
5.46
3.41

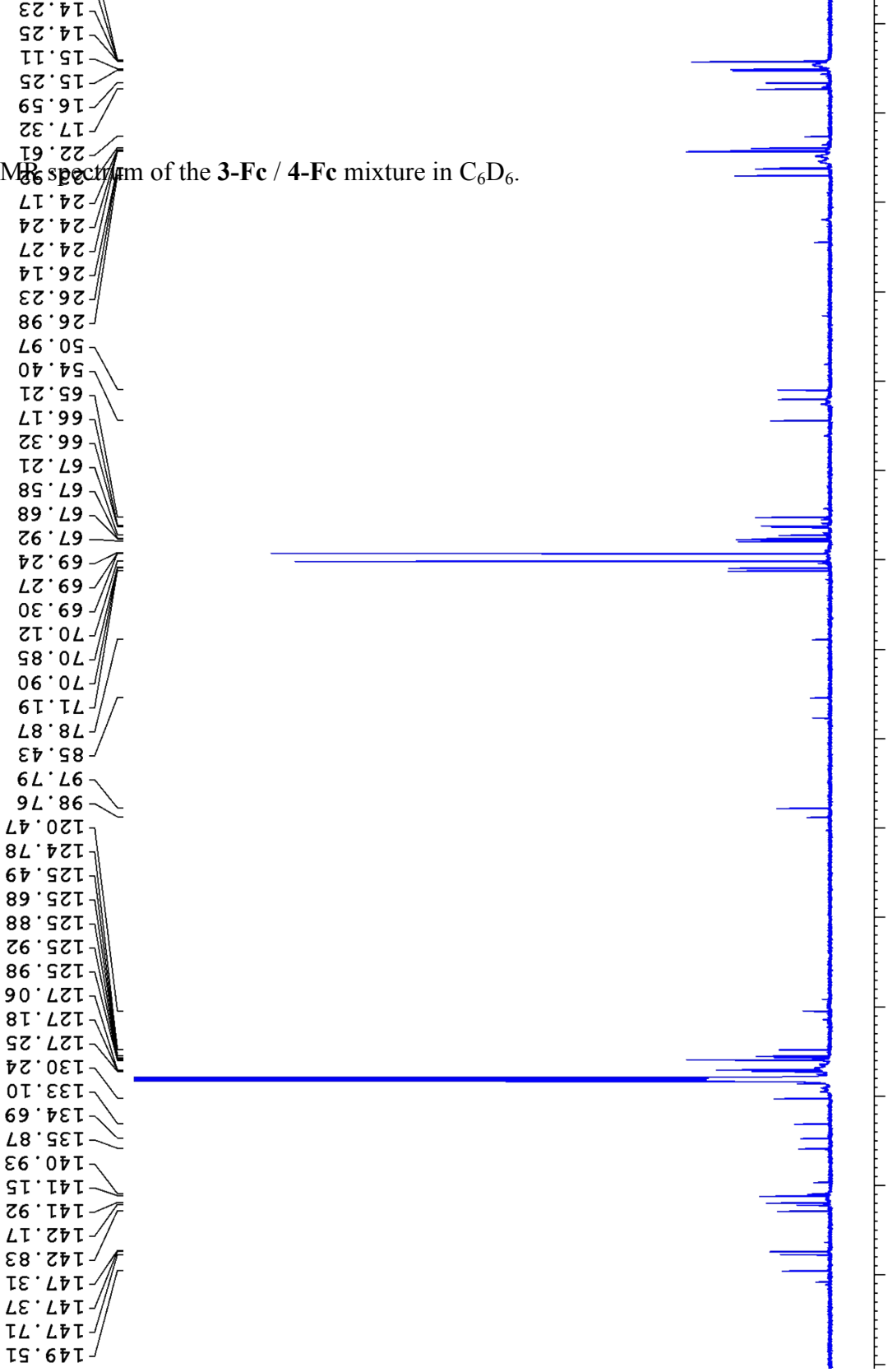

Figure S53. $^{13}C\{^{1}H\}$ NMR spectrum of the **3-Fc** / **4-Fc** mixture in C_6D_6.

Figure S54. ^{11}B NMR spectrum of the **3-Fc** / **4-Fc** mixture in C_6D_6.

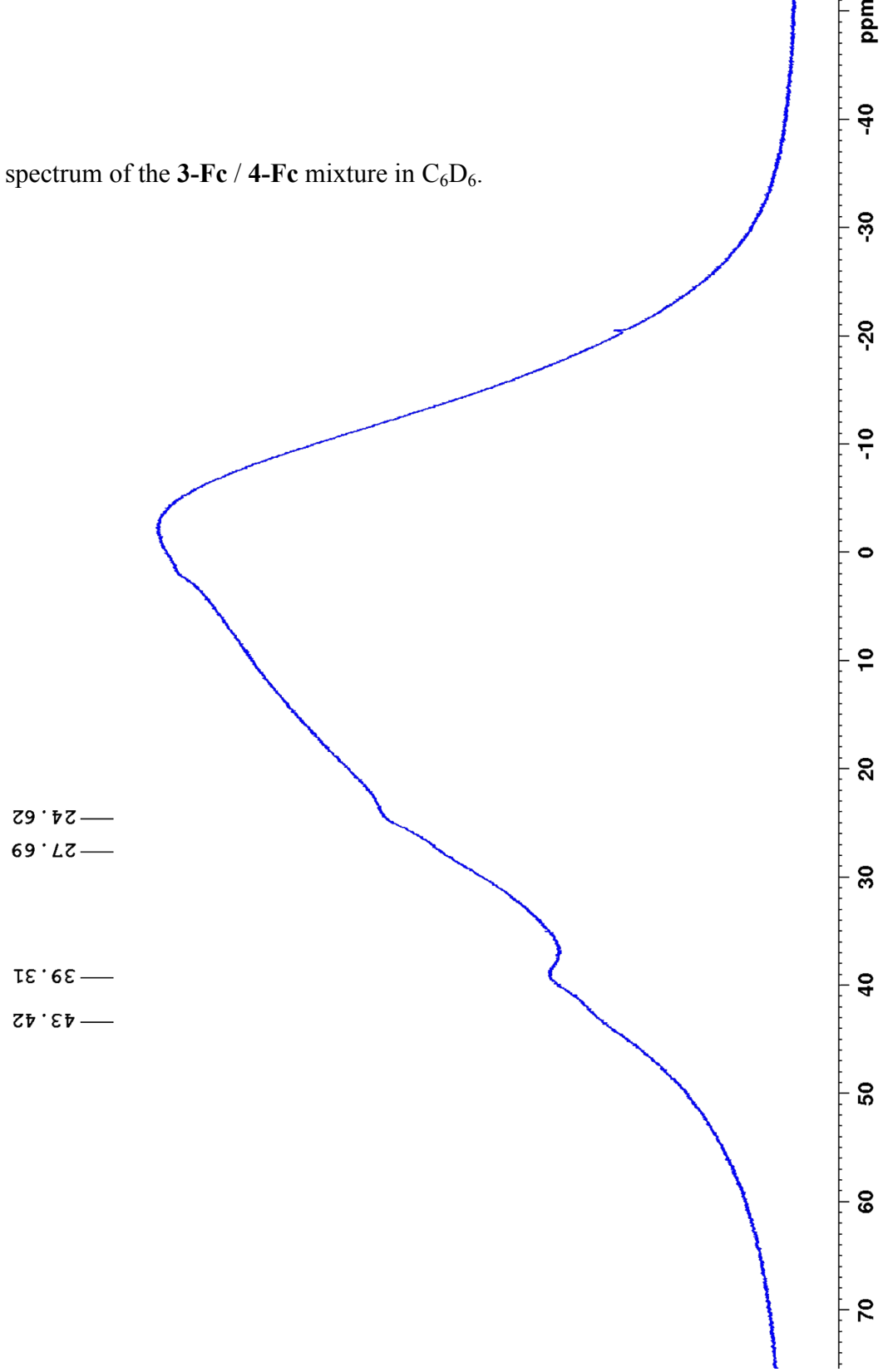

Figure S55. ^{1}H NMR spectrum of **5-Ph$_2$** in C_6D_6.

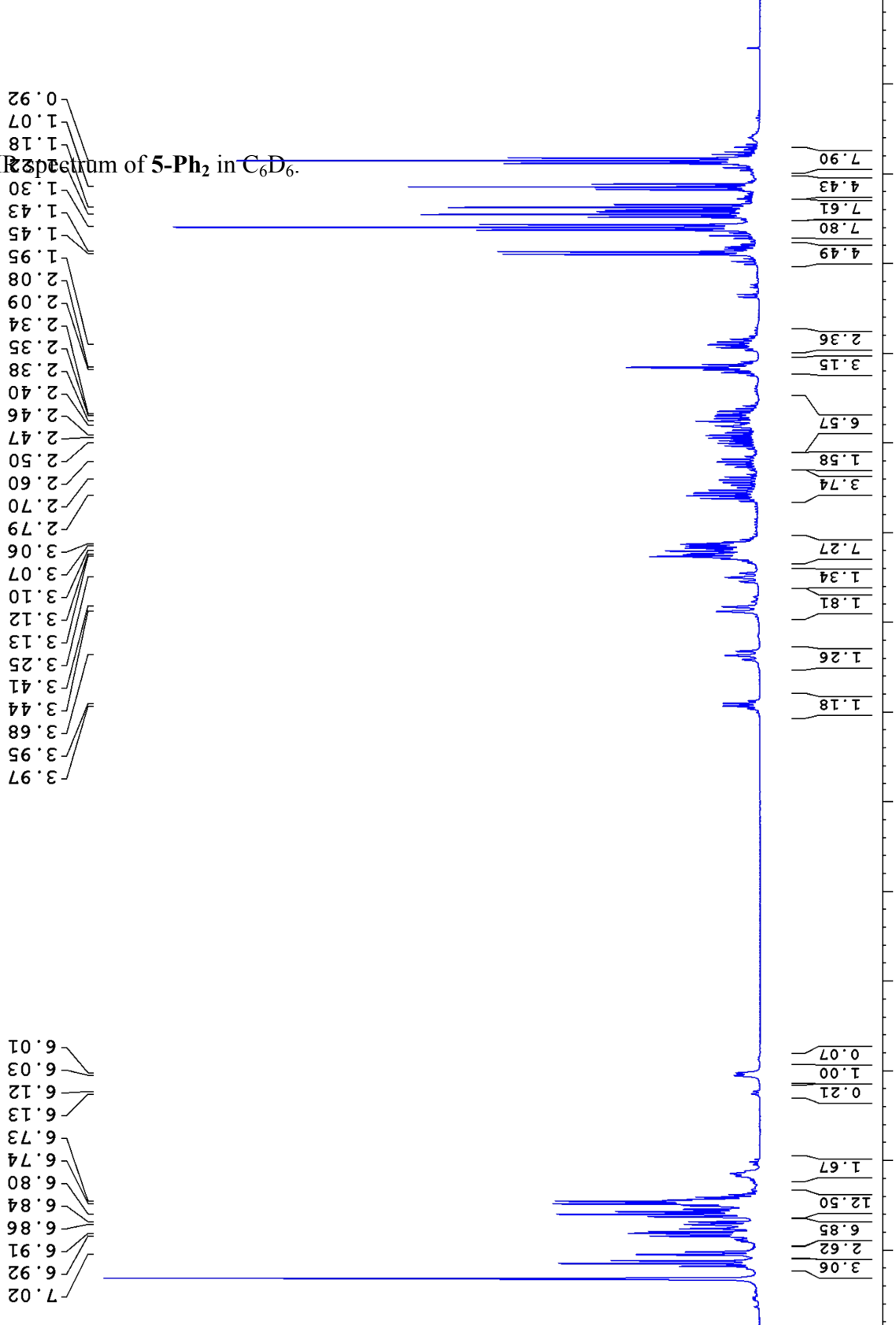

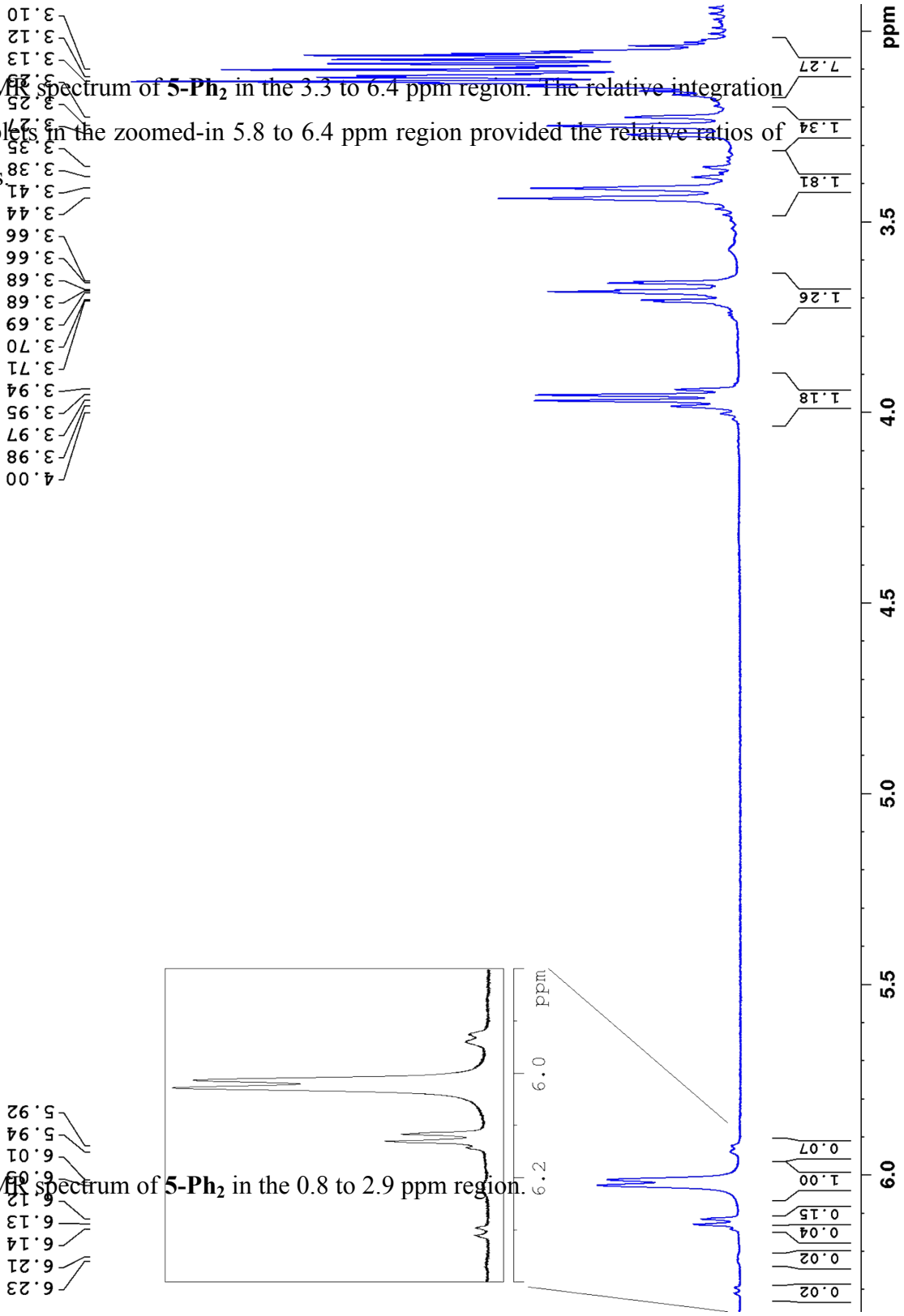

Figure S56. ^{1}H NMR spectrum of **5-Ph$_2$** in the 3.3 to 6.4 ppm region. The relative integration of the phenyl doublets in the zoomed-in 5.8 to 6.4 ppm region provided the relative ratios of the 6 diastereomers.

Figure S57. ^{1}H NMR spectrum of **5-Ph$_2$** in the 0.8 to 2.9 ppm region.

0.91
0.92
0.94
1.05
1.07
1.08
1.17
1.18
1.20
1.21
1.22
1.24
1.28
1.30
1.31
1.43
1.45
1.62
1.63
1.67
1.68
1.95
2.08
2.09
2.34
2.35
2.38
2.40
2.46
2.47
2.50
2.60
2.70
2.79
0.45
0.50
6.36
0.68
4.43
3.53
3.66
6.92
0.85
3.22
0.53
0.19
0.30
2.36
3.15
3.81
2.65
1.58
1.20
2.47

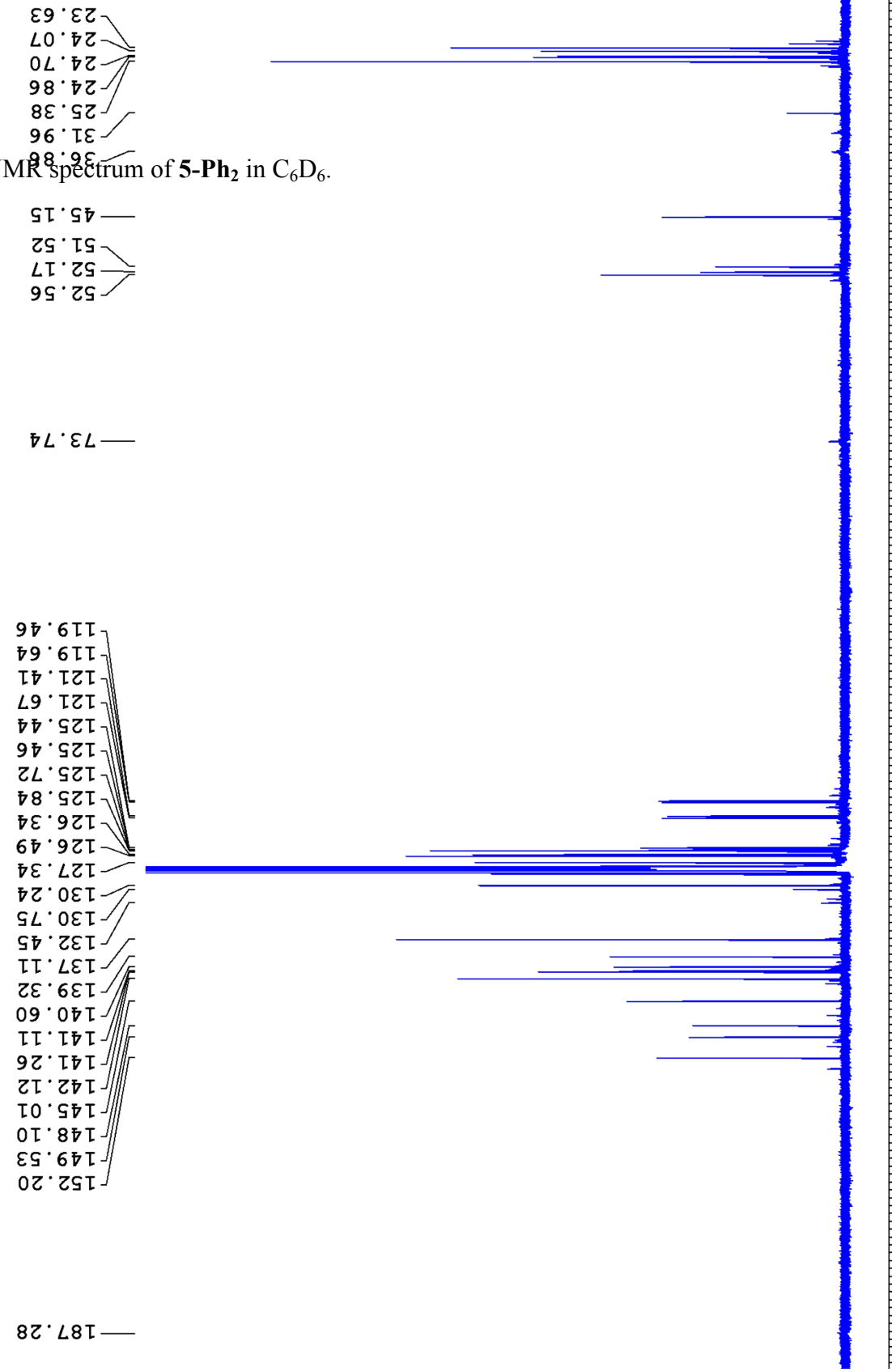

Figure S58. $^{13}C\{^{1}H\}$ NMR spectrum of **5-Ph$_2$** in C_6D_6.

Figure S59. HSQC plot of **5-Ph$_2$** in C_6D_6.

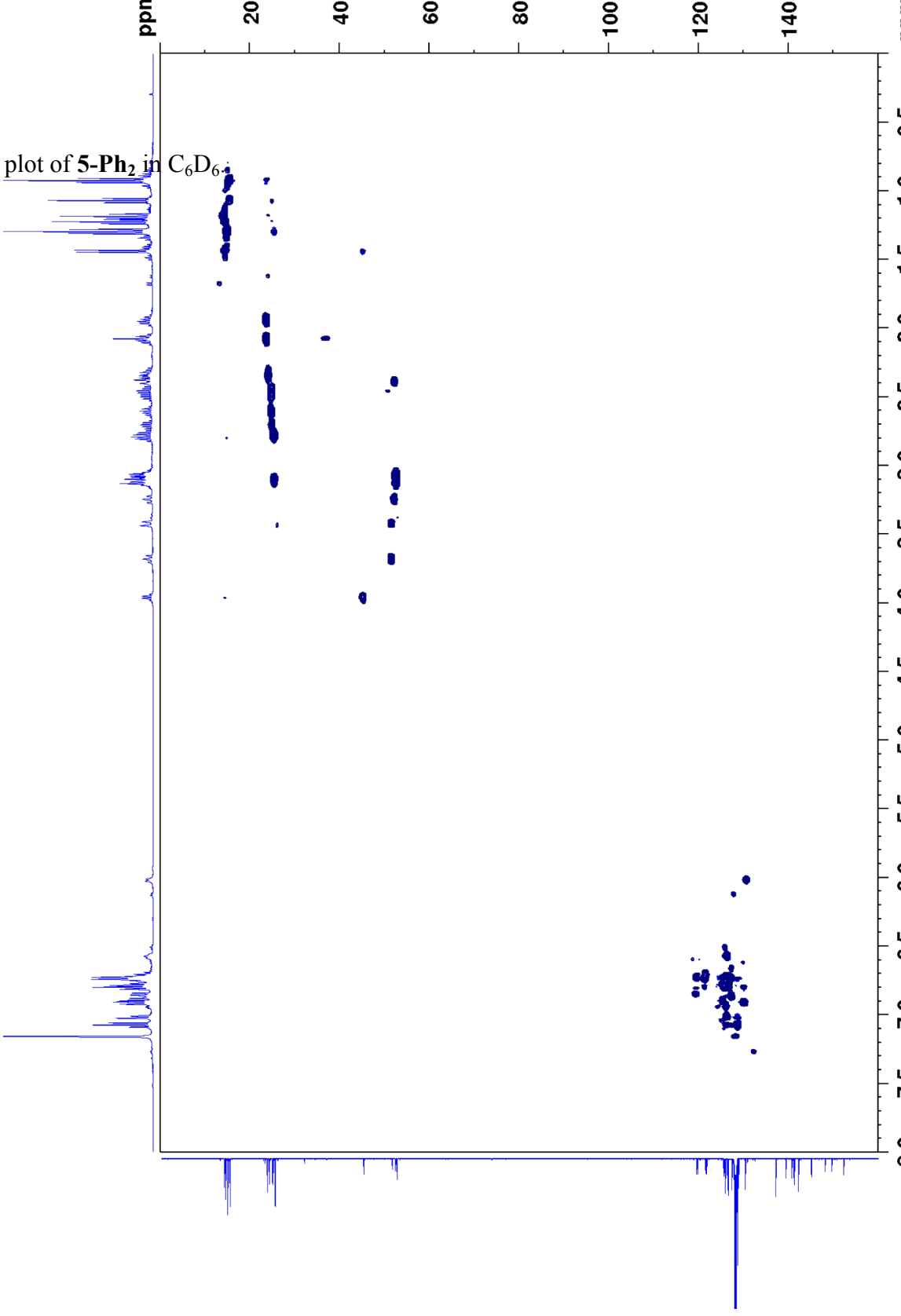

Figure S60. HMBC plot of **5-Ph$_2$** in C_6D_6.

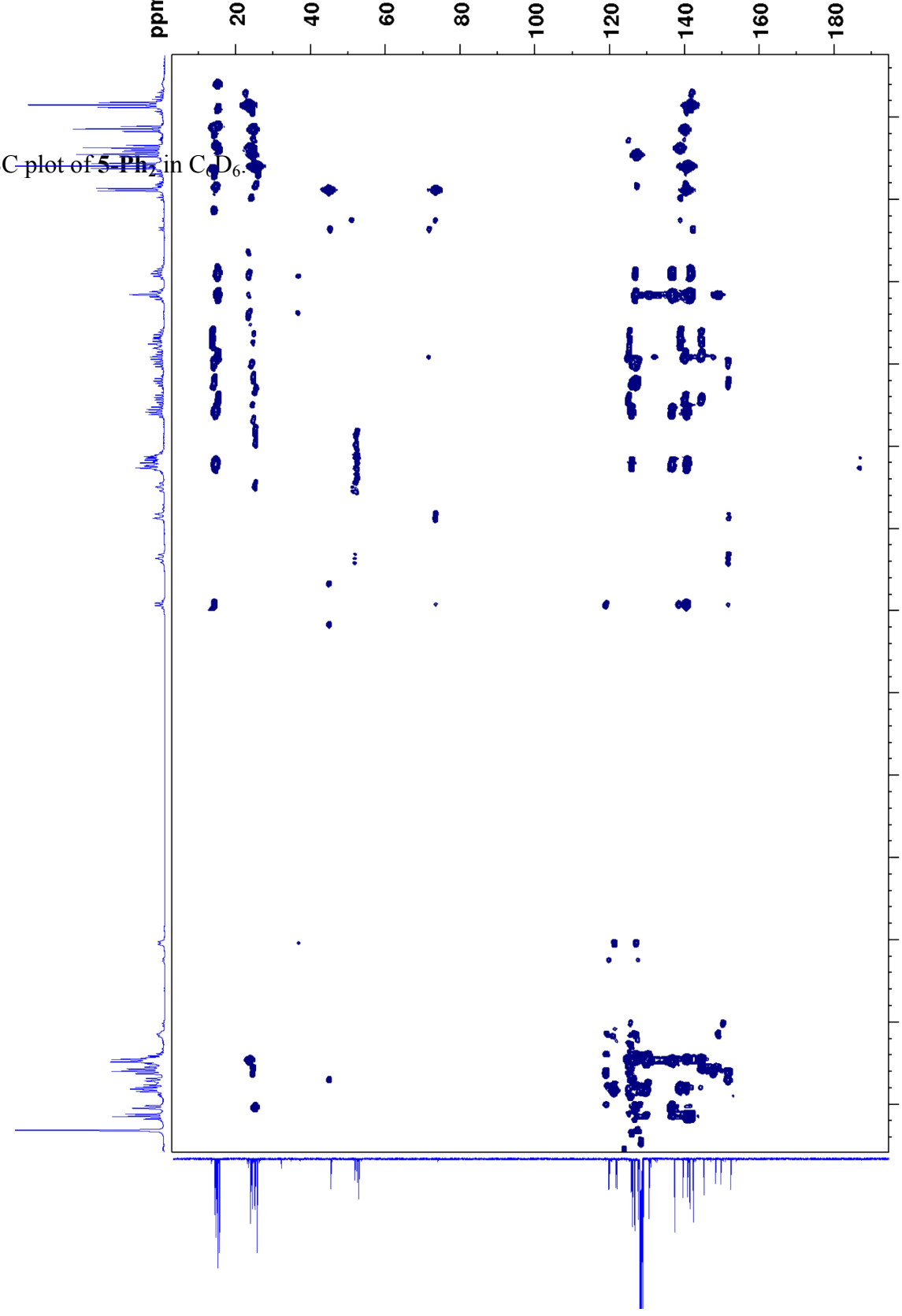

Figure S61. ^{11}B NMR spectrum of **5-Ph$_2$** in C_6D_6.

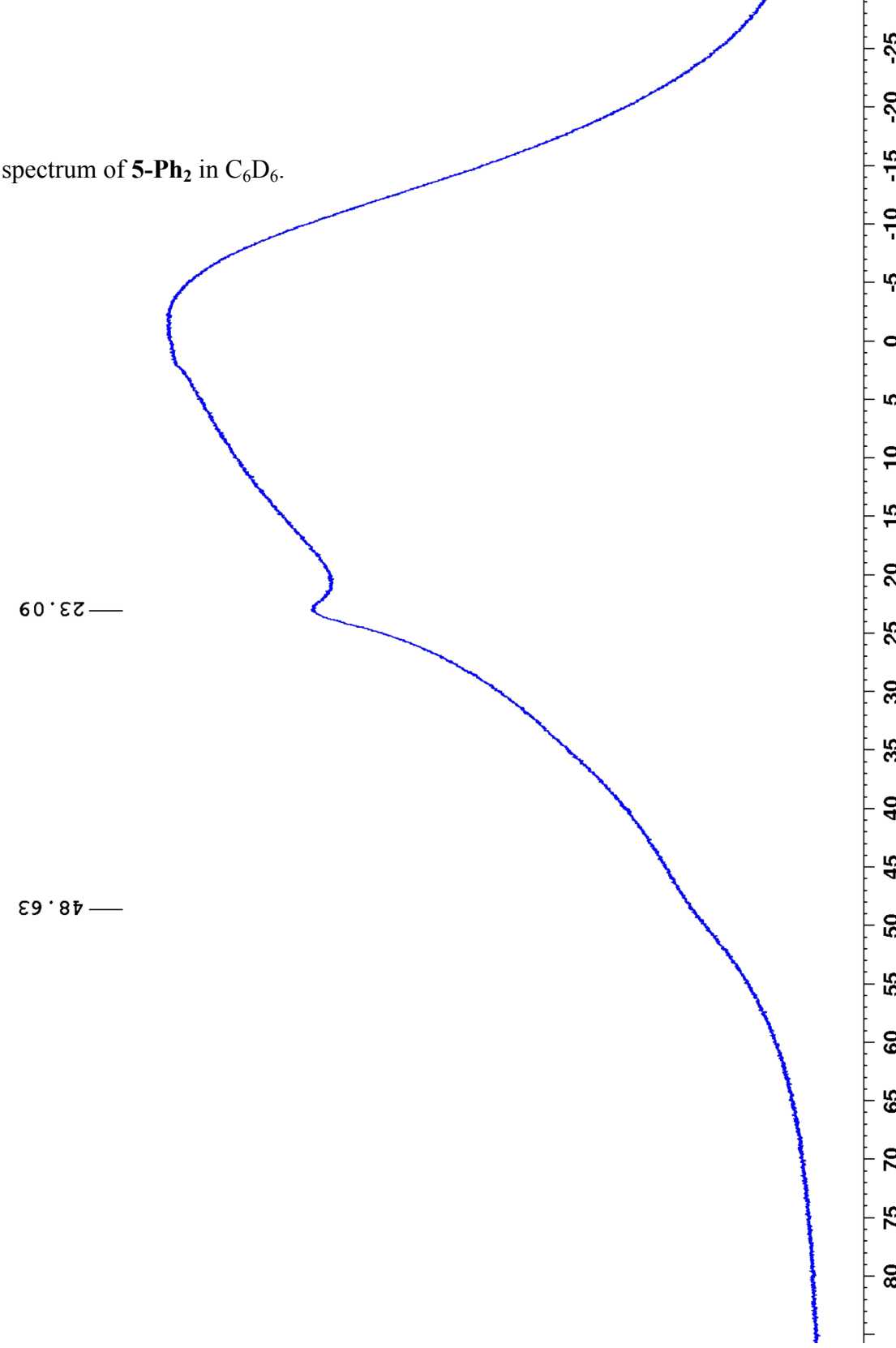

Crystallographic Details

The crystal data of **2a-Ph**, **2a-PhC^{F3}**, **3-Fc**, **4-Fc** and **5-Ph$_2$** were collected on a Bruker D8 Quest diffractometer with a CMOS area detector and multi-layer mirror monochromated $Mo_{K\alpha}$ radiation. The crystal data of **2-H** and **2a-Ph^{NMe2}** were collected on a Bruker X8-APEX II diffractometer with a CCD area detector and multi-layer mirror monochromated $Mo_{K\alpha}$ radiation. The structures were solved using intrinsic phasing method,[5] refined with the ShelXL program[6] and expanded using Fourier techniques. All non-hydrogen atoms were refined anisotropically. Hydrogen atoms were included in structure factor calculations. All hydrogen atoms were assigned to idealised geometric positions.

Crystallographic data have been deposited with the Cambridge Crystallographic Data Centre as supplementary publication no. CCDC 1907157-1907164. These data can be obtained free of charge from The Cambridge Crystallographic Data Centre *via* www.ccdc.cam.ac.uk/data_request/cif

Refinement details for 2-H: The asymmetric unit contains 3 crystallographically distinct molecules of the same compound (RESI 1, 2 and 3) displaying various disorders. RESI 1 displays no disorder. RESI displays a twofold disorder in the CH3-groups of the ethyl substituents C13 C14 (RESI 9 and 91 Ethy), and C29 C30 (RESI 11 and 111 Ethl) both modelled in an 86:14 ratio with SIMU 0.01 and SADI restraints. RESI 3 displays two fully twofold disordered Dep groups on the ring-expanded NHC, C21 > C30 (RESI 4 and 41) and C11 > C20 (RESI 5 and 51), modelled in a 65:35 ratio each. The ADPs in RESI 4 and 41 were restrained with SIMU 0.005 and the C28 C29 bond lengths in each residue equalized with SADI. On the intact NHC ligand, three ethyl substituents are twofold disordered: C33 C34 (RESI 6 and 61) and C39 C40 (RESI 7 and 71) both in a 60:40 ratio, and the CH3-group of C49 C59 (RESI 8 and 81) in a 89:11 ratio (bond lengths equalized in both residues with SADI). To avoid short H-H contacts due to disorders a BUMP instruction was used throughout

Refinement details for 2a-Ph: The asymmetric unit contained six heavily disordered benzene molecules, which were removed with the Platon program Squeeze.[7] Overall 255 electrons were removed per unit cell, corresponding to 6 benzene molecules (C_6H_6 = 42 electrons). Furthermore, the asymmetric unit contains two structurally distinct molecules (RESI MAIN 1 and 2) of the compound of interest displaying various degrees of disorder.

In RESI MAIN 1:

Three ethyl groups are twofold disordered in the terminal CH_3 group and modelled using separate free variables and PART 1 and -1, namely C32 (ratio = 43:57), C40 (ratio = 31:69) and C50 (ratio = 47:53). In each case the hydrogen atoms of the adjacent CH_2 unit (C31, C39 and C49, respectively) were also modelled with the same disorder in PART 1 and -1 to avoid bumping. The ADPS within these ethyl groups were restrained with SIMU 0.005 and the C31 C32 bond lengths equalized with SADI 0.005.

Furthermore, the entire Dep group C53 > C62 (RESI Dep 30 and 31) is twofold disordered and was modelled using a separate free variable and PART 1 and -1 (ratio = 31:69). The ADPs within these two residues were restrained with SIMU 0.005 and the benzene rings with AFIX 66.

In RESI MAIN 2:

Three ethyl groups are twofold disordered in the terminal CH_3 group and modelled using separate free variables and PART 1 and -1, namely C40 (ratio = 31:69), C52 (ratio = 75:25) and C60 (ratio = 73:27). In each case the hydrogen atoms of the adjacent CH_2 unit (C39, C51 and C59, respectively) were also modelled with the same disorder in PART 1 and -1 to avoid bumping. The ADPS within these ethyl groups were restrained with SIMU 0.005 (0.002 for C51 C52).

The ethyl group C41 C42 (RESI Eth 40 and 41) was modelled as twofold disordered in both atoms using a separate free variable and PART 1 and -1 (ratio = 88:12). The ADPS within the parts were restrained with SIMU 0.005 and the C41 C42 and C34 C41 bond lengths fixed with DFIX 1.51 0.005.

Refinement details for 2a-Ph^{CF3}: The asymmetric unit contained half of a highly disordered disordered and partially occupied benzene molecule which could not be modelled in a satisfactory manner and were therefore removed with the Platon programme Squeeze.[7] The number of electrons squeezed corresponds to 150 per unit cell, i.e. 3.6 benzene molecules.

The CF_3 group on the alkynyl fragment is twofold disordered in F1, F2, F3 in a 73:27 ratio (RESI 5 and 51 F3). ADPs were restrained using SIMU 0.005. The CF_3 group on the aromatic ring attached to the B_2C_3 ring is threefold disordered in C24, F4, F5, F6 in a 41:53:6 ratio (RESI 4, 41 and 411 CF3). ADPs were restrained with SIMU 0.002 and the C20-C24 and F-F distances in all three residues equalized with SADI. One ethyl group on the intact NHC, C47 C48 (RESI 8 and 81 Eth), is twofold disordered in a 88:12 ratio, with ADPs restrained using SIMU 0.003.

Furthermore, one Dep group on the ring-expanded NHC is partially twofold disordered C35 + C40 > C44 (RESI 6 and 7 Ar), modelled in a 62:38 ratio, the ADPs being restrained with SIMU 0.003. The other Dep group has one ethyl substituent, C27 C28 (RESI 2 and 3 Ethyl), which is twofold disordered in a 41:59 ratio. The ADPs of the carbon atoms of that Dep group, C25 > C31, were restrained with SIMU 0.002 (elongation due to disorder in the ring which could not be satisfyingly modelled). A BUMP restraint had to be applied to prevent short intermolecular H-H distances. The three most disagreeable reflexions were omitted.

Refinement details for 2a-Ph^{NMe2}: The asymmetric unit contains two distinct molecules of the compound (RESI 1 and 2) and two molecules of benzene. RESI 2 shows no disorder. In RESI, two ethyl groups on the ring-expanded NHC ligand are twofold disordered: C35 C35 (RESI 3 and 31) in a 69:31 ratio and C45 C46 (RESI 4 and 41) in a 70:30 ratio. SIMU were applied to these disorders. Furthermore, the intact NHC ligand presents a twofold disorder (RESI 5 and 51) in its central ring (C6, N3, C7, C8) and one of the Dep groups (C47 > C56) modelled in a 60:40 ratio with a default SIMU restraint and the aryl Dep ring idealized with AFIX 66/65. Finally, ADPs of the 4-NMe_2-C_6H_4 residues attached to the central B_2C_3 rings were restrained with SIMU because of a slight rotational disorder which could not be modelled.

Refinement details for 2-TMS: The asymmetric unit contains two distinct molecules of the compound, one of them displaying a twofold disorder in the ethyl group C35 C36 modelled in a 78:22 ratio, the ADPs being restrained with SIMU 0.01.

Refinement details for 3-Fc: The asymmetric unit contains 0.5 benzene molecules positioned on an inversion centre. The ring-expanded moiety of the molecule displays two disorders. One ethyl substituent (C27 C28) is twofold disordered in C28 refined to a 56:44 ratio. The two protons on C27 were also modelled as disordered using parts 1 and -1. The Dep substituent C11 > C20 (RESI 4 and 5 Dep) was fully disordered over two positions refined to a 57:43 ratio. The benzene ring in these residues was modelled with AFIX 66 and the ADPs restrained using SIMU 0.005.

Refinement details for 4-Fc: The asymmetric unit contains two distinct molecules of the title compound (RESI 1 and 2) and two benzene molecules. RESI 1 presents a twofold disorder in one ethyl substituent, C27 C28 (RESI 3 and 31) modelled in a 61:39 ratio and with ADP SIMU 0.01 restraints. RESI 2 also presents a twofold disorder in one ethyl substituent, C21 C22 (RESI

4 and 41) modelled in a 82:18 ratio and with ADP SIMU 0.01 restraints. The benzene molecule C70 > C75 was modelled with an idealised ring using AFIX 66/65.

Refinement details for 5-Ph$_2$: The compound presents one twofold disordered ethyl group in C39 C40 modelled in a 77:23 ratio without further restraints. The two most disagreeable reflexions were omitted.

Crystal data for 2-H: $C_{50}H_{64}B_2N_4$, $M_r = 742.67$, yellow block, 0.325×0.222×0.202 mm^3, monoclinic space group $P2_1/n$, $a = 11.2520(3)$ Å, $b = 57.9972(13)$ Å, $c = 20.3572(6)$ Å, $\beta = 96.869(2)°$, $V = 13189.4(6)$ Å^3, $Z = 12$, $\rho_{calcd} = 1.122$ g·cm^{-3}, $\mu = 0.064$ mm^{-1}, $F(000) = 4824$, $T = 100(2)$ K, $R_1 = 0.0769$, $wR^2 = 0.1708$, 25948 independent reflections [$2\theta \leq 52.044°$] and 1744 parameters.

Crystal data for 2a-Ph: $C_{62}H_{72}B_2N_4$ (+ 3 squeezed C_6H_6), $M_r = 1789.70$, yellow block, 0.297×0.246×0.231 mm^3, triclinic space group $P\bar{1}$, $a = 10.9015(13)$ Å, $b = 23.701(3)$ Å, $c = 24.120(3)$ Å, $\alpha = 97.712(4)°$, $\beta = 97.821(4)°$, $\gamma = 90.381(4)°$, $V = 6116.5(13)$ Å^3, $Z = 2$, $\rho_{calcd} = 0.972$ g·cm^{-3}, $\mu = 0.056$ mm^{-1}, $F(000) = 1928$, $T = 101(2)$ K, $R_1 = 0.0632$, $wR^2 = 0.1967$, 24104 independent reflections [$2\theta \leq 52.044°$] and 1386 parameters.

Crystal data for 2a-Ph^{CF3}: $C_{64}H_{70}B_2F_6N_4$, $M_r = 1030.86$, yellow block, 0.253×0.216×0.163 mm^3, monoclinic space group $C2/c$, $a = 43.9042(16)$ Å, $b = 11.6825(5)$ Å, $c = 26.7007(11)$ Å, $\beta = 123.0460(10)°$, $V = 11479.7(8)$ Å^3, $Z = 8$, $\rho_{calcd} = 1.193$ g·cm^{-3}, $\mu = 0.082$ mm^{-1}, $F(000) = 4368$, $T = 100(2)$ K, $R_1 = 0.0492$, $wR^2 = 0.1306$, 11273 independent reflections [$2\theta \leq 52.044°$] and 865 parameters.

Crystal data for 2a-Ph^{NMe2}: $C_{66}H_{82}B_2N_6 \cdot C_6H_6$ $M_r = 1059.1$, yellow block, 0.399×0.242×0.222 mm^3, triclinic space group $P\bar{1}$, $a = 10.9162(6)$ Å, $b = 20.7562(13)$ Å, $c = 28.3310(17)$ Å, $\alpha = 88.333(2)°$, $\beta = 82.473(2)°$, $\gamma = 76.374(2)°$, $V = 6184.8(6)$ Å^3, $Z = 4$, $\rho_{calcd} = 1.137$ g·cm^{-3}, $\mu = 0.066$ mm^{-1}, $F(000) = 2288$, $T = 100(2)$ K, $R_1 = 0.0682$, $wR^2 = 0.1951$, 24378 independent reflections [$2\theta \leq 52.044°$] and 1611 parameters.

Crystal data for 2-TMS: $C_{53}H_{72}B_2N_4Si$, $M_r = 814.85$, yellow plate, 0.238×0.228×0.189 mm^3, triclinic space group $P\bar{1}$, $a = 14.3768(5)$ Å, $b = 17.7360(7)$ Å, $c = 19.9449(7)$ Å,

α = 94.5010(10)°, β = 100.3180(10)°, γ = 100.3410(10)°, V = 4889.9(3) Å^3, Z = 4, ρ_{calcd} = 1.107 g·cm^{-3}, μ = 0.086 mm^{-1}, F(000) = 1768, T = 100(2) K, R_1 = 0.0487, wR^2 = 0.1359, 19111 independent reflections [$2\theta \leq$ 52.044°] and 1123 parameters.

Crystal data for 3-Fc: $C_{73}H_{83}B_2Fe_2N_4$, M_r = 1149.75, red block, 0.207×0.159×0.111 mm^3, triclinic space group $P\bar{1}$, a = 13.254(3) Å, b = 13.786(3) Å, c = 18.567(4) Å, α = 75.387(7)°, β = 80.073(8)°, γ = 64.354(6)°, V = 2951.7(12) Å^3, Z = 2, ρ_{calcd} = 1.294 g·cm^{-3}, μ = 0.540 mm^{-1}, F(000) = 1222, T = 100(2) K, R_1 = 0.0672, wR^2 = 0.1773, 11628 independent reflections [$2\theta \leq$ 52.036°] and 814 parameters.

Crystal data for 4-Fc: $C_{64}H_{76}B_2FeN_4$, M_r = 1957.51, colourless block, 0.28×0.198×0.144 mm^3, monoclinic space group $P2_1/c$, a = 39.5261(17) Å, b = 12.8542(6) Å, c = 22.1018(9) Å, β = 105.9140(10)°, V = 10799.0(8) Å^3, Z = 4, ρ_{calcd} = 1.204 g·cm^{-3}, μ = 0.323 mm^{-1}, F(000) = 4192, T = 100(2) K, R_1 = 0.0573, wR^2 = 0.1302, 21255 independent reflections [$2\theta \leq$ 52.044°] and 1323 parameters.

Crystal data for 5-Ph$_2$: $C_{60}H_{70}B_2N_4$, M_r = 868.82, yellow block, 0.401×0.374×0.256 mm^3, monoclinic space group $P2_1/c$, a = 11.5634(5) Å, b = 22.8149(8) Å, c = 18.8309(7) Å, β = 99.871(2)°, V = 4894.4(3) Å^3, Z = 4, ρ_{calcd} = 1.179 g·cm^{-3}, μ = 0.067 mm^{-1}, F(000) = 1872, T = 100(2) K, R_1 = 0.0473, wR^2 = 0.1246, 9636 independent reflections [$2\theta \leq$ 52.044°] and 618 parameters.

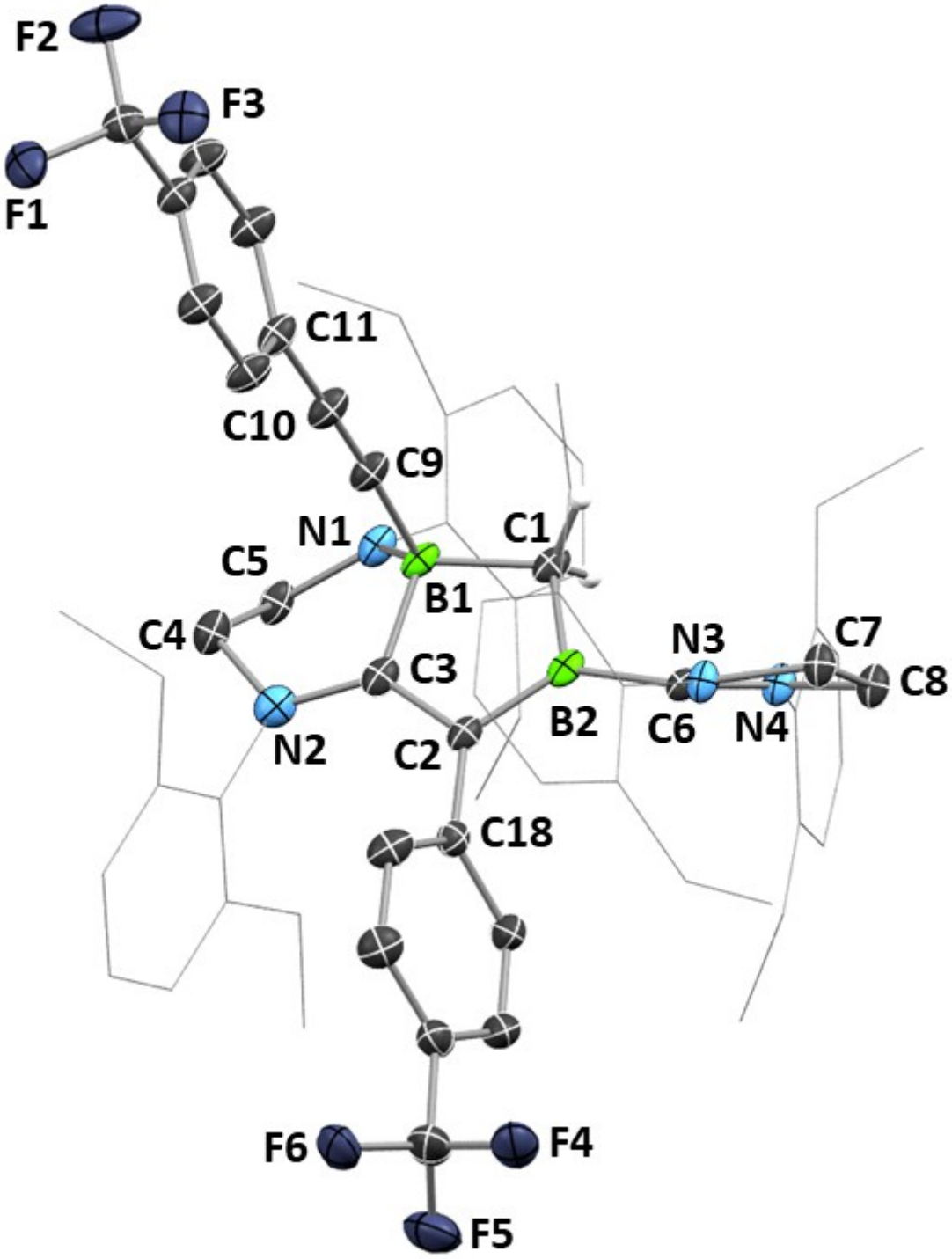

Figure S62. Crystallographically-derived molecular structure of **2a-Ph^{CF3}**. Thermal ellipsoids drawn at the 50% probability level. Dep groups represented in framework style and hydrogen atoms omitted for clarity, except for the diagnostic protons bound to C1.

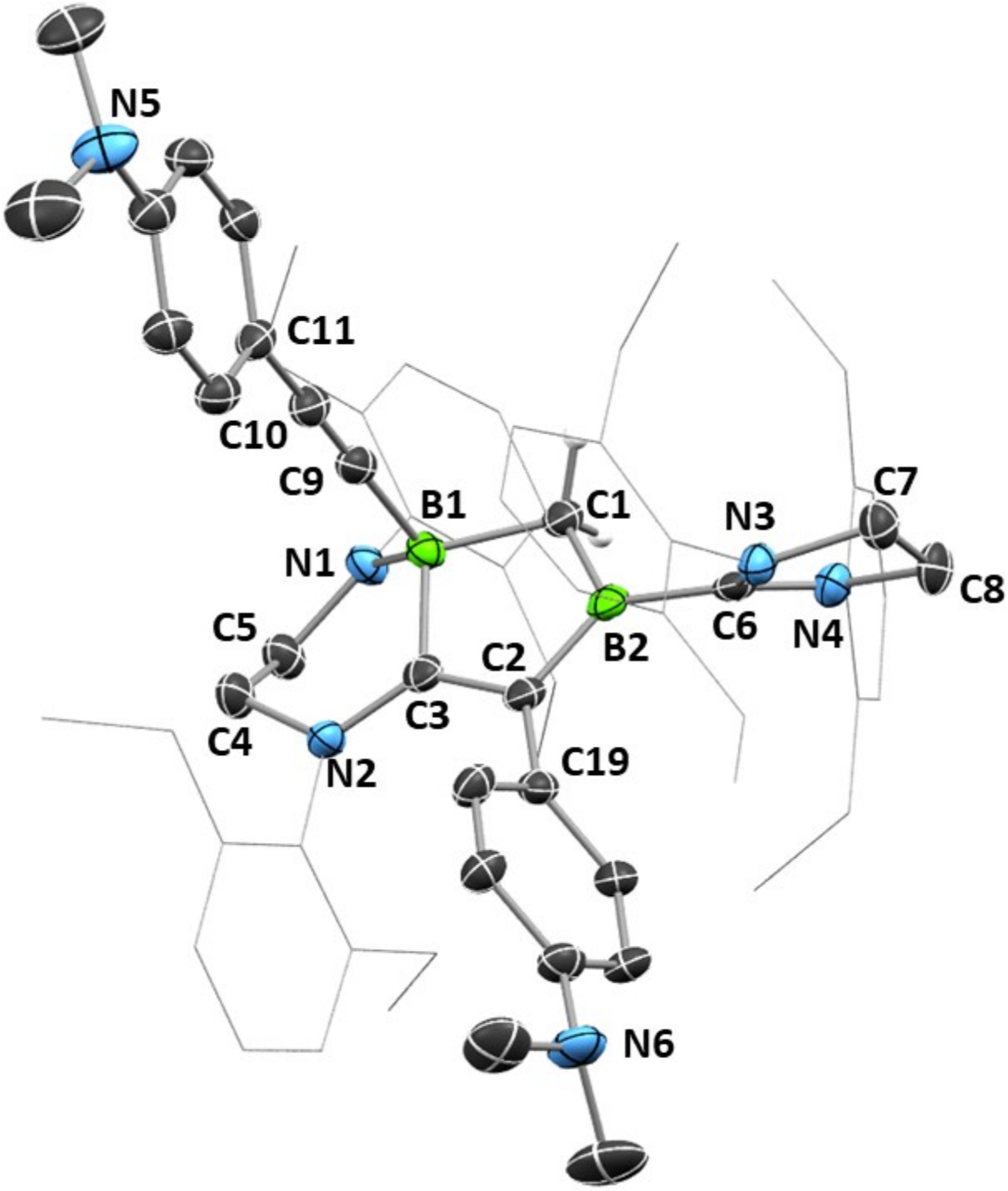

Figure S63. Crystallographically-derived molecular structure of **2a-Ph^{NMe2}**. Thermal ellipsoids drawn at the 50% probability level. Dep groups represented in framework style and hydrogen atoms omitted for clarity, except for the diagnostic protons bound to C1.

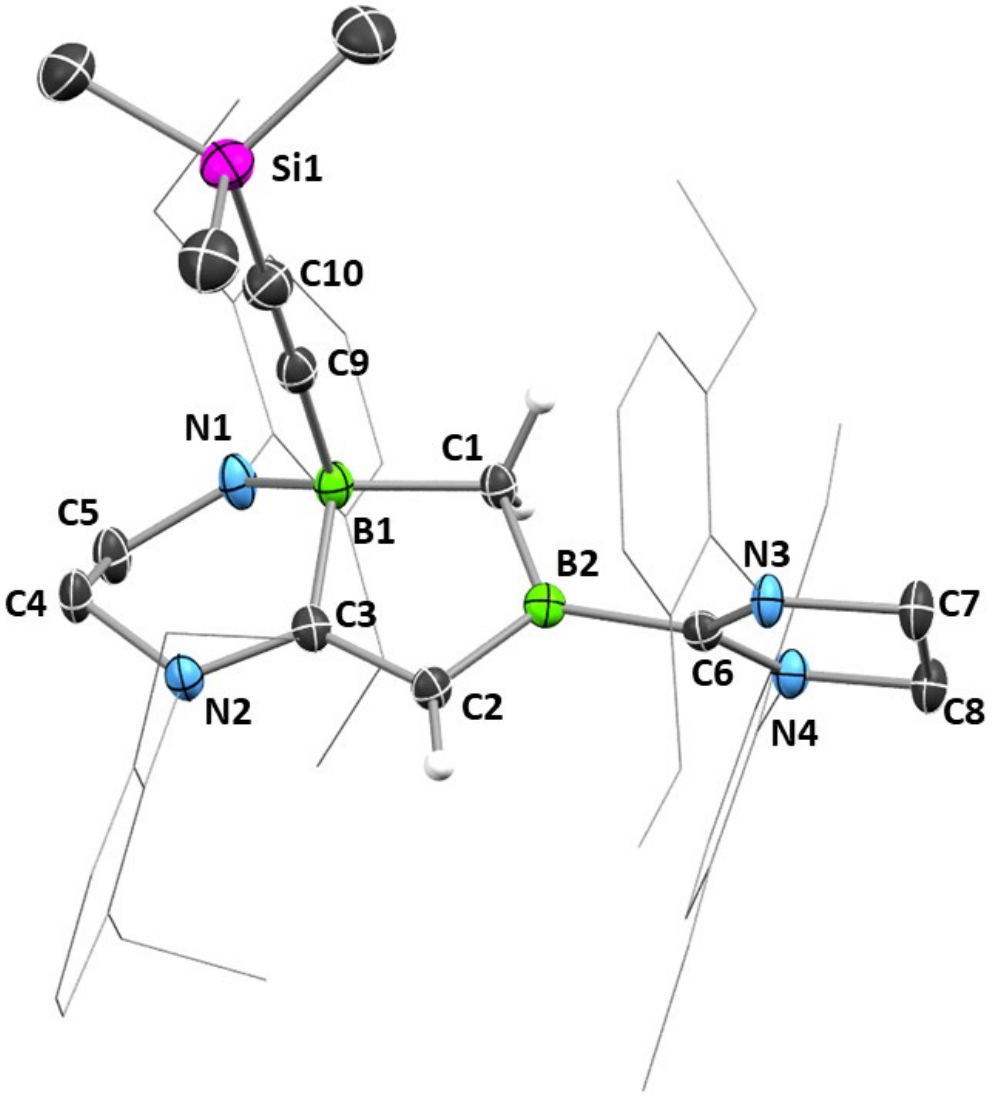

Figure S64. Crystallographically-derived molecular structure of **2-TMS** (only the second of the two independent molecules is the asymmetric unit is shown, the other one is its mirror image). Thermal ellipsoids drawn at the 50% probability level. Dep groups represented in framework style and hydrogen atoms omitted for clarity, except for the diagnostic protons bound to C1 and C2.

Calculation of ^{11}B NMR shifts

Calculations of the ^{11}B NMR shifts of **2-H**, **3-Fc** and **4-Fc** were performed on the optimized structures at the B3LYP/6-311G(d)[8] level against a $BF_3{\cdot}Et_2O$ standard using the Gaussian 09, Revision D.01 program package.[9] These were used to identify the ^{11}B NMR resonances of all other **2a/2b/3-R** compounds by analogy.

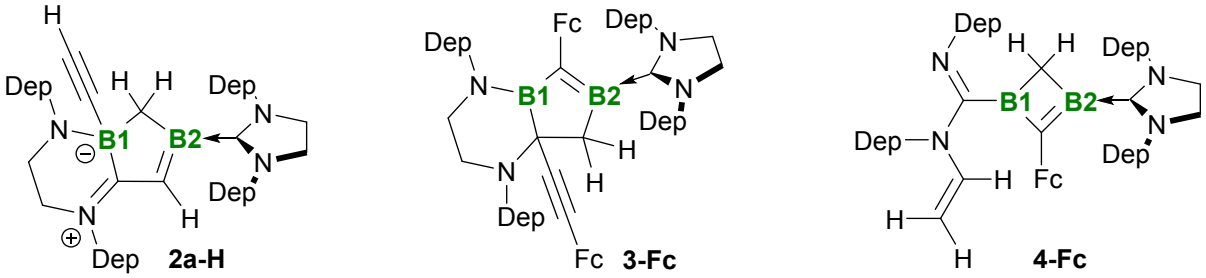

Exp:	54.0 **B2**, −10.2 **B1**	43.4 **B2**, 39.3 **B1**	27.7 **B1**, 24.6 **B2**
Calcd:	53.5 **B2**, −13.5 **B1**	42.2 **B2**, 37.0 **B1**	28.6 **B1**, 25.5 **B2**

Figure S65. Experimental and theoretical ^{11}B NMR shifts (B3LYP/6-311G(d) level) of compounds **2-H**, **3-Fc** and **4-Fc**.

References

1 K. M. Kuhn and R. H. Grubbs, *Org. Lett.*, 2008, **10**, 2075.

2 H.-C. Chiu and I. A. Tonks, *Angew. Chem. Int. Ed.*, 2018, **57**, 6090.

3 G. Doisneau, G. Balavoine and T. Fillebeen-Khan, *J. Organomet. Chem*., 1992, **425**, 113.

4 M. Arrowsmith, J. Böhnke, M. Celik, T. Dellermann, K. Hammond and H. Braunschweig, *Chem. Eur. J.*, 2016, **22**, 17169.

5 G. Sheldrick, *Acta Cryst.*, 2015, **A71**, 3.

6 G. Sheldrick, *Acta Cryst.*, 2008, **A64**, 112.

7 A. L. Spek, *Acta Cryst*., 2015, **C71**, 9.

8 (a) A. D. Becke, *J. Chem. Phys.* 1993, **98**, 5648; (b) M. P. McGrath and L. Radom, *J. Chem. Phys.*, 1991, **94**, 511; (c) A. J. H. Wachters, *J. Chem. Phys.*, 1970, **52**, 1033.

9 Gaussian 09, Revision A.02, M. J. Frisch, G. W. Trucks, H. B. Schlegel, G. E. Scuseria, M. A. Robb, J. R. Cheeseman, G. Scalmani, V. Barone, G. A. Petersson, H. Nakatsuji, X. Li, M. Caricato, A. Marenich, J. Bloino, B. G. Janesko, R. Gomperts, B. Mennucci, H. P. Hratchian, J. V. Ortiz, A. F. Izmaylov, J. L. Sonnenberg, D. Williams-Young, F. Ding, F. Lipparini, F. Egidi, J. Goings, B. Peng, A. Petrone, T. Henderson, D. Ranasinghe, V. G. Zakrzewski, J. Gao, N. Rega, G. Zheng, W. Liang, M. Hada, M. Ehara, K. Toyota, R. Fukuda, J. Hasegawa, M. Ishida, T. Nakajima, Y. Honda, O. Kitao, H. Nakai, T. Vreven, K. Throssell, J. A. Montgomery, Jr., J. E. Peralta, F. Ogliaro, M. Bearpark, J. J. Heyd, E. Brothers, K. N. Kudin, V. N. Staroverov, T. Keith, R. Kobayashi, J. Normand, K. Raghavachari, A. Rendell, J. C. Burant, S. S. Iyengar, J. Tomasi, M. Cossi, J. M. Millam, M. Klene, C. Adamo, R. Cammi, J. W. Ochterski, R. L. Martin, K. Morokuma, O. Farkas, J. B. Foresman and D. J. Fox, Gaussian, Inc. Wallingford CT, **2016**.